

INVESTIGATION ON THERMO-PHYSICAL
PROPERTIES AND THERMAL-HYDRAULIC
PERFORMANCE OF $\text{TiO}_2\text{-SiO}_2$ NANOFLUIDS

MUHAMMAD NABIL FIKRI BIN MOHAMAD



UMP

Master of Science

UNIVERSITI MALAYSIA PAHANG

UNIVERSITI MALAYSIA PAHANG

DECLARATION OF THESIS AND COPYRIGHT

Author's Full Name : MUHAMMAD NABIL FIKRI BIN MOHAMAD

Date of Birth : 01 DISEMBER 1993

Title : INVESTIGATION ON THERMO-PHYSICAL
PROPERTIES AND THERMAL-HYDRAULIC
PERFORMANCE OF TiO₂-SiO₂ NANOFLUIDS

Academic Session : 2017/2018

I declare that this thesis is classified as:

- CONFIDENTIAL (Contains confidential information under the Official Secret Act 1997)*
- RESTRICTED (Contains restricted information as specified by the organization where research was done)*
- OPEN ACCESS I agree that my thesis to be published as online open access (Full Text)

I acknowledge that Universiti Malaysia Pahang reserves the following rights:

1. The Thesis is the Property of Universiti Malaysia Pahang
2. The Library of Universiti Malaysia Pahang has the right to make copies of the thesis for the purpose of research only.
3. The Library has the right to make copies of the thesis for academic exchange.

Certified by:

(Student's Signature)

MUHAMMAD NABIL FIKRI
BIN MOHAMAD

New IC: 931201-03-5353

Date: 8 JUNE 2018

(Supervisor's Signature)

ASSOC. PROF. DR. WAN AZMI
BIN WAN HAMZAH

Name of Supervisor

Date: 8 JUNE 2018

NOTE : * If the thesis is CONFIDENTIAL or RESTRICTED, please attach a thesis declaration letter.

SUPERVISOR'S DECLARATION

We hereby declare that we have checked this thesis and in our opinion, this thesis is adequate in terms of scope and quality for the award of the degree of Master of Science in Mechanical Engineering.

(Supervisor's Signature)

Full Name : DR. WAN AZMI BIN WAN HAMZAH

Position : ASSOCIATE PROFESSOR

Date : 8 JUNE 2018



(Co-supervisor's Signature)

Full Name : DR. AZRI BIN ALIAS

Position : SENIOR LECTURER

Date : 8 JUNE 2018

STUDENT'S DECLARATION

I hereby declare that the work in this thesis is based on my original work except for quotations and citations which have been duly acknowledged. I also declare that it has not been previously or concurrently submitted for any other degree at Universiti Malaysia Pahang or any other institutions.

(Student's Signature)

Full Name : MUHAMMAD NABIL FIKRI BIN MOHAMAD
ID Number : MMM16014
Date : 8 JUNE 2018



UMP

INVESTIGATION ON THERMO-PHYSICAL PROPERTIES AND
THERMAL-HYDRAULIC PERFORMANCE OF TiO₂-SiO₂ NANOFLUIDS



MUHAMMAD NABIL FIKRI BIN MOHAMAD

Thesis submitted in fulfillment of the requirements
for the award of the degree of
Master of Science

UMP

Faculty of Mechanical Engineering
UNIVERSITI MALAYSIA PAHANG

JUNE 2018

ACKNOWLEDGEMENTS

In the name of Allah, Most Gracious, Most Merciful.

First and foremost, I am most thankful to The Almighty for granting me such a lifetime opportunity. A very thankful to my supervisor; Assoc. Prof. Dr. Wan Azmi Bin Wan Hamzah and my co-supervisor; Dr. Azri Bin Alias, for their guidance, and support from the initial to the final stage of the research study. The completion of this thesis would not have been possible without their review and correction of my mistakes, accompanied by the countless valuable suggestions.

My sincere thanks to all my labmates from Advanced Automotive Liquids Laboratory especially Miss Khamisah Binti Abdul Hamid, Miss Nurul Nadia Binti Mohd Zawawi, Mr. Mohamad Redhwan Bin Abd.Aziz and Mr. Sharif Bin Mohd Zaki that always advice and help me during my research study. Special thanks to Final Year Project (FYP) members of nanofluids research group for their good commitment, co-operation, inspirations and supports during this research. Not to forget to all members who helped me in many ways and made my stay at UMP pleasant and unforgettable.

I acknowledge my sincere indebtedness and gratitude to my late parents for their love, dream and sacrifice throughout my life. I acknowledge the sincerity of my sisters, who consistently support and give an unbelievable spirit for me to carry on my studies at UMP. It is a pleasure to thank my beloved family for their continuing encouragement and moral support whenever needed. I am sincerely grateful to my fellow friends for their willingness of going through all the years together here. Lastly, special thanks should be given to all of those who have supported me in any aspect during the completion of my research study.

Thank you all. Praise be to Allah.



UMP

ABSTRAK

Keperluan prestasi terma dalam sesuatu sistem telah meningkat sejak beberapa tahun kebelakangan ini dan mendorong para penyelidik untuk mencari kaedah baru bagi meningkatkan prestasi pemindahan haba. Salah satu kaedah adalah melalui gabungan dua atau lebih nanopartikel ke dalam bendalir asas untuk menghasilkan hibrid/komposit *nanofluid* yang boleh memberikan prestasi pemindahan haba yang lebih baik. Kecenderungan utama bagi prestasi sistem penyejukan yang sedia ada adalah untuk meminimumkan rintangan aliran di samping itu dapat meningkatkan pekali pemindahan haba. Selain itu, bendalir pemindahan haba konvensional seperti air, etilena glikol (EG) dan minyak mempunyai tahap penyerapan haba yang terhad kerana nilai sifat terma yang rendah terutamanya pekali kekonduksian haba. Oleh itu, adalah penting untuk membangunkan kaedah baru bagi meningkatkan prestasi sistem penyejukan. Tujuan eksperimen ini adalah untuk mengkaji sifat fizikal terma, prestasi pemindahan haba dan pekali geseran $\text{TiO}_2\text{-SiO}_2$ *nanofluid* untuk aliran gelora di dalam tiub bulat. $\text{TiO}_2\text{-SiO}_2$ *nanofluid* dihasilkan melalui kaedah dua langkah bagi kepekatan 0.5 hingga 3.0% dengan nisbah campuran nanopartikel 50:50 dan dicampurkan ke dalam bendalir asas iaitu campuran air/EG dengan nisbah isipadu 60:40. Pengukuran pekali kekonduksian terma dan kelikatan dinamik telah dilakukan pada julat suhu 30 hingga 80 °C dengan menggunakan *KD2 Pro Thermal Properties Analyzer* dan *Brookfield LVDV III Ultra Rheometer*. Eksperimen pemindahan haba dilakukan dalam julat nombor *Reynolds* dari 3,000 hingga 24,000 pada suhu 30, 50 dan 70 °C. Eksperimen dijalankan dalam keadaan fluks haba yang tetap. Nilai kekonduksian haba $\text{TiO}_2\text{-SiO}_2$ *nanofluid* telah ditambahbaik dengan peningkatan kepekatan dan suhu. Di mana peningkatan maksimum kekonduksian haba adalah 22.8% berbanding dengan bendalir asas manakala peningkatan sebanyak 7.5% berbanding dengan TiO_2 *nanofluid*. Pekali kelikatan pula menunjukkan peningkatan dengan pertambahan nilai kepekatan dan suhu. Pekali pemindahan haba untuk $\text{TiO}_2\text{-SiO}_2$ *nanofluid* telah meningkat dengan peningkatan kepekatan dan suhu. Peningkatan maksimum pekali pemindahan haba adalah 81% lebih tinggi daripada bendalir asas untuk kepekatan 3.0% pada suhu 70 °C. Di samping itu, pekali geseran $\text{TiO}_2\text{-SiO}_2$ *nanofluid* meningkat sedikit dengan pertambahan nilai kepekatan namun ianya boleh diabaikan. Model persamaan-persamaan Matematik telah dihasilkan menggunakan data eksperimen bagi pekali kekonduksian, pekali kelikatan dinamik, nombor *Nusselt* dan pekali geseran. Justeru itu, melalui ujikaji ini dapat disimpulkan bahawa prestasi termal-hidraulik $\text{TiO}_2\text{-SiO}_2$ *nanofluid* telah bertambah dengan lebih baik berbanding TiO_2 atau SiO_2 *nanofluid*. Oleh itu, disyorkan bagi aplikasi pemindahan haba dalam sistem dengan suhu operasi 70 °C menggunakan $\text{TiO}_2\text{-SiO}_2$ *nanofluid* dalam campuran air/EG (60:40) berkepekatan isipadu 3.0%.

ABSTRACT

The need of thermal performance in the system has increased in recent years and motivated the researchers to find a new method to enhance the heat transfer performance. One of the methods is the combination of two or more nanoparticles into a base fluid to form the nanofluids and it is known as hybrid/ nanofluids which can give better performance of heat transfer. The main challenge for the existing cooling system performance is to minimize the flow resistance while enhancing the heat transfer coefficients. Beside that, conventional heat transfer fluids including water, ethylene glycol and oil have limitation to absorb the heat due to their poor thermal properties values especially the thermal conductivity. Therefore, it is vital to develop techniques to enhance the performance of the cooling system. The aims of the experimental study are to investigate the thermo-physical properties, heat transfer performance and friction factor of $\text{TiO}_2\text{-SiO}_2$ nanofluids in a circular tube under turbulent flow. The $\text{TiO}_2\text{-SiO}_2$ nanofluids are prepared by using the two-step method for 0.5 to 3.0% volume concentration with nanoparticles mixture ratio of 50:50 and dispersed in a base fluid of water/EG mixture with 60:40 volume ratio. The measurements of thermal conductivity and dynamic viscosity were performed at a temperature range of 30 to 80 °C by using KD2 Pro Thermal Properties Analyser and Brookfield LVDV III Ultra Rheometer, respectively. The experimental determination of forced convection heat transfer is conducted in the Reynolds numbers range from 3,000 to 24,000 at a bulk temperatures of 30, 50 and 70 °C. The experiments are undertaken for constant heat flux boundary condition. The thermal conductivity of $\text{TiO}_2\text{-SiO}_2$ nanofluids was improved by increasing the volume concentration and temperature with 22.8% maximum enhancement compared with base fluid and 7.5% improvement compared with single TiO_2 nanofluids. The viscosity showed evidence of being influenced by nanoparticles concentration and nanofluids temperature. The heat transfer coefficient of $\text{TiO}_2\text{-SiO}_2$ nanofluids is enhanced with increasing of volume concentration and temperature. It was observed that the maximum enhancement of convective heat transfer is 81% higher than the base fluid for volume concentration and temperature of 3.0% and 70 °C, respectively. Furthermore, the friction factor of $\text{TiO}_2\text{-SiO}_2$ nanofluids is slightly increased with volume concentration. The regression correlation model was developed from the experimental result for the thermal conductivity, dynamic viscosity, Nusselt number and friction factor. Finally, it can be concluded that the thermal-hydraulic performance of $\text{TiO}_2\text{-SiO}_2$ nanofluids improved further as compared to single TiO_2 or SiO_2 nanofluids. Therefore, it is recommended to use $\text{TiO}_2\text{-SiO}_2$ nanofluids in water/EG mixture (60:40) for the heat transfer applications at temperature of 70 °C and 3.0% volume concentration.

TABLE OF CONTENT

DECLARATION	
TITLE PAGE	
ACKNOWLEDGEMENTS	ii
ABSTRAK	iii
ABSTRACT	iv
TABLE OF CONTENT	v
LIST OF TABLES	ix
LIST OF FIGURES	x
LIST OF SYMBOLS	xii
LIST OF ABBREVIATIONS	xiv
CHAPTER 1 INTRODUCTION	1
1.1 Background of Study	1
1.2 Problem Statement	4
1.3 Significance of Study	4
1.4 Research Objectives	5
1.5 Research Scopes	5
1.6 Thesis Overview	6
CHAPTER 2 LITERATURE REVIEW	7
2.1 Literature Overview	7
2.2 Background of Hybrid Nanofluids	7
2.3 Review on Preparation of Hybrid Nanofluids	8

2.4	Review on Stability and Characterization of Hybrid Nanofluids	13
2.5	Development and Current Progress of Hybrid Nanofluids	19
2.6	Thermo-physical Properties of Hybrid Nanofluids	21
2.6.1	Thermal Conductivity and Dynamic Viscosity	21
2.6.2	Density and Specific Heat	27
2.7	Heat Transfer Performance of Hybrid Nanofluids	27
2.8	Challenges and Potential Applications of Hybrid Nanofluids	30
2.9	Summary	32
CHAPTER 3 METHODOLOGY		33
3.1	Research Overview	33
3.2	TiO ₂ - SiO ₂ Nanofluids Preparation	37
3.2.1	Nanoparticles Materials and Base Dilutions	37
3.2.2	Procedure for Preparation	38
3.3	TiO ₂ - SiO ₂ Nanofluids Stability	40
3.3.1	Sedimentation Observation	40
3.3.2	Transmission Electron Microscope (TEM)	41
3.4	Thermo-physical Properties Measurement	42
3.4.1	TiO ₂ - SiO ₂ Nanofluids Thermal Conductivity	43
3.4.2	Procedure for Thermal Conductivity Measurement	43
3.4.3	TiO ₂ - SiO ₂ Nanofluids Dynamic Viscosity	44
3.4.4	Procedure for Dynamic Viscosity Measurement	45
3.4.5	Density and Specific Heat Relation	46
3.5	Experimental Setup for Forced Convection Heat Transfer	46
3.5.1	Data Logger Connection	48
3.5.2	Pressure Transducer Calibration	50

3.5.3	Test Section Setup	52
3.6	Experimental Procedures	53
3.7	Heat Transfer Analysis	54
3.7.1	The Rate of Heat Transfer	55
3.7.2	Dimensionless Parameters	56
3.7.3	Friction Factor and Pressure Drop	57
3.8	Uncertainty Analysis	58
CHAPTER 4 RESULTS AND DISCUSSION		61
4.1	Introduction	61
4.2	Stability of TiO ₂ -SiO ₂ Nanofluids	61
4.2.1	Sedimentation Observation	61
4.2.2	UV-Vis Spectrophotometer Evaluation	62
4.2.3	Characterization of TiO ₂ -SiO ₂ Nanofluids	63
4.3	Thermo-physical Properties	64
4.3.1	Properties Measurement Validation	65
4.3.2	Thermal Conductivity of TiO ₂ -SiO ₂ Nanofluids	66
4.3.3	Dynamic Viscosity of TiO ₂ -SiO ₂ Nanofluids	68
4.3.4	Properties Regression Equations	70
4.3.5	Comparison with Literature	72
4.3.6	Properties Enhancement Ratio	74
4.4	Convective Heat Transfer Experimental Study	75
4.4.1	Experimental Validation	75
4.4.2	Heat Transfer Coefficient and Nusselt Number	77
4.4.3	Friction Factor and Pressure Drop	82
4.5	Experimental Regression Correlation	85

4.5.1	Nusselt Number	85
4.5.2	Friction Factor	86
4.6	Thermal Hydraulic Performance	87
4.6.1	Nusselt Number Ratio	87
4.6.2	Friction Factor Ratio	88
4.6.3	Thermal Performance Factor	89
CHAPTER 5 CONCLUSIONS		91
5.1	Introduction	91
5.2	Conclusions	91
5.3	Recommendations for the Future Work	92
REFERENCES		93
APPENDIX A Ethylene Glycol		108
APPENDIX B Titanium Oxide (TiO₂) Nanofluids		109
APPENDIX C Silicon Oxide (SiO₂) Nanofluids		111
APPENDIX D Stirring Hotplate		113
APPENDIX E Ultrasonic Bath		114
APPENDIX F UV-Vis Spectrophotometer		115
APPENDIX G Transmission Electron Microscope (TEM)		117
APPENDIX H KD2 Pro Thermal Property Analyzer		119
APPENDIX I Brookfield LVDV III Ultra Rheometer		120
APPENDIX J Sample Calculation of the Effect of Tube Thickness		121
APPENDIX K Uncertainty of Parameter Analysis		122
APPENDIX L List of Publications		124

LIST OF TABLES

Table 2.1	Summary of preparation method for hybrid nanofluids	14
Table 2.2	Summary of stability, characterization, thermo-physical properties and instrumentations of hybrid nanofluids	17
Table 2.3	Summary of development and current progress	20
Table 2.4	Summary thermal conductivity and viscosity of hybrid nanofluids	26
Table 2.5	Summary of heat transfer performance and pressure drop of hybrid nanofluids	28
Table 3.1	Nanofluids concentration and nanoparticles properties	37
Table 3.2	Physical and chemical properties of ethylene glycol	38
Table 3.3	Description of each component in the test rig	47
Table 3.4	Terminal of Data Logger	50
Table 3.5	Calibration readings	51
Table 3.6	The uncertainty of parameter	59
Table 3.7	Uncertainty of Instrument	60

The logo for UWP (Universitas Widyadarmas Purwokerto) is a large, stylized letter 'W' shape. It is composed of four triangular sections meeting at a central point. The top-left and bottom-right sections are light blue, the top-right and bottom-left sections are a slightly darker blue, and the central point is white. The letters 'UWP' are printed in a bold, white, sans-serif font across the center of the 'W' shape.

UWP

LIST OF FIGURES

Figure 3.1	Experimental Flow Chart	36
Figure 3.2	Process of hybrid nanofluids preparation	40
Figure 3.3	UV-Vis Spectrophotometer	41
Figure 3.4	Transmission Electron Microscope (TEM) (Model Philips CM120)	42
Figure 3.5	KD-2 Pro Thermal Property Analyser equipment	43
Figure 3.6	KD2 Pro Thermal Properties Analyzer	44
Figure 3.7	Brookfield LVDV III Rheometer Component	45
Figure 3.8	Forced Convection Test Rig	47
Figure 3.9	Schematic Diagram of Test Rig	48
Figure 3.10	Data Logger Setup	49
Figure 3.11	Schematic Diagram for Data Logger	49
Figure 3.12	Pressure Transducer Calibration Setup	51
Figure 3.13	Calibration line for 1.0 psi pressure transducer	52
Figure 3.14	Test Section Setup	53
Figure 3.15	Process flow for experimental of forced convection test rig	54
Figure 4.1	Observation of TiO ₂ - SiO ₂ samples	62
Figure 4.2	Absorbance ratio for difference sonication time	63
Figure 4.3	TEM images (100 nm scales) for single type nanofluid of TiO ₂ and SiO ₂ , and TiO ₂ - SiO ₂ hybrid nanofluids for 1.0% volume concentrations	64
Figure 4.4	Comparison of water/EG (60:40) thermal conductivity and viscosity experimental results with ASHRAE (2009)	66
Figure 4.5	Thermal conductivity of TiO ₂ -SiO ₂ and single TiO ₂ nanofluids	68
Figure 4.6	Variation of dynamic viscosity of TiO ₂ -SiO ₂ and TiO ₂ nanofluids	70
Figure 4.7	Comparison of thermal conductivity ratio with Eq. (4.1)	71
Figure 4.8	Comparison of relative viscosity with Eq. (4.2)	72
Figure 4.9	Comparison of TiO ₂ -SiO ₂ nanofluids properties with the data from literatures	73
Figure 4.10	Variation of property enhancement ratio with concentration and temperature	74
Figure 4.11	Validation of Nusselt number	75
Figure 4.12	Validation of friction factor and pressure drop	77

Figure 4.13	Variation of the Nusselt number and heat transfer coefficient with Reynolds number of TiO ₂ -SiO ₂ hybrid nanofluids at various temperature.	80
Figure 4.14	Variations of experimental Nusselt number comparison and heat transfer enhancement	81
Figure 4.15	Friction factor in bulk temperature at 30, 50 and 70 °C	82
Figure 4.16	Variation of the Pressure drop with Reynolds number of TiO ₂ -SiO ₂ nanofluids at various temperatures	84
Figure 4.17	Comparison of Nusselt number regression model with experimental data	86
Figure 4.18	Comparison of friction factor regression model with experimental data	87
Figure 4.19	Variation of Nusselt number ratio with Reynolds number for different volume concentration of TiO ₂ -SiO ₂ nanofluids at various temperature	88
Figure 4.20	Variation of friction factor ratio with Reynolds number for different volume concentration of TiO ₂ -SiO ₂ nanofluids at various temperature	89
Figure 4.21	Variation of thermal performance factor with Reynolds number for TiO ₂ -SiO ₂ nanofluids at various temperatures	90

UMP

LIST OF SYMBOLS

A	Area
Abs	Absorbance
C_{bf}	Specific heat of base fluid
C_{hnf}	Specific heat of hybrid nanofluids
C_p	Specific heat of particles
D	Diameter
d	Diameter
d_i	Inner diameter
d_o	Outer diameter
ΔV	Additional volume
ΔP	Pressure drop
f	Friction factor
$f_{Blasius}$	Blasius friction factor
f_{exp}	Experimental friction factor
ϕ	Volume concentration
ϕ_1	Initial volume concentration
ϕ_2	Final volume concentration
φ	Volume fraction
h	Heat transfer coefficient
h_{exp}	Experimental heat transfer coefficient
I	Current
k	Thermal conductivity
k_{bf}	Thermal conductivity of base fluid
k_{hnf}	Thermal conductivity of hybrid nanofluids
L	Length
μ	Viscosity
μ_{bf}	Viscosity of base fluid
μ_{hnf}	Viscosity of hybrid nanofluids
\dot{m}	Mass flow rate
Nu	Nusselt number
Nu_{DB}	Nusselt number of Dittus-Boelter

Nu_{hnf}	Nusselt number of hybrid nanofluids
Nu_{exp}	Experimental Nusselt number
ω	Weight concentration
P	Pressure
P_{exp}	Experimental pressure drop
P_{theory}	Theoretical pressure drop
Pr	Prandtl number
Pr_{hnf}	Prandtl number of hybrid nanofluids
q	Rate of heat transfer
Q	Heat transfer
Re_{hnf}	Reynolds number of hybrid nanofluids
ρ	Density
ρ_{bf}	Density of base fluid
ρ_{hnf}	Density of hybrid nanofluids
ρ_{TiO_2}	Density of TiO_2
ρ_{SiO_2}	Density of SiO_2
T	Temperature
T_b	Bulk temperature
T_s	Surface temperature
v	Velocity
\bar{V}	Average Velocity
V_t	Voltage
V	Volume
V_1	Initial volume
V_2	Final volume
V_b	Bulk volume

LIST OF ABBREVIATIONS



ASHRAE	American Society of Heating, Refrigerating and Air-Conditioning
ASTM	American Society for Testing and Materials
Al ₂ O ₃	Aluminium Oxide
AuNP	Gold Nanoparticles
BG	Bio-Glycol
CCVP	Catalytic Chemical Vapor Deposition
CNT	Carbon Nano-tube
CHF	Critical Heat Flux
Cu	Copper
CuO	Copper Oxide
DI	Deionized Water
EG	Ethylene Glycol
Fe ₃ O ₄	Iron Oxide
FESEM	Field Emission Scanning Electron Microscopy
GO	Graphene Oxide
HEG	Hydrogen Exfoliated Graphene
HP	Horse Power
HTC	Heat transfer coefficient
LPM	Liter per minute
MWCNT	Multi Walled Carbon Nano-tube
NIOSH	National Institute for Occupational Safety and Health
TiO ₂	Titanium Oxide
TEM	Transmission Electron Microscopy
SiO ₂	Silicon Oxide
SiC	Silicon Carbide
W	Water
ZnO	Zinc Oxide
ZrO	Zirconium Oxide

CHAPTER 1

INTRODUCTION

1.1 Background of Study

Currently, the demand of heat transfer is increasing due to the evolution of the industry that involves the heating and cooling processes. The enhancement in heat transfer are needed in order to reduce the processing time, save energy, increase the thermal rating and lengthen the working life of the system (Sivashanmugam, 2012). Generally, the heat transfer enhancement methods are classified into three categories which are (i) active method, (ii) passive method, (iii) compound method (Ahuja, 1975; Dewan et al., 2004; Mahesh et al., 2016; Sonawane et al., 2016). The active method requires external energy to enhance the heat transfer such as mechanical aids, surface vibration, and electrostatic fields whereas passive method does not require any external energy. The heat transfer performance of the passive method can be increased by introducing rough surfaces, extended surfaces, coiled tubes, displaced enhancement devices, swirl flow devices and additives for gasses or liquids. The compound method or also known as the hybrid method is a combination of active and passive methods. This method has a limitation on application due to its complicated design. However, the previous study shows that passive method is the best in augmenting heat transfer (Dewan et al., 2004; Sonawane et al., 2016).

Heat transfer fluid is very important for use in heat transfer systems such as for applications in automotive, buildings, and industrial processes (Choi & Stephen, 1995). The best methods to develop the heat transfer efficiency is improving the thermal conductivity of the working fluids by dispersing particles. The particles can be categorized into two groups which are metallic and non-metallic (Choi & Stephen, 1995). Conventional heat transfer fluids such as water, ethylene glycol and oil used in forced convection heat transfers has relatively poor thermal conductivity when

compared with solid particles. Since solid particles has higher thermal conductivity than conventional fluids, through adding small portions of solid particles in the fluids, it is likely to enhance the thermal properties especially thermal conductivity and further improve the heat transfer performance.

Initially, the addition of micron-sized particles as an additive in a base fluid is proposed for the improvement of heat transfer. The micron-sized solid particles caused some problems such as clogging, stability problems as it settles down rapidly, erosion of heat transfer devices and significant pressure drop increase due to large particle size (Das et al., 2006). Therefore, the researchers have shown more interest in nanometer-sized particles for novel dispersion in the base fluids. These fluids are known as “nanofluids”. The term was introduced by Choi and Stephen (1995). Nanofluids materialized from the dispersion of nanoparticles in a conventional working fluid such as water, ethylene glycol and oil with principal dimensions of less than 100 nm in a liquid (Azmi et al., 2013a; Azmi et al., 2016d; Azmi et al., 2010; Choi & Stephen, 1995; Duangthongsuk & Wongwises, 2008). In the past decades, the previous investigations showed that the nanofluids have greatly improved the thermo-physical properties such as thermal conductivity and dynamic viscosity (Sundar et al., 2013a; Sundar et al., 2013c; Sundar et al., 2012). The nanofluids have a potential for wide applications in industries because of some features such as (i) high thermal conductivity and large surface area that improves the rate of heat transfer, (ii) pressure drop is minimum because of small-sized particles, (iii) most effective in rapid heating and cooling systems (Hatwar & Kriplani, 2014).

Studies were conducted by Sundar et al. (2013a) and Zakaria et al. (2015) for the thermal conductivity of nanofluids in a mixture of water and ethylene glycol base fluid. In their study, the researchers found that the temperature and volume concentrations strongly affected the enhancement of thermal conductivity. In another study, it was stated that the other factors that contributed to the improvement in effective thermal conductivity are particle size and stability of nanofluids (Javadi et al., 2013a; Paul et al., 2011). Most of the previous researchers agreed that the best performance of nanofluids can be achieved in a combination of higher thermal conductivity and lower dynamic viscosity (Azmi et al., 2014b; Garg et al., 2008). Azmi et al. (2014b) found a decreasing pattern for the dynamic viscosity using TiO_2 and SiO_2

water-based nanoparticles up to 3.0% concentration at 30°C. They observed that the viscosity of TiO₂ nanofluids is larger than SiO₂ nanofluids. Meanwhile, the maximum improvement of heat transfer of TiO₂ and SiO₂ nanofluids are attained for 1.0% volume concentration up to 26% enhancement and 3.0% concentration up to 33% enhancement, respectively.

In a continuation of nanofluids research, a few studies have recently discussed the topic of hybrid or composite nanofluids (Hemmat Esfe et al., 2015d; Moghadassi et al., 2015; Sarkar et al., 2015; Suresh et al., 2012). The hybrid and composite nanofluids are considered the extension of research work for single nanofluids, which can be prepared through the combination of two or more dissimilar nanoparticles-either in a mixture or composite form dispersed in base fluids (Sarkar et al., 2015). A hybrid and composite material is an element that combines the chemical and physical properties. A hybrid and composite material consisting of carbon nanotubes (CNTs) have been used in electrochemical sensors, bio-sensors, and nanocatalysts, however these nanomaterials are still not used as an hybrid and composite type of nanofluids as such (Gou et al., 2008). The purpose of synthesizing hybrid and composite nanofluids is to improve the properties of single materials where great enhancement in thermal properties or rheological properties might be achieved. Furthermore, hybrid nanofluids are expected to achieve better thermal performance compared to a single type of nanofluids. Until recently, the convective heat transfer study by using hybrid and composite nanofluids either experimental or numerical, are very limited. Suresh et al. (2012) studied on the effect of Al₂O₃-Cu/water hybrid nanofluids in heat transfer. They found that the Nusselt number was improved up to 13.56% higher than the base fluid. This implies that the rate of heat transfer can be improved with addition of copper nanoparticles to Al₂O₃/water single nanofluids.

Researchers used various types of nanofluids to improve the heat transfer performance (Agarwal et al., 2015; Deepak Selvakumar & Dhinakaran, 2016; Kumar & Sonawane, 2016; Mehmood & Iqbal, 2016; Naghash et al., 2016; Saleh et al., 2014). They investigated the thermo-physical properties of nanofluids and its relation to the heat transfer and friction parameter, namely heat transfer coefficient and pressure drop, respectively. Primarily, the investigation on thermal conductivity and viscosity of hybrid nanofluids is essential to provide more information and understanding on its

behaviour towards heat transfer performance. Therefore, in the present work, the nanofluids consisting of $\text{TiO}_2\text{-SiO}_2$ nanoparticles were investigated at various volume concentrations and temperatures for heat transfer performance.

1.2 Problem Statement

The main concern for the existing cooling system performance is to reduce resistance flow and at the same time to enhance the heat transfer coefficients. Thus, it is important to find the best techniques for the enhancement of cooling system performance. Various techniques can be used for the improvement of cooling system performance. The use of nanofluids was considered as the most effective technique for heat transfer augmentation (Hormozi et al., 2016). Conventional heat transfer fluids including water, ethylene glycol and oil has limitation to absorb the heat due to their poor thermal properties value especially the thermal conductivity value. This circumstance lowers the overall thermal efficiency of any type of cooling system. Although the thermal properties and performance of heat transfer for the base fluid was improved by using single nanofluid, however some of the nanoparticles still have relatively low thermal properties. Recently, the researchers tried to enhance the nanoparticles properties value. For this reason, hybrid nanofluids are developed to enhance the performance of heat transfer fluids (Afrand, 2017). Hence, this study is focused on the experimental investigation of thermo-physical properties of hybrid nanofluids as a thermal fluid for heat transfer applications. The concentration of hybrid nanofluids and their base fluids including water and ethylene glycol are investigated in this study. Therefore, the fundamental study of hybrid nanofluids on thermo-physical properties and heat transfer performance are necessary for applications in the cooling system (Sundar et al., 2017). At the end of the study, it is expected to establish the best working conditions (temperature, and concentration) using hybrid nanofluids.

1.3 Significance of Study

This study could provide information on the limitation of conventional heat transfer fluids to absorb the heat. The research was motivated by a need to improve the thermo-physical properties of nanofluids by combining two types of nanoparticles in water/ethylene glycol mixture as a base fluids. Furthermore, this study also would be a benchmark for application of forced convection heat transfer by using $\text{TiO}_2\text{-SiO}_2$

nanofluids at different concentrations and temperatures. The findings from this study also will give beneficial for future application since nanofluids had been used in industrial application such as automotive, solar energy and refrigeration system. Hybrid nanofluids are a new topic in nanofluids and still under early stage. The hybrid nanofluids are expected to achieve higher thermal conductivity and better heat transfer performance compared to single nanofluids. Consequently, this study can provide a reference to show potential of hybrid nanofluids for various engineering applications.

1.4 Research Objectives

The present research work is aimed to formulate the hybrid nanofluids for the combination of $\text{TiO}_2\text{-SiO}_2$ nanoparticles in water/EG mixture. Therefore, the determination of thermo-physical properties of $\text{TiO}_2\text{-SiO}_2$ nanofluids are essential for the investigation of thermal-hydraulic performance at various operating temperatures.

Hence, the main objectives of this study are:

- i. To evaluate the thermal conductivity and dynamic viscosity of $\text{TiO}_2\text{-SiO}_2$ nanofluids.
- ii. To evaluate the thermal-hydraulic performance of $\text{TiO}_2\text{-SiO}_2$ nanofluids at different working temperatures.

1.5 Research Scopes

The scopes of this study are:

- i. The hybrid nanofluids are prepared using two-step method for combination of TiO_2 and SiO_2 nanoparticles (50:50 volume ratio) in base fluids of water-ethylene glycol mixture (60:40 volume ratio) at volume concentrations of 0.5 to 3.0%.
- ii. The thermal conductivity and dynamic viscosity is conducted for $\text{TiO}_2\text{-SiO}_2$ nanofluids under temperatures in the range of 30 to 70 °C whereas specific heat capacity and the density were used the mixture relation from the previous study.
- iii. The forced convection heat transfer experiment is conducted using a modified version of the existing experimental setup at working temperatures of 30, 50 and

70 °C under a fully developed turbulent region with a constant heat flux condition of 7,955 W/m².

- iv. The heat transfer performance (heat transfer coefficient and pressure drop) was evaluated with the measured nanofluids properties under turbulent flow Reynolds number from 3,000 to 24,000.
- v. The development of regression equations for Nusselt number and friction factor of TiO₂-SiO₂ nanofluids using the experimental data and useful in the design of thermal systems.

1.6 Thesis Overview

Chapter 1 explains the background of study from previous literature, the objectives and scopes of the study. Review of the literature in Chapter 2 provides information on the related studies which including the method of preparations, the characterizations and the experimental investigations by various investigators. Further, the experimental setup and the comprehensive procedures are presented in the Chapter 3. Chapter 4 presents the results for the experimental works and comprehensive discussion to answer the objectives of the present study. Finally, Chapter 5 concludes the entire contents of the thesis and to provide suggestions and recommendations for improvement in the future research.

CHAPTER 2

LITERATURE REVIEW

2.1 Literature Overview

This chapter summarizes the previous research works related to the method of hybrid nanofluids preparation, stability and characterization, development and current progress. Moreover, the thermo-physical properties and performances in term of heat transfer, pressure drop and friction factor of hybrid nanofluids are reviewed. Some reviews of the challenges and applications of hybrid nanofluids was also discussed. Recent researches showed that the hybrid nanofluids improved the performance of the single nanofluids. Various studies of hybrid nanofluids were carried out to investigate the thermal conductivity whereas the other thermo-physical properties such as viscosity, density and specific heat are limited in the literature. Thus, comprehensive studies on the other thermo-physical properties of the hybrid nanofluids are required for future applications in any engineering system. The chapter also reviewed the heat transfer performance, the challenges and the potential applications of hybrid nanofluids. Besides that, the performance of the hybrid nanofluids are also discussed for heat transfer, pressure drop and friction factor. Lastly, the challenges and several applications of hybrid nanofluids were also discussed.

2.2 Background of Hybrid Nanofluids

Nanofluids are defined as the dispersion of metallic or non-metallic nanoparticles with principal dimensions of less than 100 nm in a liquid. From previous investigations, the efficiency of heat transfer greatly enhances the thermo-physical properties such as thermal conductivity, thermal diffusivity, viscosity and convective heat transfer coefficients of nanofluids that have been dispersed in a continuous medium such as water, ethylene glycol, and engine oil (Wong & De Leon, 2015).

Keblinski et al. (2005) conducted investigations on thermal conductivity of Cu nanoparticle and found that the thermal conductivity for ethylene glycol and oil increased with the dispersion of less than 1% volume concentration of Cu nanoparticles. Different studies by various researchers were conducted with nanofluids prepared in different base fluids and concentrations using metal or metal oxide nanoparticles such as Al₂O₃ (Aluminium oxide), Cu (Pure copper), CuO (Copper oxide), Fe₃O₄ (Iron oxide), SiC (Silicon carbide), SiO₂ (Silicon dioxide), TiO₂ (Titanium oxide), ZnO (Zinc oxide), and ZrO₂ (Zirconium dioxide) (Azmi et al., 2016c; Azmi et al., 2014b; Sundar et al., 2013a; Yu et al., 2012; Zamzamian et al., 2011).

Hybrid nanofluids are considered as an extension of nanofluids in research work, which can be prepared by suspending two or more dissimilar nanoparticles either in mixture or composite form in the base fluids (Sarkar et al., 2015). A hybrid material is a substance that combines the physical and chemical properties. Hybrid material consisting of carbon nanotubes (CNTs) have been used in electrochemical-sensors, bio-sensors and nanocatalysts, but the use of these hybrid nanomaterials in nanofluids has not developed as such (Gou et al., 2008). The main objective of synthesizing hybrid nanofluids is to improve the properties of single materials where great enhancement in thermal properties or rheological properties can be achieved. Furthermore, the hybrid nanofluids are expected to achieve better thermal conductivity compared to a single type of nanofluid. Investigations on hybrid nanofluids, either experimental or numerical, are very limited. Until recently, only two review papers on hybrid nanofluids have been done by Sarkar et al. (2015) and Sidik et al. (2016). However, both papers concentrated on the development and the recent progress and the review was only limited to the hybrid nanofluids.

2.3 Review on Preparation of Hybrid Nanofluids

In order to increase the stability of the nanofluids and to minimize the agglomeration of nanoparticles, the one-step method was chosen. The one-step method is a process of synthesising the nanoparticles and simultaneously dispersing them in a base fluid. However, this method is not practical for industrial functions and only applicable for low vapour pressure host fluids (Hatwar & Kriplani, 2014). The other method of nanofluid preparation is known as the two-step method. There are two processes in this method, which are (i) synthesis of the nanoparticles in the powder

form (ii) dispersion of the nanoparticles into the base fluids to form a stable and homogeneous solution (Hatwar & Kriplani, 2014). Most nanofluids and nanolubricants used oxide particles and carbon nanotubes and are produced by the two-step method (Azmi et al., 2012; Baby & Ramaprabhu, 2011; Baby & Ramaprabhu, 2013; Kumaresan et al., 2013; Kumaresan & Velraj, 2012). This method is usually produced in large scales because nanopowder synthesis techniques have already been scaled up to industrial production levels. However, the challenges of using the two-step method in preparing nanofluids are the agglomerations and that the nanoparticles tend to settle down quickly (Hatwar & Kriplani, 2014; Yu & Xie, 2012).

The two-step method is the more dominant method compared to the one-step method. There are three types of base fluids used in preparing the hybrid solution, which are water and ethylene glycol for hybrid nanofluids whereas oil based fluids and lubricant for hybrid nanolubricants. A study by Jana et al. (2007) used CNT-AuNP hybrid nanofluids. First, they used different volume fractions of CNT added into the water to produce different volume fractions of CNT suspensions whereas AuNP was added to DI water to produce AuNP suspensions. After that, AuNP suspensions were added to different volume fractions of CNT suspensions to achieve CNT-AuNP suspensions. Laurate salt and DI water were added in CuNP to form CuNP suspensions. Laurate salt acted as a catalyst to enhance the stability of CuNP suspensions. Then, CNT suspensions were added in CuNP suspensions to reduce the sedimentation of CuNP and improve the stability.

Ho et al. (2010, 2011) prepared the PCM suspensions using interfacial polycondensation and emulsion technique. The PCM suspensions were formulated by mixing appropriate quantities of MEPCM particles with ultra-pure Milli-Q water in a flask. They then dispersed the nanoparticles in the solution using an ultrasonic vibration bath. The water based hybrid nanofluids was set up by scattering Al_2O_3 nanoparticles at different mass fractions in ultra-pure Milli-Q water by utilizing an attractive stirrer. Baby and Ramaprabhu (2011) synthesized MWNT by catalytic chemical vapour deposition (CCVD) and hydrogen exfoliated graphene from graphite oxide (GO). The as-synthesized HEG was not solvent in water due to the exfoliation of oxygen containing functional groups from the specimen; making it hydrophobic. So as to make it hydrophilic, HEG and MWNT was functionalized in H_2SO_4 and HNO_3 acid medium.

The nanostructure of the mixture was set up by mixing the same amounts of *f*-MWNT and *f*-HEG in a specified volume of water after functionalization. Further, the arrangement was ultrasonicated for 1 hour and stirred for another 24 hours. The final mixture was separated, dried and utilized to produce nanofluids. The same was done for other different combinations of Ag/HEG/MWNT to form hybrid nanofluids.

Botha et al. (2011) prepared nanofluids containing silica using the one-step method. The magnetic stirrer was used to mix the silica to the base fluids at a temperature of 130 °C. Silver nanoparticles supported on silica were prepared correspondingly by mixing the silver nitrate and silica to the base liquid. The oxidation of oil is achieved on high temperature and the reductions of Ag⁺ ions to Ag particles by electron transfer reaction, the temperature was thus increased to 130 °C. Suresh et al. (2011, 2012) synthesized nanocrystalline alumina-copper hybrid (Al₂O₃-Cu) powder by the thermochemical method which consisted of the following stages; (i) Spray-drying, (ii) Oxidation of precursor powder, and (iii) Reduction by hydrogen and homogenisation. The water solution of soluble nitrates of copper and aluminium, Cu (NO₃)₂·3H₂O and Al (NO₃)₃·9H₂O was prepared with 90:10 of alumina and copper oxide in the powder mixture.

Baghbanzadeh et al. (2012) synthesized the hybrid nanostructures using the wet chemical method. Graphitic surfaces of carbon nanotubes were activated in order to achieve synthesis of CNT-based nano hybrid effectively. This is because the graphitic surfaces are chemically inactive. At first, sodium silicate was added to distilled water and then functionalized MWCNTs were added to the previous solution. The new suspension was sonicated by an ultrasonic bath to disperse the suspension with functionalized MWCNTs. CTAB was added to distilled water and dimethylformamide and mixed using a magnetic stirrer. The mixture was then added to the first suspension. After the response, the products were separated and washed by ethanol and distilled water. The gray products were dried in a vacuum oven at 60 °C. Surfactant and impurities were removed from the products. A study by Abbasi et al. (2013) used hybrid γ -Al₂O₃/MWCNT hybrid nanofluids. They prepared the hybrid nanofluids using a solvothermal process in ethanol. By completely dissolving aluminium acetate powder in ethanol, the pure MWCNTs and functionalized MWCNTs were added to this suspension. The mixture was then dispersed using an ultrasonic water bath to avoid

particle agglomeration. Finally, the mixture was placed under vacuum (50 cm Hg) at room temperature and an ammonia solution was slowly added to the mixture.

Other processes of preparing hybrid nanofluid is presented by Bhosale and Borse (2013). The samples of CuO and Al₂O₃ were mixed in distilled water by adding different concentrations of nanofluids. The number of reading for CHF enhancement was taken to analyse the effect of Nichrome wire size on CHF value. Then the reading for Nichrome wire size and distilled water for different concentrations of Al₂O₃-CuO hybrid nanofluids were taken. Madhesh et al. (2014) employed a method involving four steps of facile preparation of the copper/titania hybrid nanocomposite (HyNC) which are: (i) Ultrasonic dispersion of an aqueous solution containing titania, (ii) Intense stirring and mixing of a copper acetate aqueous solution, containing ascorbic acid and sodium borohydride reducing agents with the prepared titania aqueous solution and ambient pressure for subsequent production of HyNC colloids, (iii) Washing and filtration of the HyNC colloids followed by vacuum drying, (iv) Ultrasonic re-dispersion of the prepared HyNC powder into the base fluid for different volume concentrations.

Sundar et al. (2014) used an in-situ method to prepare nanocomposite samples. At first, carboxylated-MWCNT was dispersed in distilled water under magnetic stirring. Then, FeCl³⁺/FeCl²⁺ salts were added in a molar ratio of 2:1 and stirred. After that, the dispersion of all the iron chlorides were added into the distilled water and simultaneously added to the aqueous sodium hydroxide solution. The solutions were stirred continuously. The reaction is completed once the colour of the solutions turned black. Hemmat Esfe et al. (2015b) prepared the nanofluid by dispersing nanoparticles into the base fluid. The suspension was stabilized with three methods, which are the addition of surface activators (surfactants), changing the pH value, and using ultrasonic vibrations. XRD was used to determine the size of nanoparticles.

Hemmat Esfe et al. (2015d) prepared the hybrid nanofluid of Cu/TiO₂-water/EG by the two-step method. Firstly, the nanoparticles were dispersed into different concentrations using a mechanical mixture. The Cu and TiO₂ nanoparticles were mixed using a magnetic stirrer in order to achieve a stable solution of nanofluids. The solution was sonicated using an ultrasonic processor. Consequently, the agglomeration of nanoparticles reduced and prevented the sedimentation in the solution. Yarmand et al.

(2015) chose the acid treatment for functionalization of graphene nanoplatelets (GNP) hydrophilic. The acid treatment process was conducted by dispersing GNP in a 1:3 ratio of HNO_3 and H_2SO_4 solution under bath-ultrasonication. Next, GNP was washed several times by DI water and then dried in an oven. The solution of ammonia-silver was prepared by adding drop ammonia to silver nitrate solution until fully reacted and the silver colour disappeared. The $\text{Ag}(\text{NH}_3)_2\text{OH}$ solution was mixed into the functionalized GNP solution. The nanofluids were stable and no sedimentations occurred up to 60 days.

Afrand et al. (2016b) investigated SiO_2 -MWCNTs/SAE40 hybrid nanofluid using the two step method. The structural properties of the dry MWCNTs and SiO_2 nanoparticles were measured using X-ray diffraction. The masses of MWCNTs, SiO_2 nanoparticles and engine oil were determined by a sensitive electronic balance. Then, the nanoparticles were dispersed in the oil and allowed to mix with a magnetic stirrer. The suspension was then proceeded using an ultrasonic processor to achieve stable condition. The nanofluids were observed to be have good stability and no sedimentation occurred. The same process was repeated for Fe_3O_4 -Ag/EG hybrid nanofluids by Afrand et al. (2016b). Asadi and Asadi (2016) also used the two-step method in their study of MWCNT/ZnO-oil hybrid nanofluid. After dispersing nanoparticles into various volume fractions, the MWCNT and ZnO nanoparticles were mixed in the base fluid using a magnetic stirrer to obtain stable nanofluids. The suspension was inserted into an ultrasonic processor to achieve a superb dispersion and to breakdown the agglomeration of nanoparticles.

Ramachandran et al. (2016) employed the two step method to prepare the hybrid nanofluid. They used Al_2O_3 and CuO nanoparticles and dispersed in a base fluid of deionized water. In order to achieve the stability of nanofluids, it was sonicated in an ultrasonic processor. Another researcher that used the two step method was Harandi et al. (2016). The dry *f*-MWCNTs and Fe_3O_4 nanoparticles were mixed in equal volumes. This mixture was dispersed in ethylene glycol with solid volume fractions. In order to attain a characterization of the sample, the structural properties of dry MWCNTs and Fe_3O_4 nanoparticles were measured using X-ray diffraction. To accomplish an appropriate dispersion, after magnetic stirring, every sample went through a sonication

process. All specimens prepared were perceived to have good stability and no sedimentation was seen in the time before the analysis.

Soltani and Akbari (2016a) prepared hybrid nanofluids with ethylene glycol as the base fluid. The mixing process was first implemented using a magnetic stirrer to mix the MgO-MWCNTs/EG into the base fluid. The suspensions then went through the sonication process using an ultrasonic processor to breakdown the agglomeration between the particles and to achieve a stable suspension. The pH measurement using the pH meter were also used as an indicator of the nanofluid stability. In a study by Yarmand et al. (2016b), the graphene oxide (GO) was dispersed in distilled water by sonication. GO and carbon samples were independently added to aqueous KOH solution. The mass ratio of KOH/carbon and KOH/GO was 4:1. The carbon sample and GO sample were combined, stirred and dried at 50 °C. The mixture was placed in a ceramic boat and kept in a heater tube. The mixture was heated and the obtained nanocomposite was washed with distilled water and HCl a few times to evacuate the impurities and then dried at a temperature of 60 °C. This sample was known as activate carbon/graphene (ACG) and used to make nanofluids. Table 2.1 summarized the methods of preparing the hybrid nanofluids.

2.4 Review on Stability and Characterization of Hybrid Nanofluids

Nanoparticles are often hydrophobic and therefore cannot typically be dispersed in most heat transfer fluids such as water or ethylene glycol without surface treatments, dispersants or surfactants (Chen & Xie, 2010; Xie et al., 2003). Furthermore, without these special treatments, the nanoparticles would most certainly agglomerate, thereby creating other problems such as channel clogging and reduction in thermal conductivity of the mixture (Yu & Xie, 2012). Surfactants or dispersion agents are therefore commonly used in nanofluids. Although they are beneficial for stabilizing the suspension, they may also create certain problems for heat transfer mediums. There are three effective methods for stabilizing the suspension namely (i) addition of surface activators (surfactants), (ii) control of the pH value, and (iii) use of ultrasonic vibrations (Duangthongsuk & Wongwises, 2008; Hemmat Esfe et al., 2015b).

Table 2.1 Summary of preparation method for hybrid nanofluids

Authors	Base fluids	Materials	Methods
Jana et al. (2007)	Water	CNT-CuNP/CNT-AuNP	two-step method
Gou et al. (2008)	Water	MWNT-Silica	two-step method
Ho et al. (2010)	Water	Al ₂ O ₃ -MEPCM	two-step method
Baby and Ramaprabhu (2011)	Water, EG	MWNT-HEG	two-step method
Botha et al. (2011)	Transformer oil	Silver-Silica	one-step method
Han and Rhi (2011)	Water	Ag-Al ₂ O ₃	one-step method
Ho et al. (2011)	Water	Al ₂ O ₃ -MEPCM	two-step method
Suresh et al. (2011)	Water	Al ₂ O ₃ -Cu	two-step method
Baghbanzadeh et al. (2012)	Water	Silica-MWCNT	two-step method
Selvakumar and Suresh (2012b)	Water	Al ₂ O ₃ -Cu	two-step method
Suresh et al. (2012)	Water	Al ₂ O ₃ -Cu	two-step method
Abbasi et al. (2013)	Gum arabic(GA) + Water	MWCNT/g-Al ₂ O ₃	two-step method
G.H.Bhosale and S.L.Borse (2013)	Water	Al ₂ O ₃ -CuO	one-step method
Madhesh et al. (2014)	Water	Cu-TiO ₂	two-step method
Sundar et al. (2014)	Water	MWCNT-Fe ₃ O ₄	two-step method
Hemmat Esfe et al. (2015a)	Water	Ag-MgO	two-step method
Hemmat Esfe et al. (2015d)	Water, EG	Cu-TiO ₂	two-step method
Mechiri et al. (2015)	Vegetable oils	Cu-Zn	two-step method
Takabi and Shokouhmand (2015)	Water	Al ₂ O ₃ -Cu	two-step method
Yarmand et al. (2015)	Water	GNP-Ag	two-step method
Afrand et al. (2016a)	SAE40	SiO ₂ -MWCNTs	two-step method
Asadi and Asadi (2016)	engine oil	MWCNT-ZnO	two-step method
S.Harandi et al. (2016)	EG	F-MWCNTs-Fe ₃ O ₄	two-step method
Soltani and Akbari (2016b)	EG	MgO-MWCNT	two-step method
Yarmand et al. (2016a)	EG	Biomass carbon-graphene oxide	two-step method

In order to stabilize the hybrid nanofluids, the specific equipment and established approaches for stability were used for dispersing the hybrid nanofluids in base fluids. The main reason for hybrid nanofluids to achieve a stable suspension is to avoid agglomeration and sedimentation. Zeta potential, spectrometer, diffractometer, ultrasonic bath and pH meter are some examples of stability instruments and approaches that were used by many (Abbasi et al., 2013; Afrand et al., 2016b; Asadi & Asadi, 2016; Baby & Ramaprabhu, 2011; Baghbanzadeh et al., 2012; Botha et al., 2011; Gou et al., 2008; Harandi et al., 2016; Hemmat Esfe et al., 2015b; Hemmat Esfe et al., 2015d; Jana et al., 2007; Li et al., 2009b; Madhesh et al., 2014; Selvakumar & Suresh, 2012a; Soltani & Akbari, 2016a; Suresh et al., 2011, 2012; Yarmand et al., 2015; Yarmand et al., 2016b). Since the particle size of nanofluids are very small with less than 100 nm, FESEM and SEM analysis were done by several researchers in literatures (Abbasi et al., 2013; Baby & Ramaprabhu, 2011; Baghbanzadeh et al., 2014; Botha et al., 2011; Gou et al., 2008; Jana et al., 2007; Li et al., 2009b; Madhesh et al., 2014; Selvakumar & Suresh, 2012a; Yarmand et al., 2015; Yarmand et al., 2016b). The surface and characteristics morphology were seen with these analyses where the size of nanoparticles were defined. Various analysts have considered and reported the types of equipment for measuring the thermal conductivity, density, viscosity and specific heat of the hybrid nanofluids. Understanding the physical and thermal properties of nanofluid is vital before utilizing hybrid nanofluids as a part of practical applications. There are a few well-known imperative types of equipment for nanofluid's thermo-physical properties evaluation, which are commonly used by various researchers.

Various researchers measured the thermal conductivity of hybrid nanofluids using KD2 Pro thermal properties analyser (Abbasi et al., 2013; Harandi et al., 2016; Hemmat Esfe et al., 2015b; Hemmat Esfe et al., 2015d; Suresh et al., 2011, 2012; Yarmand et al., 2015; Yarmand et al., 2016b). The KD2 Pro is a battery-worked, menu - driven device that measures thermal conductivity and resistivity, volumetric specific heat capacity and thermal diffusivity. It comprises a handheld microcontroller and sensor needles that contained both a heating component and a thermistor. The controller module contains a battery, a 16-bit microcontroller/AD converter, and force control hardware. The sensor needle utilized was KS-1, which is made of stainless steel with a length of 60 mm and a diameter of 1.3 mm and nearly approximating the interminable line heat source which gives minimum aggravation to the specimen during each

measurement that takes 90 s/cycle. The KD2 Pro thermal property analyser was used by Baby and Ramaprabhu (2011) and Selvakumar and Suresh (2012a) in their thermal conductivity measurements. The test sensor utilized for these estimations was 6 cm long and 1.3 mm in distance across. In consideration of the temperature impact on the thermal conductivity of the nanofluids, a thermostat bath was utilized. In another paper, Madhesh et al. (2014) used the NanoFlash equipment for the measurement of thermal conductivity of hybrid nanofluids. The precision of the equipment was $\pm 3\%$ and the range of thermal conductivity estimation varied from 0.1 W/m K to 2000 W/m K.

Viscosity is another important parameter of thermo-physical properties of hybrid nanofluids. The investigations were done by various researchers as stated in previously published literature (Afrand et al., 2016b; Hemmat Esfe et al., 2015b; Soltani & Akbari, 2016a; Suresh et al., 2011, 2012). The viscosity of the nanofluids was measured using the Brookfield cone and plate viscometer (LV DV-I PRIME C/P) equipped with a 2.4 cm 0.8° cone. The cone is associated with the shaft drive while the plate is mounted in the sample container. The shaft utilized was CPE-40, which can be utilized for tests as a part of the viscosity range of 0.3–1028 cP. A gap of 0.013 mm between the cone and the plate is considered during the measurements. As the shaft is turned, the thick drag of the fluids against the axle is measured by the diversion of the aligned spring. The axle speed accessible with this viscometer falls in the range of 0 to 100 rpm and the shear rate is 0 to 750 s^{-1} . With a specific end goal to guarantee the precision of the estimations, the viscosity was recorded again by (i) taking the same amount of fluid specimen (0.5 to 2 ml), (ii) keeping up the same torque required to turn the shaft (10 to 100% for all paces of pivots) and (iii) keeping up a unistrucre gap of 0.013 mm between the cone and the plate inside on which the test fluids are set (utilizing the electronic gap modifying highlight expert provided with the viscometer). Furthermore, Yarmand et al. (2016b) used a rheometer (Physica MCR, Anton Paar) in measuring the viscosity of EG and ACG/EG hybrid nanofluids. The rotational rheometer comprises a moving tube shaped plate and a stationary barrel shaped surface, which are parallel with a small gap.

A different viscometer (Viscometer, CAP 2000+) was used by Afrand et al. (2016b) and Asadi and Asadi (2016) to measure the viscosity of the hybrid nanofluids. The viscometer was set at medium to high shear rate instrument with Cone Plate

geometry and coordinated temperature control of the test material. The measurements were performed at the shear rate scope of 667 to 6667 s⁻¹. The scope of exactness and repeatability of the viscometer were respectively ±2.0% and ±0.5% of the full scale consistency territory. Prior to the estimations, the viscometer was aligned with the motor oil (SAE40) at room temperature. All measurements were repeated at various shear rates for every volume concentration and temperature to ensure the consistency in reading. In the density evaluation of hybrid nanofluids, Yarmand et al. (2016b) measured the densities of EG and hybrid nanofluids with the Mettler Toledo DE-40 density meter. The precision of density estimation is 0.0001 g/cm³. For each temperature and test sample, the estimations were recorded three times. For evaluation of specific heat, Yarmand et al. (2016b) measured the specific heat of the base liquid and the hybrid nanofluids using a differential scanning calorimeter (DSC 8000, Perkin Elmer) with a precision of ±1.0%. The summary of stability, characterization, thermo-physical properties and instrumentations of hybrid nanofluids are shown in Table 2.2.

Table 2.2 Summary of stability, characterization, thermo-physical properties and instrumentations of hybrid nanofluids

i. Stability Instruments			
Instruments	Type / Model	Measurement	Authors
Spectrophotometer	UV-vis-NIR / Cary 500 UV-vis-NIR / ESCALAB-MKII / Bruker FT-IR / WITEC alpha 300 / Perkin-Elmer 330	Stability	(Baby & Ramaprabhu, 2011; Botha et al., 2011; Gou et al., 2008; Jana et al., 2007; Li et al., 2009a)
Diffractometer	PANalytical X'PERT Pro X-ray / Bruker AXS D8 Advance / JCPDS (Joint Committee on Powder Diffraction Standards) / X-ray diffractometer (XRD, EMPYREAN, PANALYTICAL) / X- ray diffractometer (XRD, EMPYREAN,PANAL YTICAL, the Netherlands)	Powder X-ray diffraction (XRD) / XRD spectra / Cubical Cu nanoparticles	(Baby & Ramaprabhu, 2011; Botha et al., 2011; Selvakumar & Suresh, 2012b; Suresh et al., 2011, 2012; Yarmand et al., 2015; Yarmand et al., 2016a)

Table 2.2 Continued

i. Stability Instruments			
Instruments	Type / Model	Measurement	Authors
Ultrasonic	A Branson Ultrasonic Cleaner 1510 / Ultrasonic vibrator (Lark, India) / Ultrasonic vibrator (UP200S-Hielscher) / Ultrasonic processor (20 kHz, 1200 W, Topsonic, Iran) / Ultrasonic bath (DaeRyun Science Inc., Korea) / Ultrasonic processor (Hielscher Company, Germany)	To disperse the nanoparticles into water / Ultrasonic pulses / To break down the agglomeration of the nanoparticles / Phase compositions	(Abbasi et al., 2013; Afrand et al., 2016a; Afrand et al., 2016b; Asadi & Asadi, 2016; Baghbanzadeh et al., 2012; Baghbanzadeh et al., 2014; Han & Rhi, 2011; Hemmat Esfe et al., 2015d; Ho et al., 2010; Jana et al., 2007; Madhesh & Kalaiselvam, 2014; S. Harandi et al., 2016; Soltani & Akbari, 2016b; Suresh et al., 2012; Yarmand et al., 2015)
pH meter	HANNA, HI 83141 / Deep Vision: Model 111/101	Measured pH value	(Soltani & Akbari, 2016b; Suresh et al., 2012)
Spectroscopy	Energy-dispersive X-ray (EDX)	Composition	(Abbasi et al., 2013; Madhesh & Kalaiselvam, 2014; Madhesh et al., 2014)
ii. Characterization Instruments			
Instruments	Type / Model	Measurement	Authors
SEM /FESEM	A XL30 ESEM / OXFORD ISIS / FESEM, FEI QUANTA/ Hitachi H 800 / JSM 6390LV/ High resolution SUPRA®55, Carl Zeiss, Germany, Electron high tension (EHT): 20 kV / SU8000, Hitachi	Optical spectra / Average size	(Baby & Ramaprabhu, 2011; Baghbanzadeh et al., 2014; Botha et al., 2011; Gou et al., 2008; Li et al., 2009a; Madhesh & Kalaiselvam, 2014; Madhesh et al., 2014; Selvakumar & Suresh, 2012b; Yarmand et al., 2015; Yarmand et al., 2016a)
TEM	JEOL TEM-2010F / JEOL 1200 EX / HT 7700, Hitachi machine / High resolution TEM	Optical spectra / Average size / Microstructure of the synthesized nanohybrids / Surface morphology	(Abbasi et al., 2013; Baby & Ramaprabhu, 2011; Baghbanzadeh et al., 2014; Botha et al., 2011; Gou et al., 2008; Jana et al., 2007; Li et al., 2009a; Yarmand et al., 2015; Yarmand et al., 2016a)

Table 2.2 Continued

iii. Thermophysical Properties Instruments			
Instruments	Type / Model	Measurement	Authors
Density meter	Model DA-505, Kyoto Electronics Manufacturing Co. / Anton Paar / Mettler Toledo DE-40	Density	(Baghbanzadeh et al., 2014; Ho et al., 2010; Yarmand et al., 2015)
KD2 Pro thermal property	Decagon, Canada / Decagon Devices, Inc., USA / Decagon Devices, Inc., Pullman, WA / NETZSCH LFA 447 NanoFlash / AB 200, Fisher scientific, USA	Thermal conductivity	(Abbasi et al., 2013; Baby & Ramaprabhu, 2011; Baghbanzadeh et al., 2012; Hemmat Esfe et al., 2015a; Hemmat Esfe et al., 2015d; Ho et al., 2010; Madhesh & Kalaiselvam, 2014; Madhesh et al., 2014; S.Harandi et al., 2016; Selvakumar & Suresh, 2012b; Suresh et al., 2011, 2012; Yarmand et al., 2015; Yarmand et al., 2016a)
Viscometer	Brookfield cone and plate viscometer (LVDV-I PRIME C/P) / Rotational viscometer (Brookfield DV-II+Pro) / ETC Bohlin / Rheometer (Physica, MCR, Anton Paar, Austria) / CAP 2000+	Viscosity	(Afrand et al., 2016a; Afrand et al., 2016b; Asadi & Asadi, 2016; Baghbanzadeh et al., 2014; Ho et al., 2010; Madhesh et al., 2014; Selvakumar & Suresh, 2012b; Soltani & Akbari, 2016b; Suresh et al., 2011, 2012; Yarmand et al., 2015; Yarmand et al., 2016a)

2.5 Development and Current Progress of Hybrid Nanofluids

The parameters studies are related to hybrid nanofluids with base fluids of water and ethylene glycol, whereas the hybrid nanolubricants with base of oil are summarized in Table 2.3. The development of hybrid nanofluids is classified according to the type of the base fluids. Most research are concerned on the temperature variation in their study and followed by the effect of mass and volume concentrations. Table 2.3 provides the summaries of the literature for the hybrid research. Water based hybrid nanofluids are mostly used in previous studies (Baghbanzadeh et al., 2014; Bhosale & Borse, 2013; Han & Rhi, 2011; Hemmat Esfe et al., 2015b; Ho et al., 2010, 2011; Jana et al., 2007; Madhesh et al., 2014; Selvakumar & Suresh, 2012a; Suresh et al., 2011, 2012; Takabi & Shokouhmand, 2015; Yarmand et al., 2015).

Table 2.3 Summary of development and current progress

Authors	Nanofluids	Temp. Range (°C)	Volume Fraction (%)	Mass Fraction (wt.%)
Jana et al. (2007)	CNT-CuNP/ water and CNT-AuNP/ water	25	CNT: 0.2, 0.3, 0.5 and 0.8 AuNP: 1.5–2.5 CuNP: 0.05, 0.1,0.2 and 0.3	-
Ho et al. (2010)	Al ₂ O ₃ -MEPCM/water	25–40	-	PCM: 2, 5, and 10 MEPCM: 3.7,9.1, and 18.2 Al₂O₃: 2-10
Botha et al. (2011)	Silver-silica/ Transformer oil	130	-	Silica: 0.07 to 4.4 Silver: 0.1 to 0.6
Han and Rhi (2011)	Ag- Al ₂ O ₃ /water	1, 10, 20	0.005, 0.05, 0.1	-
Ho et al. (2011)	Al ₂ O ₃ -MEPCM/water	<40	-	PCM: 2, 5, and 10 MEPCM: 2–10
Suresh et al. (2011)	Al ₂ O ₃ -Cu/water	-	0.1, 0.33, 0.75, 1, 2	-
Selvakumar and Suresh (2012b)	Al ₂ O ₃ -Cu/water	-	0.1	-
Suresh et al. (2012)	Al ₂ O ₃ -Cu/water	40	0.1	-
Abbasi et al. (2013)	MWCNT+g-Al ₂ O ₃ /Gum arabic(GA)+water	60	0.1	-
G.H.Bhosale and S.L.Borse (2013)	Al ₂ O ₃ -CuO/water	<40	0.25, 0.5 and 1	-
Baghbanzadeh et al. (2014)	Silica-MWCNT/water	20	-	Hybrid 1: 80:20 Hybrid 2: 50:50
Madhesh and Kalaiselvam (2014)	Cu-TiO ₂ /water	-	0.1 to 1.0	-
Hemmat Esfe et al. (2015a)	Ag-MgO/water	-	0 to 2	50:50
Hemmat Esfe et al. (2015d)	Cu-TiO ₂ /Water-EG	30-60	0.1,0.2,0.4,0.8,1, 1.5 and 2	-
Takabi and Shokouhmand (2015)	Al ₂ O ₃ -Cu/water	-	0 to 2	-
Yarmand et al. (2015)	GNP-Ag/water	<45	-	0.02, 0.06 and 0.1
Afrand et al. (2016b)	Fe ₃ O ₄ -Ag/EG	25-50	0.0375, 0.075, 0.15, 0.3, 0.6 and 1.2	-
Asadi and Asadi (2016)	MWCNT-ZnO/engine oil	5-55	0.125, 0.25, 0.5, 0.75 and 1	-

The range of temperature that has been used for water based hybrid nanofluids were less than 45 °C with volume and mass concentrations of not more than 2.5% and 50 wt.%, respectively. However, an investigation of gum Arabic (GA) with water based hybrid nanofluids was performed by Abbasi et al. (2013). They conducted the experiment for temperature of 60 °C and 0.1% volume concentration. In other papers, Afrand et al. (2016b), Harandi et al. (2016), and Soltani and Akbari (2016a) used ethylene glycol as a base fluid with the temperature range of 25 to 60 °C and volume concentrations of up to 2.3%. The combination of water-EG base fluids with the temperature range of 30 to 60 °C and volume concentration of 0.1 to 2% was provided by Hemmat Esfe et al. (2015d). For hybrid nanolubricants, the investigation at high boiling points up to 130 °C for transformer and engine oil (SAE40) based were undertaken by Botha et al. (2011), Afrand et al. (2016b), and Asadi and Asadi (2016). They considered volume and mass concentrations of not more than 1% and 4.4 wt.% respectively.

2.6 Thermo-physical Properties of Hybrid Nanofluids

The evaluation of thermo-physical properties especially the four properties namely thermal conductivity, dynamic viscosity, specific heat and density are required for the investigation of forced convection heat transfer. The early studies stated that the enhancement of heat transfer coefficients were influenced by the effectiveness of its thermo-physical properties of the nanofluids (Chiam et al., 2017; Choi & Stephen, 1995; Duangthongsuk & Wongwises, 2008; Mariano et al., 2013). Based on the previous investigations, the best performance of heat transfer is expected with the highest thermal conductivity and lowest dynamic viscosity of the nanofluids.

2.6.1 Thermal Conductivity and Dynamic Viscosity

In recent years, several studies on the thermal conductivity and viscosity of hybrid nanofluids were conducted by many researchers (Afrand et al., 2016b; Asadi & Asadi, 2016; Bahrami et al., 2016; Hemmat Esfe et al., 2015b; Madhesh et al., 2014; Minea, 2017; Soltani & Akbari, 2016a). One of the earlier studies on thermal conductivity of hybrid SiO₂/MWCNT nanofluids was presented by Baghbanzadeh et al. (2012). The effective thermal conductivity of the hybrid nanofluid increased with the increase of nanofluid concentration. However, the enhancement was found to be at a

minimum at high concentrations. The higher percentage of MWCNT compared to SiO₂ in the hybrid nanofluid provided the highest effective thermal conductivity. S.Harandi et al. (2016) studied the effects of temperature and concentrations of *f*-MWCNTs–Fe₃O₄/EG nanofluid for concentrations of up to 2.3% and temperatures of 25 to 50 °C. The results showed that hybrid nanofluids significantly affected the thermal conductivity ratio at high concentrations. Another study on thermal conductivity of hybrid nanofluids was performed by Kumar et al. (2016b). They used Cu-Zn nanoparticles in different base fluids, namely vegetable oil, paraffin oil and SAE oil. As a result, the Cu-Zn in vegetable oil was found to be the best combination compared to the others with 53% difference. Minea (2017) conducted a study on hybrid nanofluid viscosity by using a numerical approach for Al₂O₃, TiO₂ and SiO₂ nanoparticles in a water base. They used a constant ratio of Al₂O₃ (at 25%) mixed with either TiO₂ or SiO₂ at 0.5, 1.0 and 1.5% concentrations. The discrepancy appeared between those combination mixtures because of the method of calculation.

The advantages of using nanofluids in applications of heat transfer are higher thermal conductivity and lower viscosity than microfluids (Azmi et al., 2016d). Hence, the investigations on these two properties, namely thermal conductivity and viscosity are essential to understand the thermal performance and physical behaviour of nanofluids, respectively. Koblinski et al. (2005) conducted investigations on thermal conductivity of Cu nanoparticle and found that the thermal conductivity for ethylene glycol and oil increased with the dispersion of less than 1% volume concentration of Cu nanoparticles. Different studies by various researchers were conducted with nanofluids prepared in diverse base fluids and concentrations using metal or metal oxide nanoparticles such as Al₂O₃ (Aluminium oxide), Cu (Pure copper), CuO (Copper oxide), Fe₃O₄ (Iron oxide), SiC (Silicon carbide), SiO₂ (Silicon dioxide), TiO₂ (Titanium oxide), ZnO (Zinc oxide), and ZrO₂ (Zirconium dioxide) (Azmi et al., 2016c; Azmi et al., 2014b; Sundar et al., 2013a; Yu et al., 2012; Zamzarian et al., 2011).

Previously, several studies were conducted for thermal conductivity and viscosity of nanofluids for the base mixture of water:ethylene glycol (EG). There were several factors that affected the enhancement in thermal conductivity such as concentration, particle size, working temperature, volume ratio of nanoparticles and stability of nanofluids (Javadi et al., 2013b; Paul et al., 2011; Sundar et al., 2013b; Yoo

et al., 2007). In most studies, the addition of nanoparticles into the base fluid increases the thermal conductivity. However, the enhancement may differ for different nanofluids as proven by Turgut et al. (2009). In their studies, they found that the temperature was independence with the enhancement of thermal conductivity. A study on viscosity was conducted by Sundar et al. (2012) with Fe_3O_4 nanoparticles was dispersed in three different mixtures ratio of EG:water for ratios of 60:40, 40:60 and 20:80. They observed that volume concentration of 1.0% nanofluid in a 60:40 mixture is enhanced by 2.94% compared to other mixture ratios of base fluids. Yu et al. (2012) used 55:45 (W:EG) mixture base fluid in their investigation. They found that the temperature and volume concentration significantly affected the nanofluids viscosity. In addition, the nanofluids exhibited Newtonian behaviours for temperatures below 45 °C. The Al_2O_3 nanoparticles in 40:60 water-EG mixture base was studied by Said et al. (2013). A similar behaviour was observed by them where the nanofluid exhibited Newtonian behaviours for low concentrations of below 40 °C.

A study was done by Jana et al. (2007) for the nanofluids with AuNPs with only a fixed volume fraction of AuNP was added to water in order to measure the thermal conductivity behaviour. To observe the impact of CNTs on thermal conductivity of AuNP suspensions, CNTs in various concentrations were added to AuNP suspensions. The findings from the study showed that the nanofluids with 1.4% volume concentration of AuNP colloids demonstrated a 37% improvement in thermal conductivity over water. The expansion of CNTs to AuNP nanofluids by 1.4 % AuNP colloid does not indicate a clear change of thermal conductivity. A CuNP–CNT hybrid nanofluid was set up with a fixed amount of CNTs and various CuNP concentrations to measure the impact on thermal conductivity of the suspensions. CNTs did not increase the thermal conductivity of the CuNP–CNT nanofluid but instead brought down the qualities when contrasted with the thermal conductivity of separate single CuNP nanofluids. Indeed, even with the increased measures of the CuNPs in CuNP–CNT suspension, thermal conductivity declines and standard deviation increases. The same phenomena were additionally found in AuNP–CNT suspensions.

Ho et al. (2010) compared the effect of dispersing Al_2O_3 nanoparticles with a pure PCM suspension. The thermal conductivity of hybrid suspension was increased with the nanoparticle mass fractions. The relative enhancements of more than 4% and

nearly 13% in the thermal conductivity were found for the PCM suspension containing nanoparticles of 2 wt.% and 10 wt.%, respectively. Further, they measured the dynamic viscosity for the hybrid suspensions containing diverse mass fractions of MEPCM nanoparticles at a temperature of 30 °C. For pure Al₂O₃–water nanofluids, the dynamic viscosity enhancement showed a marginal increase with the mass fraction of the nanoparticles contrasted with that of pure water while the pure PCM suspensions turn out to be fundamentally improved. Scattering the nanoparticles in the PCM suspension has a tendency to further increase of the compelling element thickness of the hybrid suspension. Specifically, the crossover suspension of PCM at 10 wt.% shows a relative increment of more than three times in the dynamic viscosity compared to water when the fraction of nanoparticles is increased up to 10 wt.%.

Baby and Ramaprabhu (2011) found that the thermal conductivity of nanofluids compared to DI water increased with increasing volume fraction. The rate improvement in thermal conductivity was ascertained utilizing the relation of $((k-k_0) \times 100) / k_0$, where ' k_0 ' is the thermal conductivity of base liquid and ' k ' is that of nanofluids. The enhancements in thermal conductivity for volume concentrations of 0.005% and 0.05% are up to 9% and 20%, respectively. The thermal conductivity of the nanofluids also increased with increasing temperature. For 0.005% volume concentration, the increments of thermal conductivity were 9% and 12% respectively at temperatures of 30 °C and 50 °C. Meanwhile for 0.05% volume concentration, the enhancements of thermal conductivity were 20% and 80% at temperatures of 30 °C and 50 °C, respectively. A comparable pattern is displayed for all volume concentrations.

The investigation by Botha et al. (2011) was concerned on the thermal conductivity of silica with concentrations extending from 0.07 to 4.4 wt%. They obtained 1.7% increase in thermal conductivity for 0.5 wt% silica and a 3.5% increment for 1.8 wt% concentration of silica alone, without the existence of silver (Ag) nanoparticles in the oil base. The highest concentration of silica under their investigation was 4.4 wt % with 5.2% enhancement in thermal conductivity. At the point when Ag was upheld on silica, the thermal conductivity was found to increase with an increment in Ag concentration. A thermal conductivity increment of 15% was found when just 0.60 wt.% Ag was supported on 0.07 wt.% silica in the hybrid solution. It is believed that the Ag nanoparticles should be sufficiently close for thermal transport

to occur among them and supporting the particles on a reasonable backing gives great grounds to a steady heat transfer system.

Suresh et al. (2011) conducted an investigation of thermal conductivity for $\text{Al}_2\text{O}_3\text{-Cu}$ /water hybrid nanofluids, measured at an interval of 15 minutes for a time of around 3 hours after sonication. Fifteen minutes was given between progressive estimations for the temperature of the sensor needle and test to re-equilibrate. The thermal conductivity improvements of $\text{Al}_2\text{O}_3\text{-Cu}$ /water hybrid nanofluids were 1.47%, 3.27%, 6.22%, 7.53%, and 12.11%, respectively for volume concentrations of 0.1%, 0.33%, 0.75%, 1% and 2%, respectively contrasted with deionised water. Thermal conductivity improvements of the hybrid nanofluids were also compared with the alumina/water nanofluids. The enhancements shown for alumina nanofluids were 0.5%, 1.31%, 3.27%, 5.36%, and 7.56%, respectively for the same concentrations. This implies that there is an extremely significant improvement in the effective thermal conductivity because of the hybridisation of alumina nanoparticles utilizing metallic copper particles.

Baghbanzadeh et al. (2012) found that the thermal conductivity of nanofluids is improved with the increase in concentration of nanomaterials, and substantial improvement in the case of MWCNTs. Silica nanofluids demonstrated a minimum increment and the improvement in effective thermal conductivity of hybrid nanofluids is within the value between the upgrade of MWCNT and silica nanofluids. Normally, solids have a more prominent thermal conductivity than fluids. The mixture with increased MWCNTs has expanded thermal conductivity of distilled water compared to the other hybrids. An explanation behind this phenomenon is that the impact of carbon nanotube concentrations inside the nanofluids implies that by increasing the amount of carbon nanotubes inside the liquid, more space within the fluids would be occupied by them and more effective networks of nanomaterials would be produced inside the liquid. The summary of thermal conductivity and viscosity of hybrid nanofluid obtained by various investigators are shown in Table 2.4.

Table 2.4 Summary thermal conductivity and viscosity of hybrid nanofluids

Authors	Nanofluids	Properties	Findings
Jana et al. (2007)	CNT-CuNP/water and CNT-AuNP/water	Thermal conductivity	Thermal conductivity for particles of CNT, CuNP, and AuNP nanofluids higher than hybrid nanofluids
Ho et al. (2010)	Al ₂ O ₃ -MEPCM/water	Thermal conductivity, dynamic viscosity	The thermal conductivity enhancement of PCM suspension by dispersion of Al ₂ O ₃ nanoparticle relative to water. The viscosity for hybrid suspension drastically increase
Baby and Ramaprabhu (2011)	MWNT-HEG/water and MWNT-HEG/EG	Thermal conductivity	The enhancement of thermal conductivity are 20% for 0.05% volume fraction whereas 289% of heat transfer coefficient (HTC) enhancement for volume fraction of 0.01% f-MWNT+f-HEG
Suresh et al. (2011)	Al ₂ O ₃ -Cu/water	Thermal conductivity, viscosity	The obviously increased in viscosity value which are higher than the increasing in thermal conductivity
Baghbanzadeh et al. (2012)	Silica-MWCNT/water	Thermal conductivity	The increasing of nanomaterial concentration affecting the effectiveness of thermal conductivity
Abbasi et al. (2013)	MWCNT+g-Al ₂ O ₃ / Gum arabic(GA) + Water	Thermal conductivity	The thermal conductivity enhancement was reached 20.68% at 0.1% of volume fraction
Hemmat Esfe et al. (2015a)	Ag-MgO/water	Thermal conductivity	Increasing in thermal conductivity and slightly increase for dynamic viscosity value of nanofluid and it showed highest value of correlation
Hemmat Esfe et al. (2015d)	Cu-TiO ₂ /water and Cu-TiO ₂ /EG	Thermal conductivity	The better performance was shown by ANN model in predicting the thermal conductivity value
S.Harandi et al. (2016)	F-MWCNTs-Fe ₃ O ₄ /EG	Thermal conductivity	The maximum enhancement of thermal conductivity for nanofluids are 30% that was occur at 2.3% volume fraction for temperature of 50 °C
Soltani and Akbari (2016b)	MgO-MWCNT /ethylene glycol	Dynamic viscosity	The dynamic viscosity were influence by volume fraction and temperature rising. The relative viscosity shows the enhancement up to 168% for 0.1 to 1% volume fraction
Yarmand et al. (2016a)	Biomass carbon-graphene oxide/EG	Thermal conductivity	The thermal conductivity enhancement of ACG-EG based fluid are 6.47% at 40 °C for 0.06% weight fraction

2.6.2 Density and Specific Heat

An experimental study of density and specific heat was done by Ho et al. (2010) for the hybrid nanofluids of Al₂O₃-MEPCM using water base fluids. The finding from the study is the experimental density values of hybrid are in good agreement by comparing with the theoretical density values. The specific heat of Al₂O₃-MEPCM hybrid nanofluids was decreased with decreasing of volume faction. The density and specific heat mixture relation is given as in Equations 2.1 and 2.2, respectively.

$$\rho_{hnf} = \phi_1 \rho_1 + \phi_2 \rho_2 + (1 - \phi_1 - \phi_2) \rho_{bf} \quad 2.1$$

$$\rho_{hnf}, C_{p,hnf} = \phi_1 \rho_1 C_1 + \phi_2 \rho_2 C_2 + (1 - \phi_1 - \phi_2) \rho_{bf} C_{p,bf} \quad 2.2$$

where ρ_{hnf} is density of hybrid nanofluids in kg/m³; ρ_{bf} is density of base fluid in kg/m³; ρ_1 is density of first nanoparticles in kg/m³; ρ_2 is density of second nanoparticles in kg/m³; ϕ_1 is initial volume concentration in %; and ϕ_2 final volume concentration in %; $C_{p,hnf}$ is specific heat of nanoparticles for hybrid nanofluids in J/kg.K; $C_{p,bf}$ is specific heat of nanoparticles for base fluid in J/kg.K; C_1 is specific heat of first nanoparticles in J/kg.K; C_2 is specific heat of second nanoparticles in J/kg.K.

2.7 Heat Transfer Performance of Hybrid Nanofluids

Performance of hybrid nanofluids has been summarized from previous research (Allahyar et al., 2016; Hjerrild et al., 2016; Ho et al., 2011; Karami & Rahimi, 2014; Madhesh et al., 2014; Ramachandran et al., 2016; Sundar et al., 2014; Takabi & Salehi, 2015). The performance of hybrid nanofluids is classified into two groups. The first group concerns research on the heat transfer observations and the other concerns the pressure drop and friction factor. Table 2.5 provides summary on heat transfer performance and pressure drop of hybrid nanofluids.

Table 2.5 Summary of heat transfer performance and pressure drop of hybrid nanofluids

Heat Transfer Observation		
Authors	Nanofluids	Findings
Baby and Ramaprabhu (2011)	MWNT-HEG / water and MWNT-HEG / EG	The heat transfer coefficient (HTC) increase with an increasing volume fraction. The highest HTC were occurred at 0.01% volume fraction
Han and Rhi (2011)	Ag-Al ₂ O ₃ / water	High in thermal resistance were influence by the increasing of nanoparticle concentration
Moghadassi et al. (2015)	Al ₂ O ₃ -Cu / water-based Al ₂ O ₃	The average of Nusselt number increase by 4.73% and 13.46% compared with Al ₂ O ₃ /water and pure water, respectively
Sundar et al. (2014)	MWCNT-Fe ₃ O ₄ / water	The Nusselt number enhancement for 0.1% of MWCNT-Fe ₃ O ₄ hybrid nanofluid is 9.35% and 20.62%, for 0.3% of MWCNT-Fe ₃ O ₄ hybrid nanofluid is 14.81% and 31.10%
Selvakumar and Suresh (2012b)	Al ₂ O ₃ -Cu / water	The convection of heat transfer is increased
Takabi and Shokouhmand (2015)	Al ₂ O ₃ -Cu / water	Hybrid nanofluid enhances the rate of heat transfer with respect to pure water and nanofluid
Yarmand et al. (2015)	GNP-Ag / water	Heat transfer efficiency showed an improvement in comparing with the based fluid
Nuim Labib et al. (2013)	CNT- Al ₂ O ₃ / water and CNT- Al ₂ O ₃ / EG	The heat transfer enhancement of ethylene glycol as a based fluid is better compared with water based fluid
Suresh et al. (2012)	Al ₂ O ₃ -Cu/water	The maximum enhancement of convective heat transfer are 13.56% in Nusselt number
G.H.Bhosale and S.L.Borse (2013)	Al ₂ O ₃ -CuO/water	The maximum critical heat flux (CHF) enhancement by 90% for 36 gauge nichrome wire at 1% volume of nanofluid
Pressure Drop and Friction Factor Observation		
Authors	Nanofluids	Findings
Ho et al. (2011)	Al ₂ O ₃ -MEPCM/water	The efficacy of heat transfer appear critically exceed through pressure drop penalty
Madhesh et al. (2014)	Cu-TiO ₂ /water	For 2.0% of the volume concentration, the friction factor and pressure drop were expected to be 1.7% and 14.9% respectively.
Huang et al. (2016)	MWCNT/water + Al ₂ O ₃ /water	The pressure drop for the mixture of hybrid nanofluid is smaller compared to Al ₂ O ₃ /water nanofluids
Selvakumar and Suresh (2012b)	Al ₂ O ₃ -Cu/water	The pumping power is increased

Baby and Ramaprabhu (2011) investigated the heat transfer evaluation and directed for various volume concentrations of hybrid f -MWNT/ f -HEG dispersed in water based nanofluids for various Reynolds numbers. For water based nanofluids, the Reynolds numbers were utilized for 4500, 8700 and 15500, which modelled the turbulent stream. The analyses focused on constant heat flux boundary conditions. The volume concentrations of 0.005% and 0.01% were used in their study. At the entrance of the test section, the improvement in the heat transfer coefficient is observed to be 181% and 264%, respectively for 0.005% and 0.01% concentrations for Reynolds number of 4500. Towards the end of the test section, the enhancements in heat transfer were improved further with 166% and 206% respectively for the same volume concentrations and Reynolds number. The heat transfer enhancement at high Reynolds number is observed to be higher than low Reynolds number measured at both the entrance and exit of the test sections. Though for EG based liquids, the heat transfer coefficient increased with increase of the volume concentrations and Reynolds numbers.

In another paper, the Nusselt numbers for Al_2O_3 -Cu hybrid nanofluids were obtained by utilizing the normal temperature of the wall, average bulk temperature, and the actual heat flux value (Moghadassi et al., 2015). They stated that the velocity profile decreased with a distinction between the normal tube wall temperature and the mass mean temperature of nanofluids. Consequently, it improved the heat transfer coefficient which resulted with a high Nusselt number. The rate of heat transfer was improved for hybrid nanofluids in contrast with water and Al_2O_3 /water nanofluids numerically. The convective heat transfer coefficient for the Al_2O_3 -Cu hybrid nanofluids is higher than the base fluids and Al_2O_3 /water nanofluids. The average Nusselt number was increased by 4.73% and 13.46% compared to Al_2O_3 /water and pure water, respectively. This implies that with an addition of copper nanoparticles, the effective heat transfer rate is increased by 5%.

A study conducted by Sundar et al. (2014) found that the Nusselt number increased with the increase of MWCNT- Fe_3O_4 hybrid nanofluid volume concentration and Reynolds number. The enhancement in the Nusselt number for 0.1% volume concentration of the hybrid nanofluids varied from 9.35% to 20.62%. Further, the heat transfer enhancements were noticed for 0.3% volume concentration with 14.81% and

31.10% respectively for the Reynolds numbers of 3000 and 22,000. The Nusselt number improvement for MWCNT-Fe₃O₄ nanofluids is additionally attributed by the molecule Brownian movement, thermo-physical properties of the nanoparticles and extensive surface range. Henceforth, the heat transport capability of MWCNT-Fe₃O₄ nanofluid also increased further. The improvement in the Nusselt number might be credited to the alluring properties of nanofluids with high thermal conductivity and high specific heat, which contrasted with the distilled water.

Suresh et al. (2012), Selvakumar and Suresh (2012a) and Takabi and Shokouhmand (2015) studied the impact of convective heat transfer performance of thin-channelled heat sink. They examined the heat transfer by utilizing the Al₂O₃-Cu hybrid nanofluids as the working liquid and deionized water as the base fluids. With the expansion of mass flow rate of the deionized water in the thin-channelled copper heat sink, the convective heat transfer coefficient also increased. Huge expansion in convective heat transfer coefficient has been observed for Al₂O₃-Cu/water hybrid nanofluids contrasted with deionized water. The stated reasons for the improvement in the convective heat transfer coefficients with the utilization of hybrid nanofluids; (i) the enhancement in thermal transport property of hybrid nanofluids is because of the inclusion of copper and alumina nanoparticles, (ii) nanoparticle thermal dispersion, and (iii) increased energy exchange between the hybrid nanoparticles/DI water and solid surface is because of the narrow channel width.

2.8 Challenges and Potential Applications of Hybrid Nanofluids

Despite the fact that a lot of research has been done on nanofluids over the previous decade and hybrid nanofluids over the past few years, the conclusions on their behaviour, characteristics, and performances remain fairly insufficient. Henceforth, it is important to engage more investigations so as to legitimately measure the impacts of particle size and shapes, sufficient scattering of particles and sedimentation, grouping of particles, surfactant impacts, nanofluid temperatures, and satisfactory experimental systems and techniques. Some of these issues have been addressed in part by a few researchers.

The preparation of homogeneous suspensions remains a specialized test because of extremely solid Van der Waals interactions. To get a stable nanofluid, physical or

chemical treatments have been conducted, for example, an increase of surfactant, and surface change of the suspended particles or applying strong force on the groups of the suspended particles. Dispersing agent and surface-dynamic agents have been utilized to scatter the nanoparticles of hydrophobic materials in aqueous solutions (Hwang et al., 2006). Generally, the long term stability of nanoparticle dispersion is one of the essential necessities of the nanofluid applications. The stability of nanofluids has a decent comparing association with the improvement of thermal conductivity where the better the dispersion conduct, the higher the thermal conductivity of nanofluids (Wu & Zhao, 2013). Eastman et al. (2001) uncovered that the thermal conductivity of ethylene glycol based nanofluids containing 0.3% copper nanoparticles diminishes with time. In their study, the thermal conductivity of nanofluids was measured twice with the first within two days and the second was two months after the preparation. It was found that the crisp nanofluids showed marginally higher thermal conductivities than nanofluids that were amassed to two months. This may be because of the reducing dispersion stability of nanoparticles with time. Nanoparticles may tend to agglomerate when kept for certain periods of time. Lee and Mudawar (2007) investigated the effects of Al₂O₃ nanofluid stability with time. It was found that nanofluids kept for 30 days displayed some settlement contrasted with crisp nanofluids. It demonstrated that long term degradation in the thermal performance of nanofluids could happen. Particle settling must be analysed precisely since it might prompt obstruction of cooling sections.

According to Sidik et al. (2014), nanofluid manufacturing has been limited to laboratory-scale productions. High costs will affect at least the near future and limit its potential widespread for applications. Until manufacturing processes allow mass productions of nanoparticles and associated with suspensions, the costs will undoubtedly remain high. As stated by Li et al. (2009c), numerous research have reported test concentrates on the thermal conductivity of nanofluids. In the last few years, many experimental investigations on the components affecting thermal conductivity of nanofluids, for example, the (i) impact of nanoparticles, (ii) impact of base fluids, and (iii) impact of the liquid–solid interface.

The different uses of nanofluids/nanolubricants have been looked into since decades ago and quantities of review articles have additionally distributed as of late covering commercial, industrial, and transportation applications. Application ranges are

generally differed, for example, electronic component cooling, automotive industry, solar energy and refrigeration systems. The hybrid nanofluids/hybrid nanolubricants are a significant new kind of nanofluid and they are still in the innovative work stage, which is similar to their applications in the industry. It is hoped that hybrid nanofluids and hybrid nanolubricants are utilized for comparative applications with better performance.

2.9 Summary

In this chapter, an inclusive review on thermo-physical properties of hybrid nanofluids were done with comprehensive studies on previous research. The hybrid nanofluids generally can be classified as new groups of nanofluids on which significantly more research studies should be done before their functional applications in the commercial ventures. Their major applications can be in the field of heat transfer applications. This is because of the synergistic impact through which they give ideal properties of the greater part of its constituents. It has been found that the enhanced thermal conductivity of nanofluids is one of the driving components for enhanced execution in various applications. The investigations on hybrid nanofluids, either experimental or numerical, are very limited and non of the study for the combination of $\text{TiO}_2\text{-SiO}_2$ nanofluids was found till now. The accentuation of the majority of the studies on hybrid nanofluids and hybrid nanolubricants is mostly focused on stability and thermal conductivity whereas the other thermo-physical properties were disregarded. Thus, many points are still left to be studied in order to test the solidness and other thermo-physical properties of hybrid nanofluids with expectations to commercial it for applications in the industry. The present review discussed in detail and summarized the methods, instrumentations of preparation, developments and current progress of hybrid nanofluids and its thermo-physical properties. The performances in terms of heat transfer, pressure drop and friction factor of hybrid nanofluids are carried out by different researchers. Some reviewed applications of hybrid nanofluids have also been discussed.

CHAPTER 3

METHODOLOGY

3.1 Research Overview

This chapter provides an explanation on methodology of the present work. Firstly, the stability of nanofluids need to be considered during the preparation of nanofluids. Next, thermo-physical properties of nanofluids were measured for thermal conductivity and dynamic viscosity. Then, the experimental setup was fabricated for the forced convection heat transfer experiment which consists of data logger, test section, flow meters, heater regulator, chiller and pressure transducer. After that, the forced convection experiment was carried out by considering the temperature and pressure drop variations for the analysis of heat transfer performance and friction factor, respectively. Finally, the analysis and experimental setup validations were undertaken by comparing the present experimental data with the previous study.

The phases of the experiment are divided into five stages. Phase one focused on preparation and stability of hybrid nanofluids. TiO_2 and SiO_2 water-based nanofluids are considered in the present heat transfer analysis. There were commercially produced by US Research Nanomaterials, Inc for research purposes in the form of liquid suspension. The procured TiO_2 and SiO_2 nanofluids will then be prepared to a new concentration by the dilution technique. In order to prepare the nanofluids by dispersing the nanoparticles in a EG/water base fluids, proper mixing and stabilization of the particles are required. In the present study, TiO_2 and SiO_2 nanoparticles will be mixed with EG/water base fluids and stabilizers, and will then be sonicated continuously by an ultrasonic bath to break down agglomeration of the nanoparticles prior to being used as the working fluid. The desired volume concentrations in the present study are between 0 and 3.0%. For each test, a new hybrid nanofluid will be prepared and used immediately.

The measurement of pH, electrical conductivity and TEM image analysis will be conducted in order to confirm the condition of agglomeration, dispersion and stability of nanofluids. To observe the distribution of the primary TiO₂ and SiO₂ nanoparticles at a nano scale, a transmission electron microscope (TEM) and FESEM will be used. Additionally, the approximate particle sizes of the nanoparticles will be measured directly from the FESEM images.

Phase 2 is thermo-physical properties measurement. The density and specific heat of nanofluids are estimated based on mixture relations. The equations were widely used by various investigators for different types of nanofluids. The equations are valid for homogeneous mixtures. The thermal conductivity of nanofluid is measured in this study using the KD2 Pro thermal property analyzer of Decagon Devices, Inc., USA. The KD2 Pro uses the transient line heat source to measure the thermal properties of solids and liquids. It consists of a handheld controller (microcontroller and power control) and two different sensors for measuring the thermal conductivity of solids and another for liquids. The apparatus meets the standards of both ASTM D5334 and IEEE 442-1981. ASTM D5334 is the standard test method for determination of thermal conductivity of soil and soft rock by the thermal needle probe procedure, whereas IEEE 442-1981 is the guide for soil thermal resistivity measurement. The sensor KS-1 is used to determine the thermal conductivity of the present sample. The dynamic viscosities of the nanofluids are measured with Brookfield LVDV-III Ultra Rheometer. The DV-III Ultra consists of a spindle model SC4-18, which is driven by a motor through a calibrated spring. The spindle is immersed in the test fluid to measure the viscosity of liquids within the range of up to 100.0 centiPoise (cP). The viscous drag of the fluid against the spindle is measured by the spring deflection. Spring deflection is measured with a rotary transducer. The range of viscosity is dependent on the rotational speed of the spindle, the size and shape of the spindle, the container in which the spindle rotates, and the full scale torque of the calibrated spring.

Phase 3 is experimental setup. The experimental setup is integrated with a circulating pump, flow meter, heater, control panel, thermocouples, pressure transducer, chiller, collecting tank, and test section. The heaters enclose a copper tube along its length of 1.5 m with an inner diameter (ID) of 16 mm and outer diameter (OD) of 19 mm, which constitutes the test section. The total length of fluid flow in the tube is 4.0

m, which ensures fully developed turbulent flow conditions at the entry of the test section. A 0.5 horsepower pump connected to a collecting tank with capacity of 0.03 m^3 is used to circulate the working fluid through the test section. The outer diameter of the test section is wrapped with two nichrome heaters each of 1500 W rating. The heat loss to the surrounding is minimized by enclosing the tube with ceramic fibre insulation. Seven K-type thermocouples are fixed at different locations; five would be spot fixed to the surface of the tube wall at 0.25, 0.5, 0.75, 1.0 and 1.25 m from the inlet and the other two would be inserted to measure the inlet and outlet temperature of the working fluid. The thermocouples are calibrated before the tests are undertaken and should have a maximum accuracy of $0.1 \text{ }^\circ\text{C}$. A digital flow meter is connected between the pump and the inlet of the test section. A chiller of 1.4 kW rating will be placed between the test section and the collecting tank.

Phase 4 is forced convection heat transfer experiment. The preliminary test should be conducted to determine the optimum input power to the heater and compatibility with the 1.4 kW capacity of the chiller. With the outer surface temperature of insulation being close to ambient temperature, the heat loss to the atmosphere is considered negligible. The chiller is adjusted to attain a liquid bulk temperature of $30 \text{ }^\circ\text{C}$ in the test section with a maximum variation of $1 \text{ }^\circ\text{C}$ at all flow rates and nanofluid concentrations. The provision of the chiller between the test section and the collecting tank will to achieve steady state condition faster. Hence, the system will be able to maintain the test section bulk temperature at $30 \text{ }^\circ\text{C}$. A pressure transducer connected across the test section will record the pressure drop for the determination of the friction factor. A data logger will record the surface and fluid temperatures every five seconds to determine the steady state nature of the experiment. The setup would be left idle for 15 to 30 minutes to achieve the steady state condition. At the steady state, the temperatures, the flow rates and the power inputs to the heater are recorded. The total length of the flow will be 4.0 m which ensures fully turbulent flow conditions at the entry of the test section. The experiments will be done with EG/water base $\text{TiO}_2\text{-SiO}_2$ hybrid nanofluids for volume concentrations of 0 to 3.0 % at various flow rates under turbulent conditions. Finally, phase 5 is analysis, results and discussion. The overall flow chart of the experiment was shown in Figure 3.1.

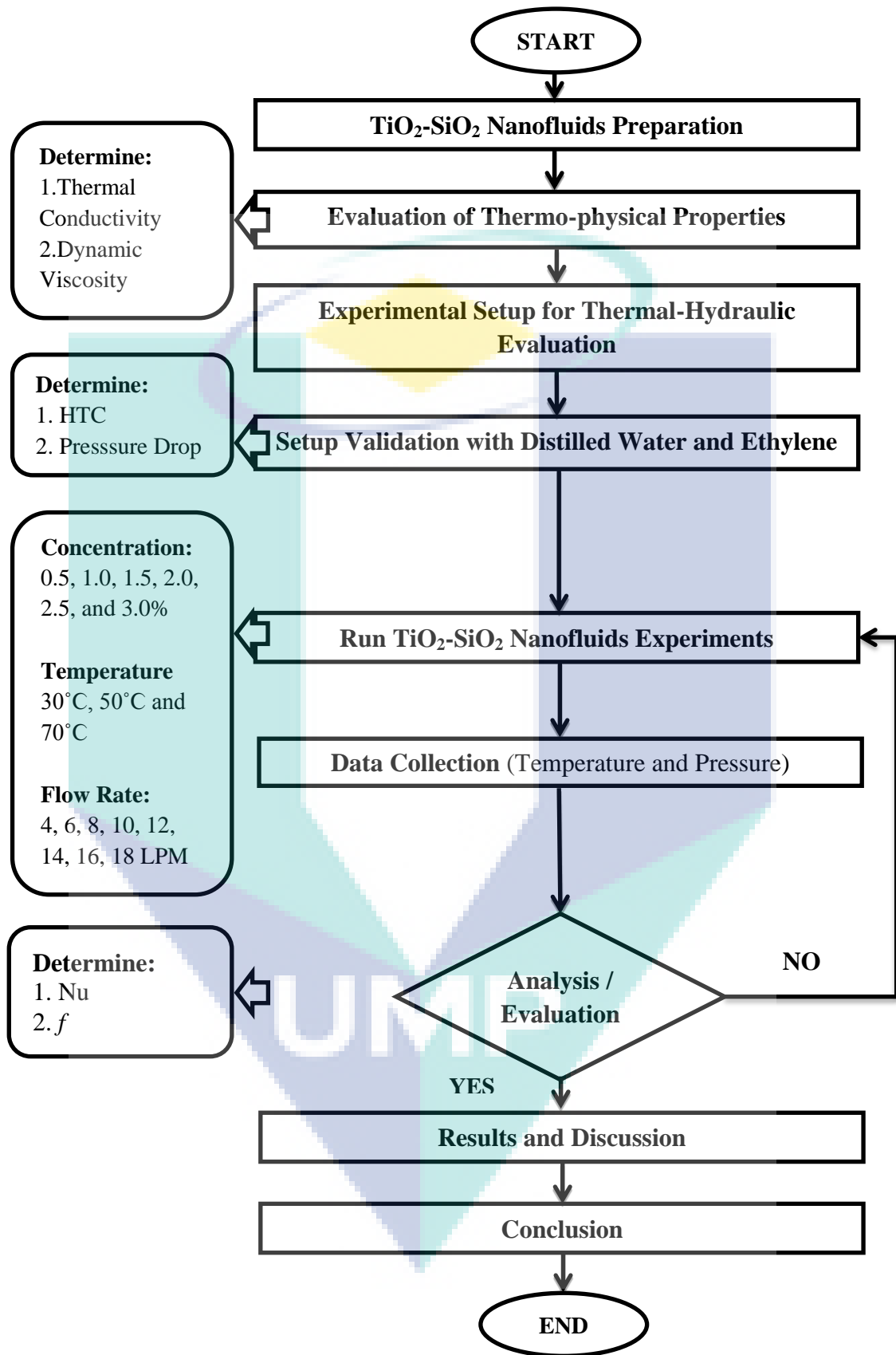


Figure 3.1 Experimental Flow Chart

3.2 TiO₂ - SiO₂ Nanofluids Preparation

The hybrid nanofluids are prepared using two-step methods. As reviewed by Hatwar and Kriplani (2014), there are two processes in this method, which are (i) synthesis of the nanoparticles in powder form (ii) scattering of the nanoparticles into the base fluids to form a stable and homogeneous solution. This method is usually produced in large scales because this techniques have already been used in industrial production. However, the challenges of using the two-step method in preparing nanofluids are agglomerations and the nanoparticles tend to settle down quickly (Hatwar & Kriplani, 2014; Yu & Xie, 2012). The selected nanoparticles for the present study are TiO₂ and SiO₂ nanoparticles dispersed in water/EG base fluids.

3.2.1 Nanoparticles Materials and Base Dilutions

The TiO₂ and SiO₂ nanoparticles with an average particle size of 50 and 30 nm, respectively, in diameter were obtained from US Research Nanomaterials, Inc. in a weight concentration of 40 ($\phi=13.62\%$) and 25 wt.% ($\phi=13.06\%$), respectively. Table 3.1 shows the nanofluids concentration and properties of TiO₂ and SiO₂ nanoparticles. In addition, mixture of distilled water and ethylene glycol was used as a base fluid. Ethylene glycol is supplied by QRec Asia Sdn. Bhd. and has density of 1113 kg/m³. The ethylene glycol is mixed with distilled water with volume ratio of 60:40 (water/EG).

Table 3.2 shows the characteristics of ethylene glycol. The detail product specification for ethylene glycol, TiO₂ and SiO₂ nanofluids are presented in Appendix A, Appendix B, and Appendix C, respectively.

Table 3.1 Nanofluids concentration and nanoparticles properties

Type of Nanoparticle	Diameter, (nm)	Weight Concen., ω (%)	Volume Concen., ϕ (%)	Specific Heat, C (J/kg.K)	Density, ρ (kg/m ³)
TiO ₂	50	40	13.62	692	4230
SiO ₂	30	25	13.06	745	2220

Table 3.2 Physical and chemical properties of ethylene glycol

Parameter	Value
pH	5.5 – 7.5
Melting Point	- 13 °C
Boiling Point	197.6 °C
Vapor Pressure	0.12 mmHg
Density	1113 kg/m ³
Molar Mass	62.07 g/mole

Source: ThermoFisher Scientific (2017).

3.2.2 Procedure for Preparation

The weight concentration of each suspended TiO₂ and SiO₂ nanofluids are converted to volume concentration by using Equation 3.1. The TiO₂-SiO₂ nanofluids was prepared for 50:50 (TiO₂:SiO₂) nanoparticle mixture ratio and dispersed in 60:40 of water/EG mixture by volume ratio. Furthermore, Equation 3.2 was used in preparation of TiO₂-SiO₂ nanofluids in different volume concentrations by the dilution process from 3.0% to 0.5%. The TiO₂-SiO₂ nanofluids were diluted from high to low volume concentrations by adding the water/EG base fluid into the solutions. The sonication process was undertaken during the preparation of TiO₂-SiO₂ nanofluids in order to maintain the stability of the suspended nanoparticles. The nanofluids are prepared through a mixing process by using a mechanical stirrer and sonication process using an ultrasonic bath for up to two hours of sonication time. A similar technique was proposed by other researchers in literature (Azmi et al., 2016a; Azmi et al., 2016b; Azmi et al., 2013b; Hamid et al., 2016; Hamid et al., 2015).

$$\phi = \frac{\omega \rho_{bf}}{\left(1 - \frac{\omega}{100}\right) \rho_p + \frac{\omega}{100} \rho_{bf}} \quad 3.1$$

$$\Delta V = (V_2 - V_1) = V_1 \left(\frac{\phi_1}{\phi_2} - 1 \right) \quad 3.2$$

where ϕ is volume concentration in %; ω is weight concentration in %; ρ_{bf} is density of base fluid in kg/m^3 ; ρ_p is density of nanoparticles in kg/m^3 ; ΔV is additional volume in mL; V_1 is initial volume in mL; V_2 is final volume in mL; ϕ_1 is initial volume concentration in %; and ϕ_2 final volume concentration in %.

The stirring process is done for more than 30 minutes to make sure the solutions are properly mixed. The magnetic stirrer was used for small quantity of nanofluids whereas bulk volume of nanofluids was used the mechanical stirrer. In order to make sure the solutions is stable, 1.5 hours sonication process is done by using ultrasonic bath. The process of preparation method was shown as in Figure 3.2. Appendix D and Appendix E shown the technical specifications of magnetic stirrer and ultrasonic bath, respectively.

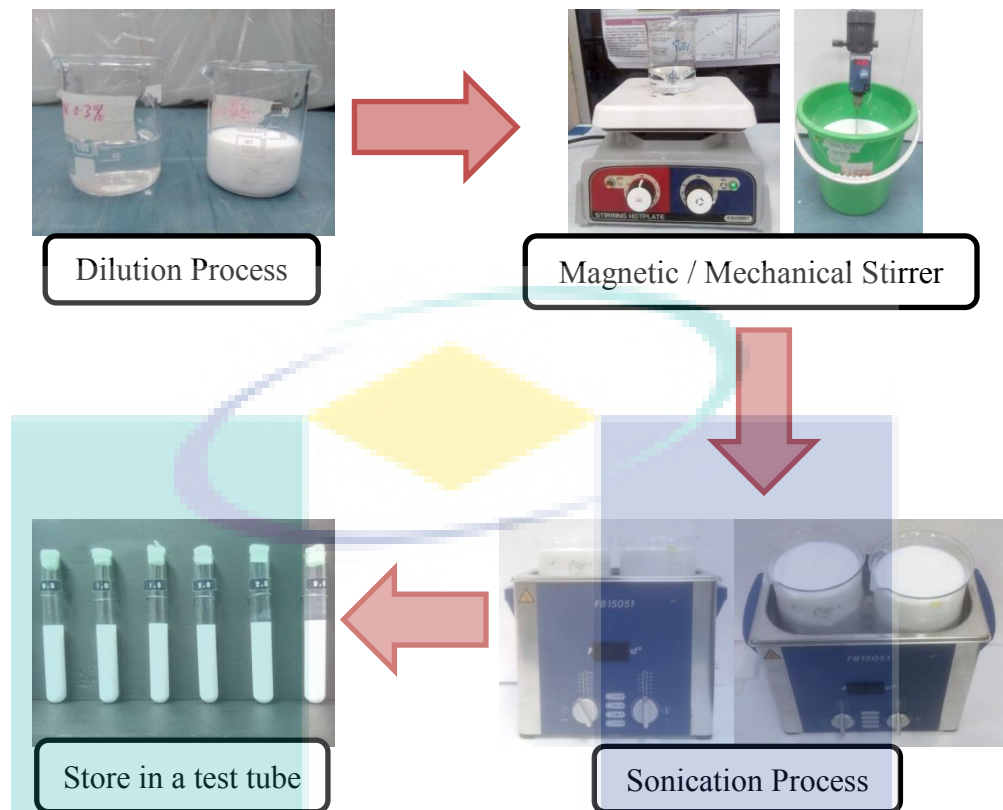


Figure 3.2 Process of hybrid nanofluids preparation

3.3 TiO_2 - SiO_2 Nanofluids Stability

The stability of nanofluids is measured through sedimentation observation and transmission electron microscope (TEM) images. Since the particle size of nanofluids are very small with less than 100 nm, FESEM and TEM micrographs has been done by several researchers as in literatures (Abbasi et al., 2013; Baby & Ramaprabhu, 2011; Baghbanzadeh et al., 2014; Botha et al., 2011; Gou et al., 2008; Jana et al., 2007; Li et al., 2009a; Madhesh & Kalaiselvam, 2014; Madhesh et al., 2014; Selvakumar & Suresh, 2012b; Yarmand et al., 2015; Yarmand et al., 2016a). The surface characteristics and morphology were measured with this methods to determine the size and distribution of nanoparticle.

3.3.1 Sedimentation Observation

The hybrid nanofluids were subjected to sonication process to enhance their stability and to reduce the agglomeration sizes (Abdolbaqi et al., 2016b; Abdolbaqi et al., 2016c). Hybrid nanofluids were prepared in 200 mL for each volume concentration

and exposed to sonication for 1.5 h. The nanofluids were found to be stable within the measurement process. The evaluation of the nanofluids stability was also determined through UV-Vis spectrophotometer (Genesis 10s) as shown in Figure 3.3. The absorption and scattering of light is measured by comparing the light intensity of the nanofluids with the base fluids (Ghadimi et al., 2011). In the previously studies, Karami et al. (2014) and Hajjar et al. (2014) were used UV-Vis spectrophotometer to evaluate the nanofluids stability. The absorbance ratio at different sonication times and various sedimentation time was observed continuously at a specific wavelength of 850 nm. Appendix F shows the technical specifications of UV-Vis spectrophotometer.



Figure 3.3 UV-Vis Spectrophotometer

3.3.2 Transmission Electron Microscope (TEM)

The characterization of nanofluids is observed using Philip CM120 Transmission Electron Microscope (TEM) as shown in Figure 3.4. Appendix G was presented the operating procedures for TEM. As reviewed in Section 2.4, the previous researchers were used the TEM for the characterization of nanofluids (Abbasi et al., 2013; Baby & Ramaprabhu, 2011; Baghbanzadeh et al., 2014; Botha et al., 2011; Gou et al., 2008; Jana et al., 2007; Li et al., 2009a; Yarmand et al., 2015; Yarmand et al., 2016a).



Figure 3.4 Transmission Electron Microscope (TEM) (Model Philips CM120)

3.4 Thermo-physical Properties Measurement

The thermo-physical properties such as thermal conductivity, dynamic viscosity, specific heat and density are considered important properties in enhancing the heat transfer performance. The thermal conductivity and dynamic viscosity of $\text{TiO}_2\text{-SiO}_2$ nanofluids in water/EG mixtures were measured by using KD2 Pro Thermal Property Analyzer and Brookfield LVDV-III Ultra Rheometer, respectively. The measurements were undertaken at wide range temperatures from 30 to 80 °C for all volume concentrations. Initially, the accuracy of the equipment were validated by measuring the properties of water/EG mixture and compared with ASHRAE (2009). Then, the properties measurements were undertaken for $\text{TiO}_2\text{-SiO}_2$ nanofluids. The similar equipment were used by previous researchers for thermal conductivity and dynamic viscosity measurements (Afrand, 2017; Asadi & Asadi, 2016; Hemmat Esfe et al., 2015d; Ho et al., 2010; Suresh et al., 2011, 2012). However, the present study was used the mixture relations for the estimation of specific heat and density of $\text{TiO}_2\text{-SiO}_2$ nanofluids.

3.4.1 TiO₂- SiO₂ Nanofluids Thermal Conductivity

The thermal conductivity of TiO₂-SiO₂ nanofluids were measured using KD2 Pro thermal property analyser of Decagon Devices, Inc. USA as shown in Figure 3.5 and its specification was presented in Appendix H. The apparatus meet the standards of both ASTM D5334 and IEEE 442-1981. It uses the transient line heat source to measure the thermal properties. The analyser consists of a handheld controller (microcontroller and power control) and a sensor for measuring the thermal conductivity of liquids. A water bath (WNB7L1, Memmert) is used to maintain a constant temperature within accuracy of 0.1 °C. The sensor is calibrated by determining the thermal conductivity of glycerin with ± 5.0% accuracy. A minimum of five measurements were collected within 15 minutes time interval for all samples and the average values were considered. The temperature of the sample is set in the range of 30 to 80 °C.

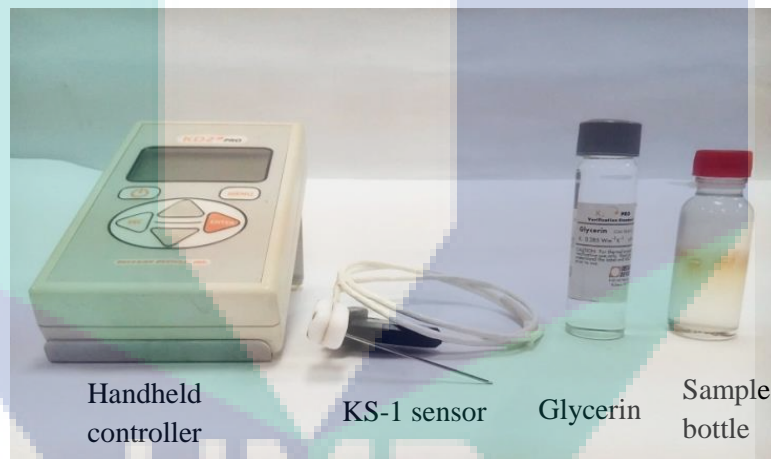


Figure 3.5 KD-2 Pro Thermal Property Analyser equipment

3.4.2 Procedure for Thermal Conductivity Measurement

KS-1 sensor of the analyser was calibrated by using a liquid verification such as glycerine. The standard liquid was provided by manufacturer. The thermal conductivity measurement was undertaken for wide range of temperature from 30 to 80 °C. The first sample measurement was conducted at 30 °C temperature for 40 ml volume of TiO₂ - SiO₂ nanofluids in a small sample container. In order to stabilize and make sure the temperature has reached a constant temperature of 30 °C, the sample bottle was immersed into water bath. The KS-1 sensor was inserted vertically into the centre of

sample bottle and sealed with the tape to ensure the sensor does not move during the measurement. Minimum 5 data of thermal conductivity value was recorded in the measurement for every 15 minutes interval time for each reading. The average data was considered for further analysis. The thermal conductivity measurement of TiO₂-SiO₂ nanofluids was repeated for the other temperatures of 40 to 80 °C. Figure 3.6 shows the setup for thermal conductivity measurement.

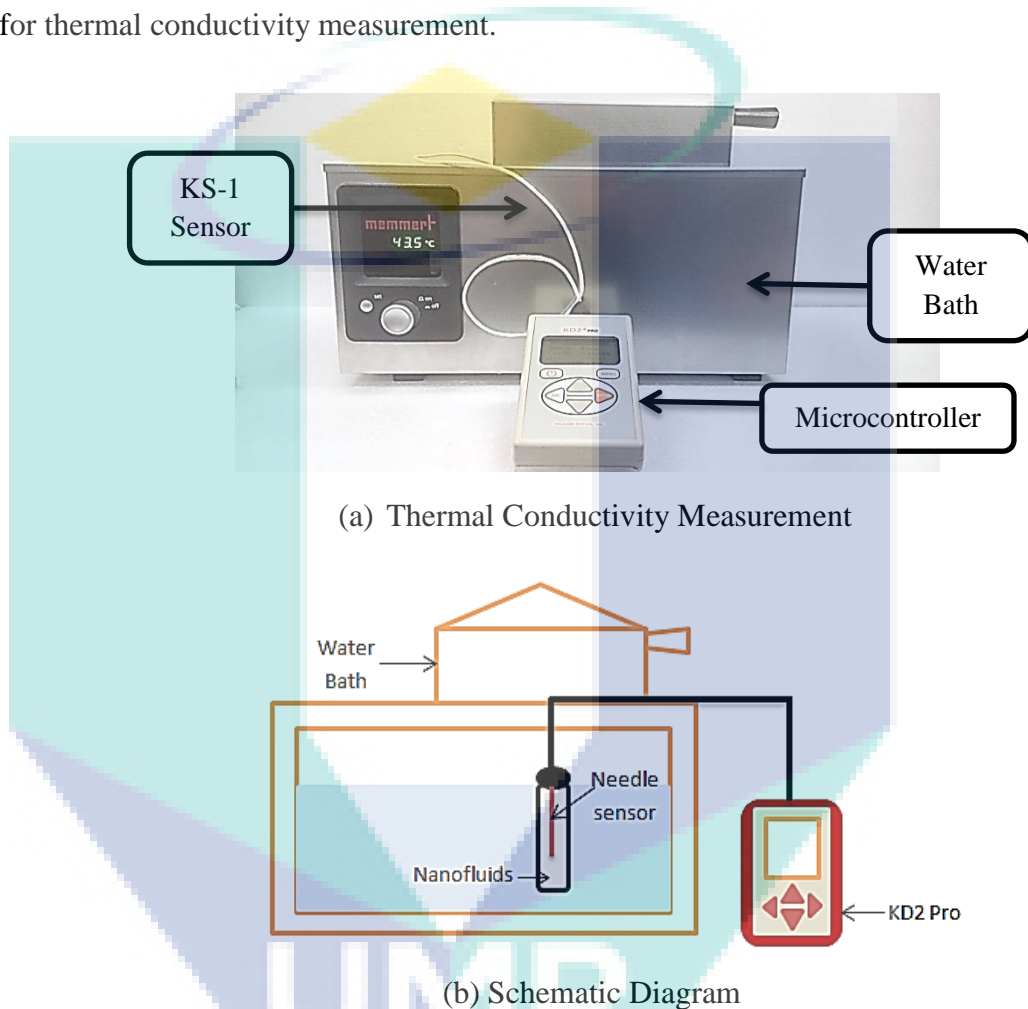


Figure 3.6 KD2 Pro Thermal Properties Analyzer

3.4.3 TiO₂- SiO₂ Nanofluids Dynamic Viscosity

Brookfield LVDV III Ultra Rheometer with circulating water bath was used for the dynamic viscosity measurement. The applicability range for the measurement is from 1 to 6 x 10⁶ mPa.s. This setup can be operated at temperature of less than 100 °C. From the current study, the variation of temperature is conducted in the range of 30 to 80 °C. Basically, the principle in handling the LVDV III Rheometer is dependent on calibrated spring which controlled the spindle. The viscous drag of the fluid against the

spindle is measured by the deflection of calibrated spring. The deflection was recorded through rotary transducers. The value of viscosity range is affected by the rotational of spindle speed, size and shape of spindle, the container of rotated spindle and torque of the calibrated spring. According to the manufacturer, the spindle speed of the viscosity measurement should be considered in range of 10 to 100% and valid for the laminar flow conditions only. Figure 3.7 and Appendix I show the setup for the viscosity measurement and technical specifications for Brookfield LVDV III Ultra Rheometer, respectively.

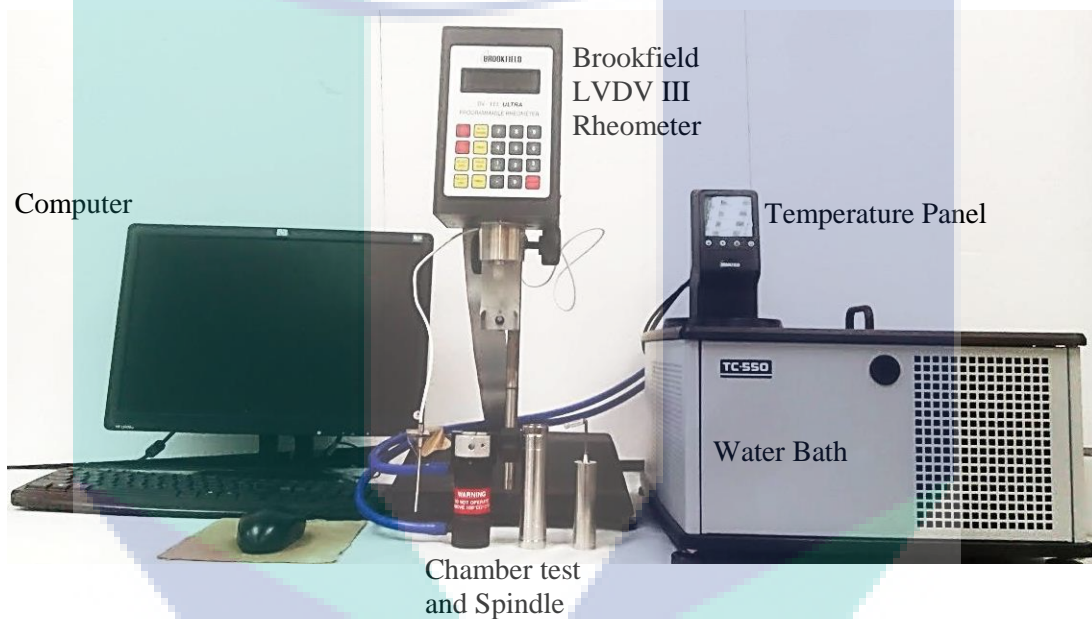


Figure 3.7 Brookfield LVDV III Rheometer Component

3.4.4 Procedure for Dynamic Viscosity Measurement

A minimum of 16 ml volume sample of $\text{TiO}_2\text{-SiO}_2$ nanofluids was poured into cylinder jacket and it was attached to the viscometer. The water bath was used in the viscosity measurement to control and maintain the temperature. The dynamic viscosity of $\text{TiO}_2\text{-SiO}_2$ nanofluids was measured for temperature of 30 to 80 °C. A *RheoCal* program was used during the measurement to extract the reading at the designated torque and temperature. Before the measurement, the spring of the viscometer was reset to zero by using auto-zero in order to minimize the systematic error during measurement. Then, a proper spindle was connected to the spring for the final

measurement. A minimum of five readings at each temperature and concentration were considered for further analysis.

3.4.5 Density and Specific Heat Relation

The density and specific heat of TiO₂-SiO₂ nanofluids for 50:50 nanoparticle mixture ratio were calculated using mixture relations as given by Equations 3.3 and 3.4, respectively (Ho et al., 2010).

$$\rho_{hnf} = (1 - \phi_p) \rho_{bf} + (0.5 \times \phi) \rho_{TiO_2} + (0.5 \times \phi) \rho_{SiO_2} \quad 3.3$$

$$C_{hnf} = \frac{(1 - \phi_p) \rho_{bf} C_{bf} + (0.5 \times \phi) \rho_{TiO_2} C_{TiO_2} + (0.5 \times \phi) \rho_{SiO_2} C_{SiO_2}}{\rho_{hnf}} \quad 3.4$$

where ρ_{hnf} is density of hybrid nanofluids in kg/m³; ρ_{bf} is density of base fluid in kg/m³; ρ_{TiO_2} is density of titanium oxide in kg/m³; ρ_{SiO_2} is density of silicon oxide in kg/m³; ϕ_p is particle volume concentration in %; ϕ is nanofluids volume concentration in %; C_{hnf} is specific heat of hybrid nanofluids in J/kg.K; C_{bf} is specific heat of base fluid in J/kg.K; C_{TiO_2} is specific heat of titanium oxide in J/kg.K; C_{SiO_2} is specific heat of silicon oxide in J/kg.K.

3.5 Experimental Setup for Forced Convection Heat Transfer

In the present study, the experimental setup for forced convection heat transfer analysis was developed by Azmi et al. (2013a); Azmi et al. (2013b); Azmi et al. (2014a); Azmi et al. (2014b). However, some modifications for the experimental setup is required to meet the requirements for the present experimental work. The setup consists of test section, thermocouples, pressure transducer, data logger, flow rate meter, collecting tank, heater regulator and chiller. The experimental setup and

schematic diagram are shown in Figure 3.8 and Figure 3.9, respectively. Table 3.3 shows the summary of each component in the test rig.

Table 3.3 Description of each component in the test rig

Components	Characterization	Function
Data logger	ADAMView Advantech Data Acquisition.	Record the readings of temperature and pressure.
Test section	Copper tube with 1.5 m length. ($d_{in}=16$ mm; $d_{out}=19$ mm)	Test section for the heat transfer analysis.
Chiller	2.8 kW	For cooling the nanofluids coming out from the test section.
Voltage Regulator	1 kW	Supply power for the heating process.
Pump	1 HP	Circulate the nanofluids to the whole system.
Flow rate meter	Range in between 5 to 30 LPM	Control the fluid flow.

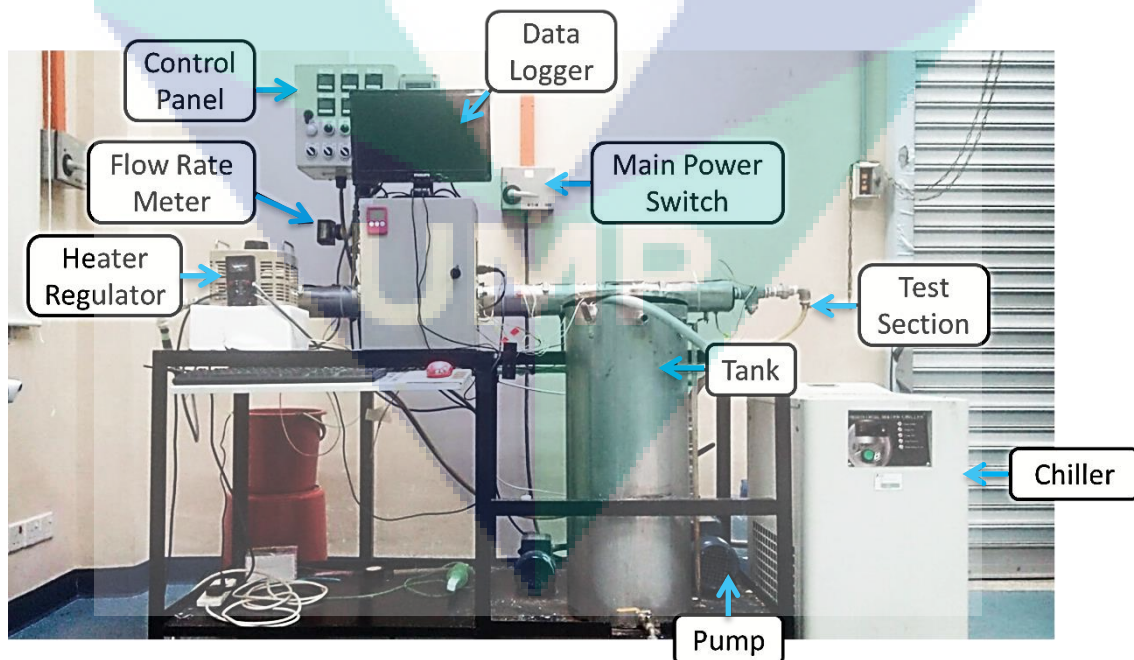


Figure 3.8 Forced Convection Test Rig

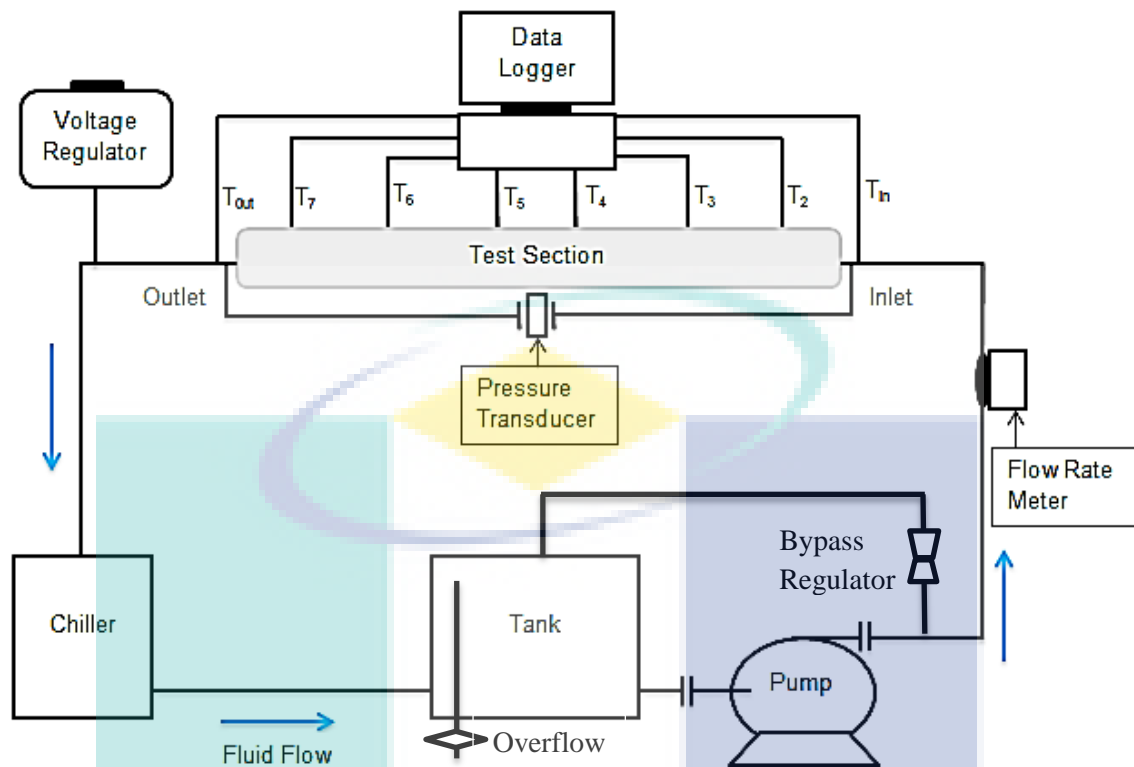


Figure 3.9 Schematic Diagram of Test Rig

3.5.1 Data Logger Connection

The thermocouple and differential pressure transducer is connected to the data acquisition system for the data logger. The experimental data for temperatures and pressure drops were recorded with the ADAMView Advantech software in data logger. The two parameters were then used in the heat transfer analysis to determine the heat transfer coefficient and friction factor of the working fluids. The thermocouples and pressure transducers were connected to the data logger and shown in Figure 3.10. The schematic diagram for the data logger connection is presented in Figure 3.11. Terminal for temperatures and pressure transducers in the data logger are shown in Table 3.4.

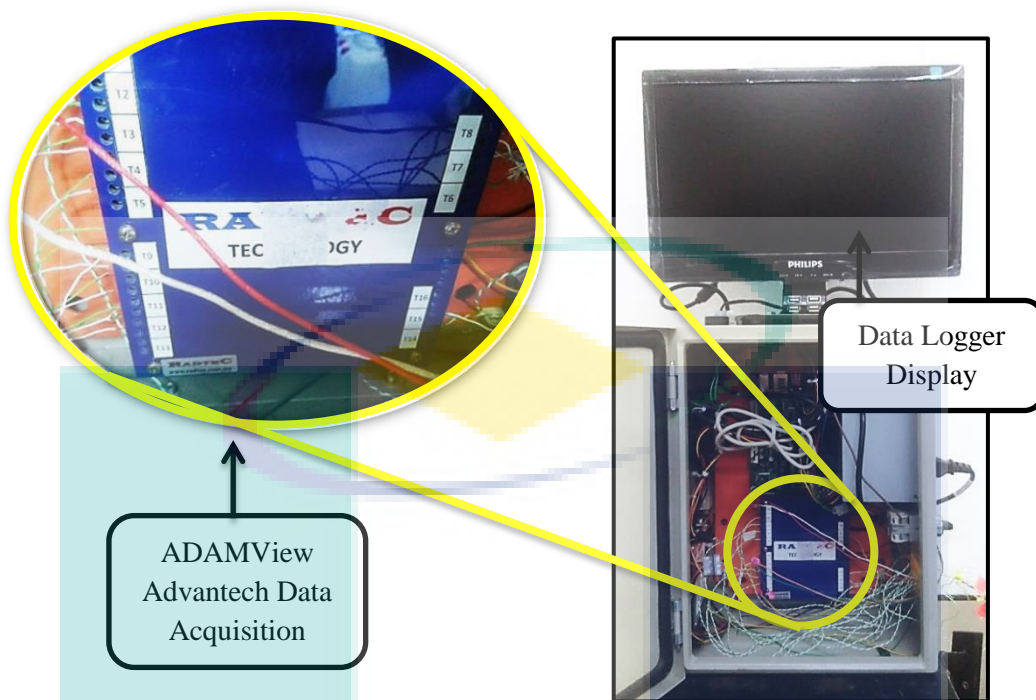


Figure 3.10 Data Logger Setup

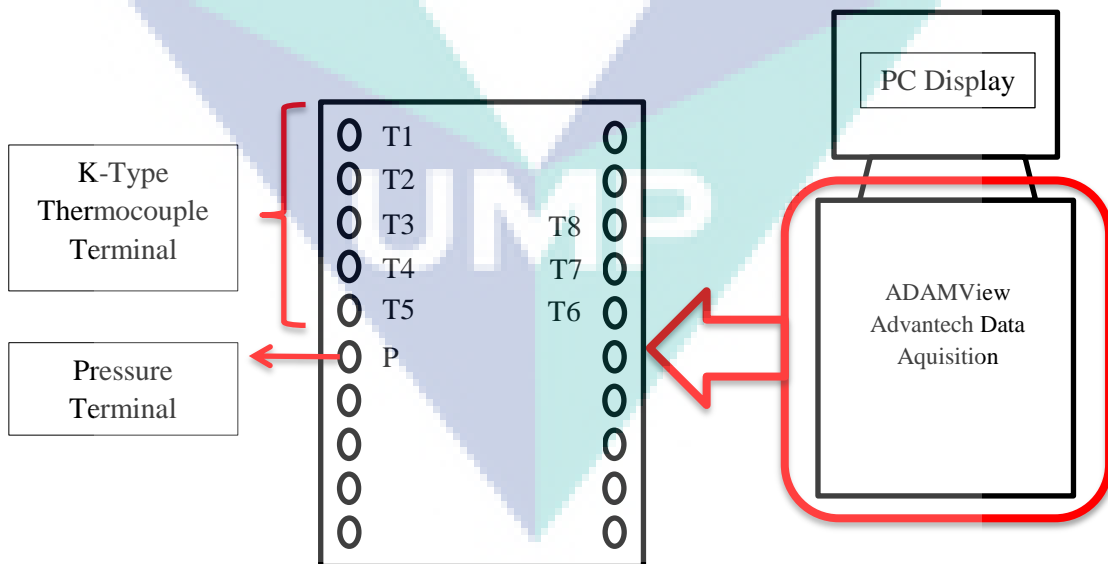


Figure 3.11 Schematic Diagram for Data Logger

Table 3.4 Terminal of Data Logger

Sensor Types	Terminal	Variable recorded in data logger
K-Type Thermocouple	T1	Inlet Temperature
	T2	
	T3	
	T4	Surface Temperature
	T5	
	T6	
	T7	
	T8	Outlet Temperature
Pressure Transducer	P	Pressure

3.5.2 Pressure Transducer Calibration

Differential pressure transducer (model 24PCEFA6D-1) was procured from RS Component and used in the present experimental work to measure the pressure drop. The transducer was specifically designed for operating temperature of -40 to 85 °C and wide range of pressure from 1.0 psi to 20 psi with sensitivity of 70 mV/psi. The transducer was connected to the pressure gauge and digital manometer by using an appropriate hose. Two transducer terminals were connected to power supply and one more terminal was attached to the multimeter for the power validation. The pressure calibration was started with zero pressure reading. The output from transducer was given by the multimeter in millivolt (mV). Then, the pressure gauge was controlled by increasing the input pressure with 0.1 psi interval. The step was repeated for up to 1.0 psi. The measurements were repeated up to three times with the average values are considered for final evaluation. Figure 3.12 shows the final setup for the pressure transducer calibration. Table 3.5 provides the final results of the pressure calibration. Finally, a linear graph for relation between pressure and voltage was plotted and shown in Figure 3.13. to get the calibration equation. Equation 3.5 was developed from the experimental data relation and useful for the estimation of the pressure drop in the present experimental work.

$$\Delta P = 155.15V - 257.89 \quad (3.5)$$

where P is pressure in Pa; V is voltage in mV.

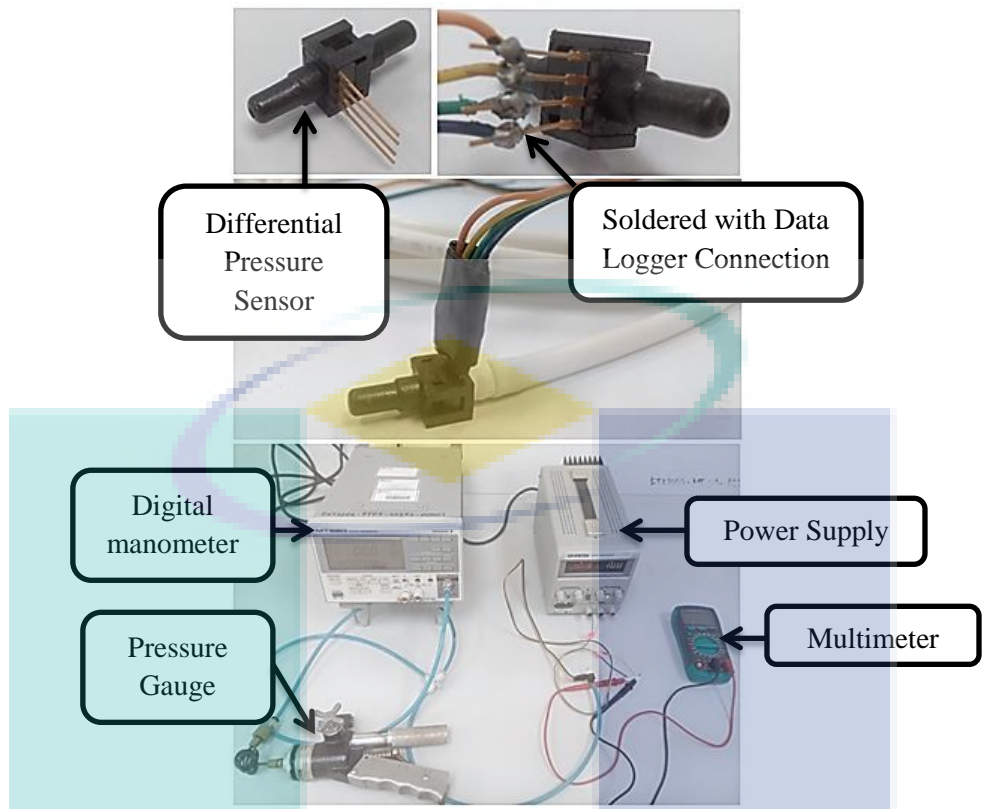


Figure 3.12 Pressure Transducer Calibration Setup

Table 3.5 Calibration readings

Pressure (Psi)	Pressure (Pa)	Voltage (mV)						
		V _{t1}	V _{t2}	V _{t3}	V _{t4}	V _{t5}	V _{t6}	V _{t_{avg}}
0	0	1.5	1.7	1.5	1.6	1.5	1.6	1.57
0.1	689.48	6.2	6.4	6.3	6.2	6.1	6.2	6.23
0.2	1378.95	10.7	10.4	10.5	10.5	10.4	10.5	10.5
0.3	2968.43	14.9	14.9	15.1	15	14.9	14.9	14.95
0.4	2757.90	19.7	19.4	19.4	19.4	19.4	19.4	19.45
0.5	3447.38	24	23.9	23.8	24	24	24	23.95
0.6	4136.86	28.5	28.4	28.4	28.3	28.3	28.4	28.38
0.7	4826.33	32.7	33	32.6	32.7	33	32.7	32.78
0.8	5515.81	37.1	37	37.1	37.3	37	37.4	37.15
0.9	6205.28	41.6	41.6	41.7	41.7	41.6	41.6	41.63

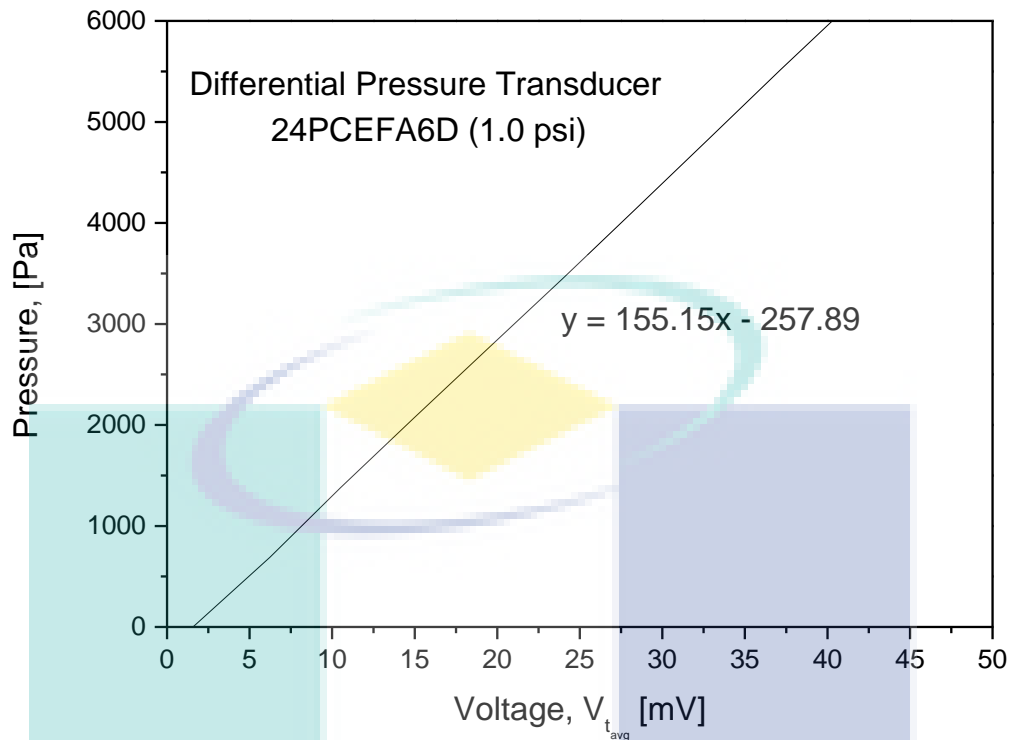


Figure 3.13 Calibration line for 1.0 psi pressure transducer

3.5.3 Test Section Setup

The setup consists of the test section as the main part of the experimental system. The test section was fabricated with a heater, 1.5 m length copper tube with an inner and outer diameter of 16 and 19 mm, respectively and well insulated with fiber glass insulators. Six thermocouples are attached to the body of the tube wall and the other two thermocouples are placed at the inlet and outlet of the test section. A constant input power was supplied by varying a voltage regulator to maintain the heat flux at 7955 W/m². A chiller is provided in the system to cool down the working fluid after being heated, hence to control the bulk temperature at 30, 50 and 70 °C. A flow meter is used to measure the flow rate of working fluids in litre per minute (LPM) and controlled by a regulator. Figure 3.14 shows the fabrication of test section.

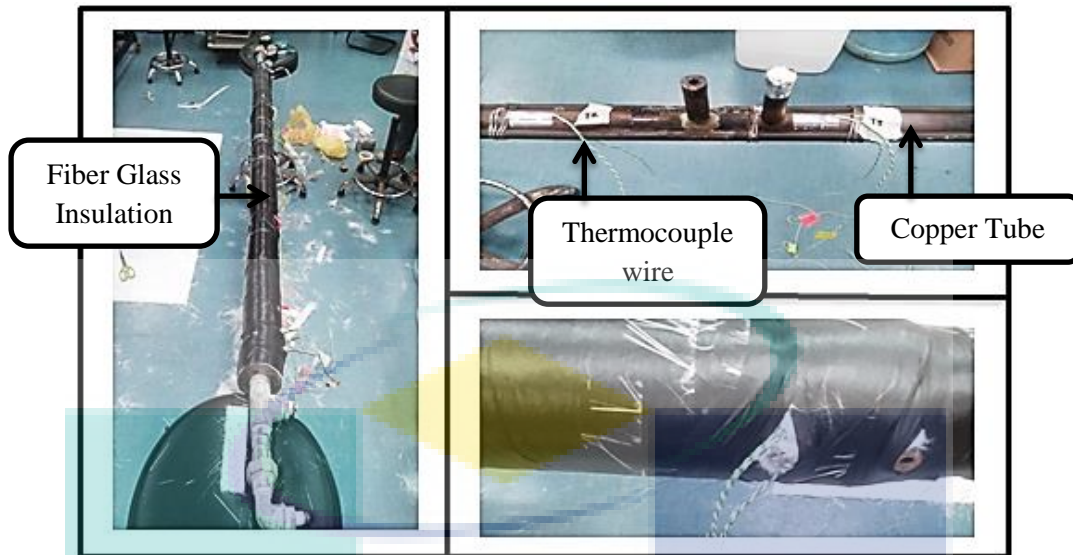


Figure 3.14 Test Section Setup

3.6 Experimental Procedures

Approximately 23 L of distilled water was placed in the collecting tank. Then, the pump was switched on to circulate the flow of fluids through the system. The flow rate of fluids was controlled and adjusted by the bypass valve regulator. Leakage should be avoided in the piping system or any connection of the experimental setup. The present experimental study was regulated the flow at nine different speed for wide range of flowrate from 2 to 22 LPM. The reliability test for the present forced convection heat transfer setup was conducted with 60:40 (water/EG) mixture at different working temperatures of 30, 50 and 70 °C. The experimental data of based fluids are then compared with the available equations in literature. Additionally, the experimental investigation of $\text{TiO}_2\text{-SiO}_2$ nanofluids is conducted for volume concentrations of 0.5 to 3.0% and temperature of 30, 50 and 70 °C. The experimental of $\text{TiO}_2\text{-SiO}_2$ nanofluids was carried out from high concentration to low concentration. The experiment was started at 3.0% volume concentration of $\text{TiO}_2\text{-SiO}_2$ nanofluids. Then, the dilution process was performed to reduce the concentration to a new low concentration. However, the volume of fluids in the collecting tank was maintained at 23 L for all volume concentration during the dilution process. Figure 3.15 shows the experimental procedure of forced convection heat transfer setup.

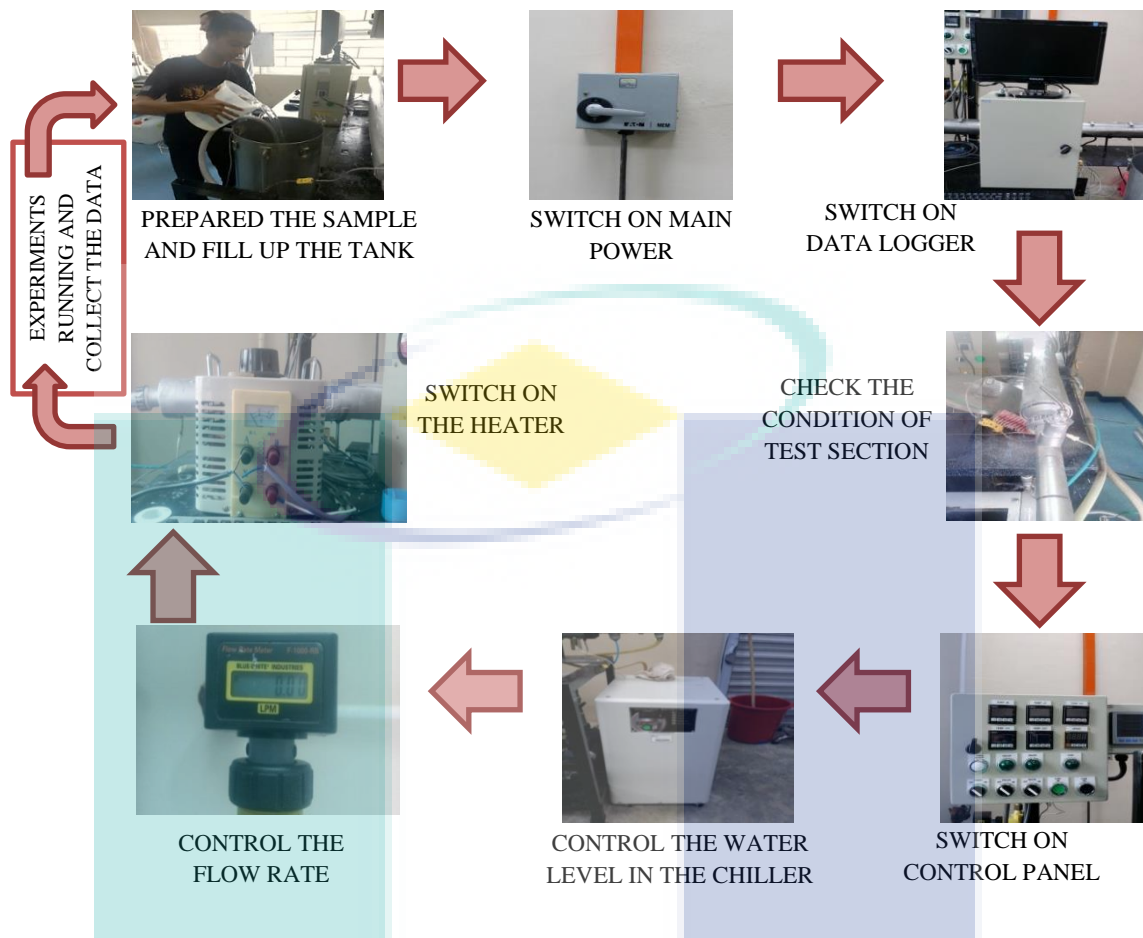


Figure 3.15 Process flow for experimental of forced convection test rig

3.7 Heat Transfer Analysis

In the present analysis, the thermo-hydraulic parameters consist of heat transfer coefficient, rate of heat transfer, pressure drop and friction factor. The rate of heat transfer was determined from heat transfer analysis inside the copper tube whereas the heat transfer coefficient was estimated from the electrical power supplied by the heater. The dimensionless parameters such as Reynolds number, Prandtl number and Nusselt number were also determined in the present analysis. The rate of heat transfer and friction factor from experimental analysis was compared with the existing models from literature (Blasius, 1913; Dittus & Boelter, 1930).

3.7.1 The Rate of Heat Transfer

Equations 3.6 to 3.9 were used for the estimation of heat transfer coefficient. The rate of heat transfer was expressed by Equation 3.6 and based on Newton's law of cooling.

$$Q = h_{\text{exp}} A_s (T_s - T_b) \quad 3.6$$

where Q is rate of heat transfer in W; h_{exp} is heat transfer coefficient in $\text{W}/\text{m}^2\cdot\text{K}$; A_s is surface area in m^2 ; T_s is surface temperature in $^\circ\text{C}$; T_b is bulk temperature in $^\circ\text{C}$.

The heat transfer coefficient was estimated from the electrical energy supplied by assuming the losses are negligible. The electrical energy supplied by the heater and absorbed by the liquid was validated with the aid of Equations 3.7 and 3.8.

$$Q = V_t \times I \quad 3.7$$

$$Q = h_{\text{exp}} A_s (T_s - T_b) = \dot{m} C_p \Delta T \quad 3.8$$

where Q is rate of heat transfer in W; h_{exp} is heat transfer coefficient in $\text{W}/\text{m}^2\cdot\text{K}$; A_s is surface area in m^2 ; T_s is surface temperature in $^\circ\text{C}$; T_b is bulk temperature in $^\circ\text{C}$; \dot{m} is mass flow rate in $\text{kg}/\text{m}^2\cdot\text{s}$; C_p is specific heat in $\text{J}/\text{kg}\cdot\text{K}$; ΔT is average temperature in $^\circ\text{C}$. V_t is voltage in volts; I is current in amps.

The difference between the electrical energy supplied and energy absorbed by the liquid is less than 2.0%. Neglecting the heat loss to the atmosphere, the heat transfer coefficients and the Nusselt numbers were respectively estimated for water and TiO_2 -

SiO₂ nanofluids with Equation 3.9. The effect of tube thickness of heat transfer through the wall of copper tube and nanofluids were shown in Appendix J. The sample calculation shows deviation of less than 0.1%.

$$h_{\text{exp}} = \frac{Q}{A_s \Delta T} = \frac{Q}{\pi D_{\text{in}} L \times (T_s - T_b)} \quad 3.9$$

where h_{exp} is experimental heat transfer coefficient in W/m².K; Q is rate of heat transfer; A_s is surface area in m²; ΔT is average temperature in °C; D_{in} is inner diameter in m; L is length in m; T_s is surface temperature in °C; T_b is bulk temperature in °C.

3.7.2 Dimensionless Parameters

The dimensionless parameters were determined with the aid of Equations 3.10 to 3.13. The Reynolds number and Prandtl number of TiO₂-SiO₂ nanofluids were determined from Equations 3.10 and 3.11, respectively. The properties were referred at the bulk temperature, T_b . Whereas, the specific heat and density of TiO₂-SiO₂ nanofluids were estimated from the mixture relations and given by Equations 3.3 and 3.4. However, thermal conductivity and viscosity of TiO₂-SiO₂ nanofluids were evaluated by using the present measurement data from experiments.

$$\text{Re}_{\text{hnf}} = \frac{\rho_{\text{hnf}} \bar{V} D}{\mu_{\text{hnf}}} \quad 3.10$$

$$\text{Pr}_{\text{hnf}} = \frac{\mu_{\text{hnf}} C_{\text{hnf}}}{k_{\text{hnf}}} \quad 3.11$$

where Re_{hnf} is Reynolds number of hybrid nanofluids; ρ_{hnf} is density of hybrid nanofluids in kg/m^3 ; \bar{V} is average velocity in m/s; D is diameter in m; μ_{hnf} is viscosity of hybrid nanofluids in mPa.s; Pr_{hnf} is prandtl number of hybrid nanofluids; C_{hnf} is specific heat of hybrid nanofluids in J/kg.K; k_{hnf} .is thermal conductivity of hybrid nanofluids in W/m.K.

The Nusselt number from experiment and Dittus-Boelter (1930) equations were estimated by using Equations 3.12 and 3.13, respectively.

$$Nu_{exp} = \frac{h_{exp} D}{k} \quad 3.12$$

$$Nu_{DB} = 0.023 Re^{0.8} Pr^{0.4} \quad 3.13$$

where Nu_{exp} is Nusselt number of experimental; h_{exp} is experimental of heat transfer coefficient in $W/m^2.K$; D is diameter in m; k is thermal conductivity in $W/m.K$; Nu_{DB} is dittus-boelter nusselt number; Re is Reynolds number; Pr .is Prandtl number.

3.7.3 Friction Factor and Pressure Drop

The pressure drop of experimental study was recorded by the pressure transducer. Blasius (1913) equation was shown by Equations 3.14 and 3.15. The experimental values recorded by the pressure transducer were used in the estimation of the Darcy friction factor by using Equation 3.16.

$$\Delta P_{Blasius} = f_{Blasius} \left(\frac{L}{D} \right) \left(\frac{\rho V^2}{2} \right) \quad 3.14$$

$$f_{Blasius} = \frac{0.3164}{Re^{0.25}} \quad 3.15$$

$$f_{exp} = \frac{\Delta P_{exp}}{\left(\frac{L}{D}\right)\left(\frac{\rho \bar{V}^2}{2}\right)} \quad 3.16$$

where $\Delta P_{Blasius}$ is Blasius pressure drop; ΔP_{exp} is experimental pressure drop; $f_{Blasius}$ is Blasius friction factor; f_{exp} is experimental friction factor; L is length in m; D is diameter in m; ρ is density in kg/m³; V is volume in m³; \bar{V} is average velocity in m/s; Re is Reynolds number; Pr is Prandtl number.

3.8 Uncertainty Analysis

The uncertainties analysis was carried out when measuring the instrumentations and variable parameter errors for the setup. A study was done by Moffat (1988) in describing the uncertainties of the experimental work. He found that the uncertainty analysis can be used to find the best method and most reliable technique for the measurement in any system. An uncertainty analysis of measurement was prepared in order to estimate the systematic error in the present experimental work. The evaluation of uncertainty estimation for Reynolds number, heat flux, heat transfer coefficient, Nusselt number and friction factor were estimated. The range of uncertainties is summarized and presented in Table 3.6 and Appendix K respectively. The instrumentation error was calculated in the range of 0.1 to 0.89%. The instrumentation error analysis of the present experimental work is shown in Table 3.7.

Table 3.6 The uncertainty of parameter

No.	Parameter	Uncertainty error (%)
1	Reynolds number, Re	0.29
2	Heat flux, q	0.18
3	Heat transfer coefficient, h	0.89
4	Nusselt number, Nu	0.89
5	Friction factor, f	0.39
6	Thermo-physical properties	0.10

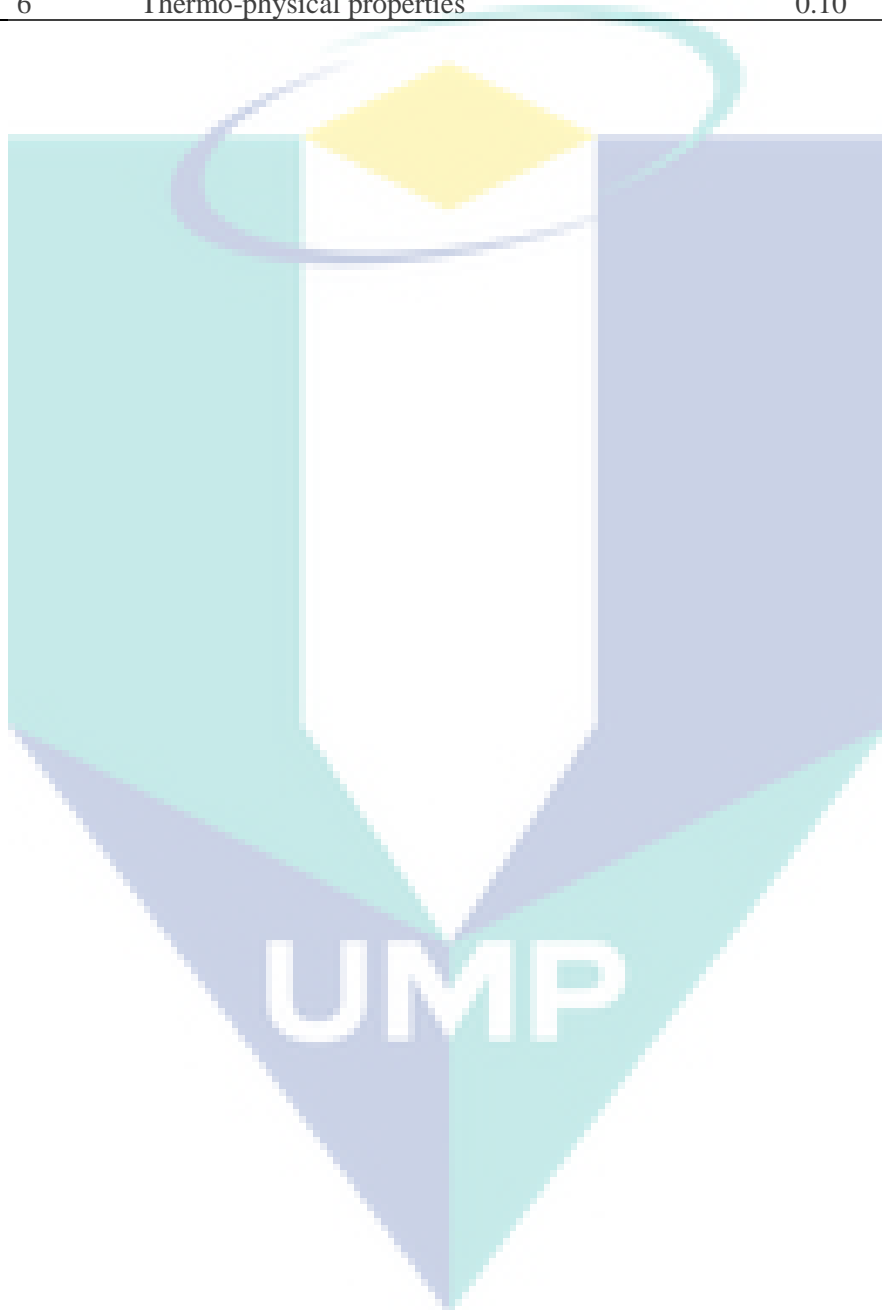


Table 3.7 Uncertainty of Instrument

No.	Name of instrument	Range of instrument	Variable measured	Least division in measuring instrument	Values measured in experiment		% uncertainty	
					Min	Max	Min	Max
1	Thermocouple	0 - 300 °C	Bulk temperature, T_b	$U_T = 0.1 \text{ }^\circ\text{C}$ $U_{T_b} = \sqrt{0.1^2 + 0.1^2}$ $= 0.14142$	29.05	70.75	0.48682	0.19989
2	Thermocouple	0 - 300 °C	Average surface temperature, T_w	$U_T = 0.1 \text{ }^\circ\text{C}$ $U_{T_b} = \sqrt{5 \times 0.1^2}$ $= 0.22361$	30.92	75.98	0.72314	0.29429
3	Flow meter	2 - 30 LPM	Volume flow rate, \dot{V}	0.01	3.99	20.4	0.25063	0.04902
			Velocity, \bar{V}	-	0.33074	1.69080	0.25063	0.04902
4	Voltage	0 - 240 V	Voltage, V	0.01	110.1	110.1	0.00908	0.00908
5	Current	0 - 15 A	Current, I	0.01	5.45	5.45	0.18349	0.18349
6	Pressure transducer	0 - 184 mV	Pressure drop, ΔP	0.01	7.5	143.75	0.13333	0.00696
		0 - 7072.4 Pa		-	226.43	5511.39	0.13333	0.00696
		0 - 1.0 psi		-	0.03283	0.79915	0.13333	0.00696

CHAPTER 4

RESULTS AND DISCUSSION

4.1 Introduction

This chapter provides the results from the experimental works and discussion for the forced convection heat transfer. The chapter also discusses the stability observation and micrograph evaluation of $\text{TiO}_2\text{-SiO}_2$ nanofluids through TEM images. In addition, the properties measurement verification and experimental validations were performed by comparing the present experimental data with the available data in the literature. This chapter also discusses the evaluation of heat transfer coefficient (HTC) and pressure drop of hybrid nanofluids. Correlation regression models were also developed for the estimation of thermal conductivity, dynamic viscosity, Nusselt number and friction factor.

4.2 Stability of $\text{TiO}_2\text{-SiO}_2$ Nanofluids

The stability of $\text{TiO}_2\text{-SiO}_2$ nanofluids was observed for a month of preparation. The stability of hybrid nanofluids is measured by using UV-Vis spectrophotometer and confirmed by Transmission Electron Microscopy (TEM).

4.2.1 Sedimentation Observation

The sedimentation observation applied for $\text{TiO}_2\text{-SiO}_2$ nanofluids just after the preparation, the samples of $\text{TiO}_2\text{-SiO}_2$ nanofluids for different concentrations were placed in a test tube for a month. It was observed that the nanofluid samples were stable without apparent sedimentation even after 30 days of preparation as shown in Figure 4.1. According to Yu and Xie (2012), the nanofluids is considered to be stable when the concentration or particle size of supernatant particles keep constant. Figure 4.1 (a)

shows the sample of $\text{TiO}_2\text{-SiO}_2$ nanofluids after preparation. After one month, the $\text{TiO}_2\text{-SiO}_2$ nanofluids samples are observed to be stable Figure 4.1 (b).

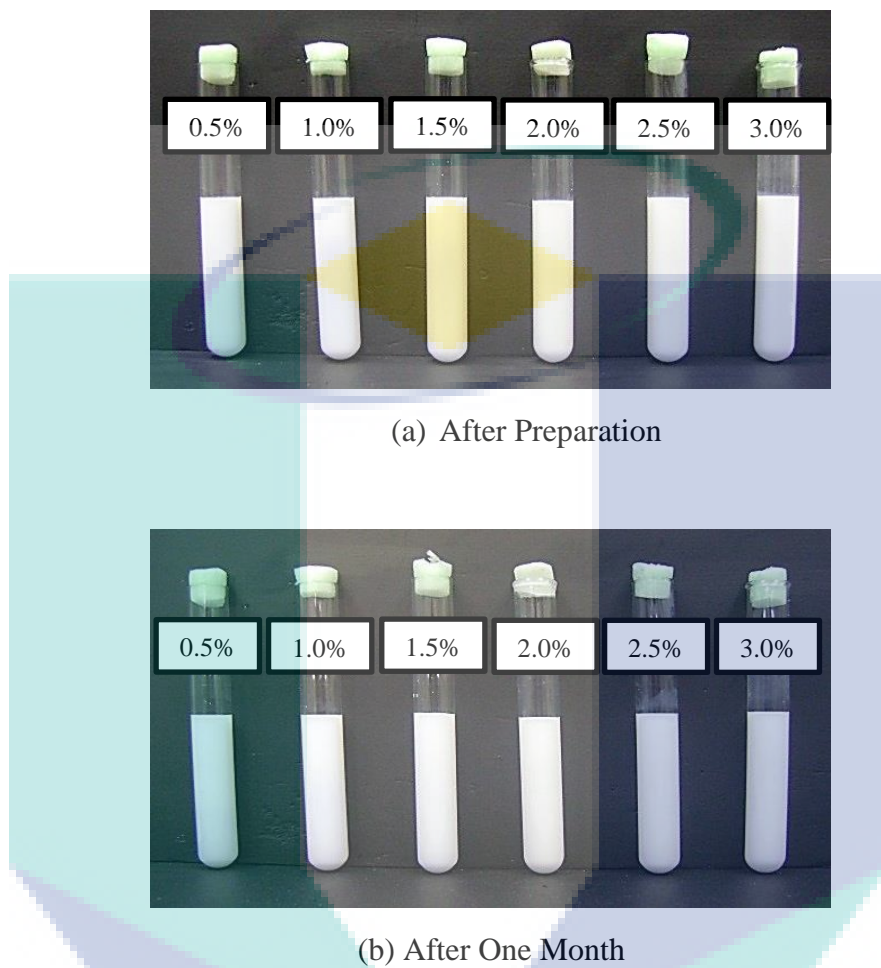


Figure 4.1 Observation of $\text{TiO}_2 - \text{SiO}_2$ samples

4.2.2 UV-Vis Spectrophotometer Evaluation

The absorbance ratio of the $\text{TiO}_2\text{-SiO}_2$ nanofluids is determined by using UV-Vis spectrophotometer to study the effect of the sonication time on the stability. Figure 4.2 represents the absorbance ratio of $\text{TiO}_2\text{-SiO}_2$ nanofluids in comparison with water/EG mixture of the base fluids. The ideal value for absorbance ratio is equal to one or 100%. The sample without sonication process was observed to be in unstable conditions with absorbance ratio of less than 30% while the sample with 1.5 hours sonication time was found to be the most stable sample with 80% absorbance ratio after 10 days of preparation. Above 1.5 hour sonication time, the absorbance ratio tends to reduce, which represents a reduction in stability. Therefore, the stability of hybrid

nanofluids is also influenced by the sonication time. Duangthongsuk and Wongwises (2008) also suggested 1.5 hour as the optimum time for sonication process. However, they studied for single TiO_2 /water nanofluids. The TiO_2 - SiO_2 nanofluids samples for thermo-physical properties study and heat transfer performance evaluation at different volume concentrations were prepared for up to 1.5 hours sonication time.

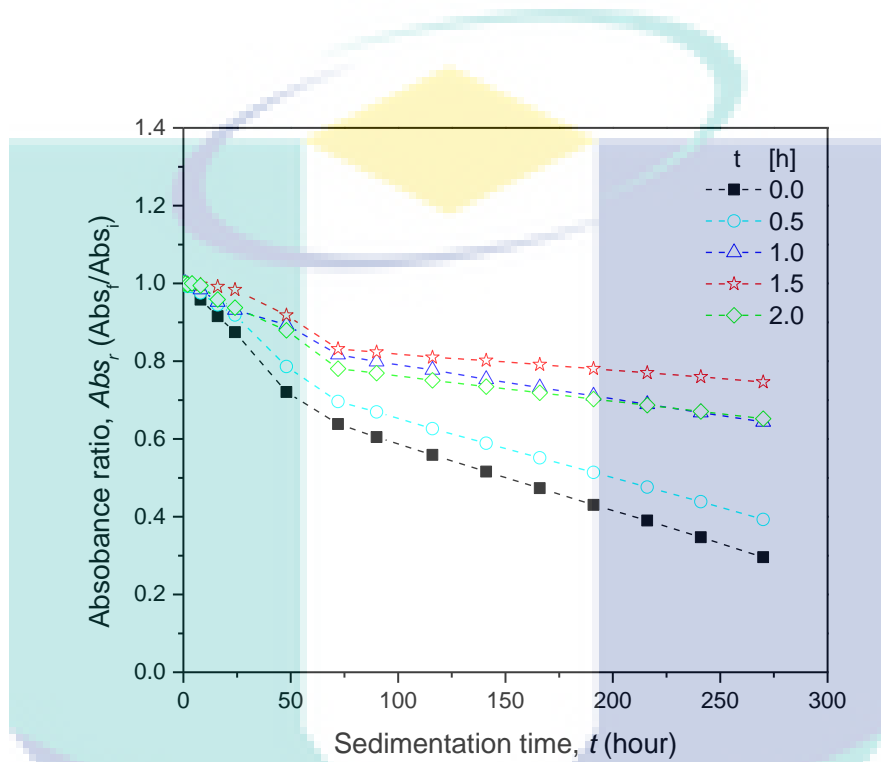


Figure 4.2 Absorbance ratio for difference sonication time

4.2.3 Characterization of TiO_2 - SiO_2 Nanofluids

The characterization of single TiO_2 and SiO_2 nanofluids were obtained by the transmission electron microscopy (TEM) techniques, which also widely used by other researchers (Sundar et al., 2016; Yarmand et al., 2016b). Figure 4.3 (a) and (b) shows the TEM images for both single TiO_2 (X 140,000 magnifications) and SiO_2 (X 17,000 magnifications) nanoparticles, respectively. The TiO_2 nanoparticles were observed to be nearly spherical with an average size of 50 nm as shown in Figure 4.3 (a). Furthermore, the SiO_2 nanoparticles were found to be spherical with an average size of 22 nm as presented in Figure 4.3 (b). Figure 4.3 (c) shows the TEM image with X 39,000 magnification for particle distribution of both SiO_2 and TiO_2 nanoparticles suspended in

W:EG based nanofluids. From Figure 4.3 (c), the bigger size of particle represents TiO_2 whereas the smaller size represents SiO_2 nanoparticles. The SiO_2 nanoparticle fills the gap between the TiO_2 nanoparticles. This condition will contribute to the reduction in space between the particles.

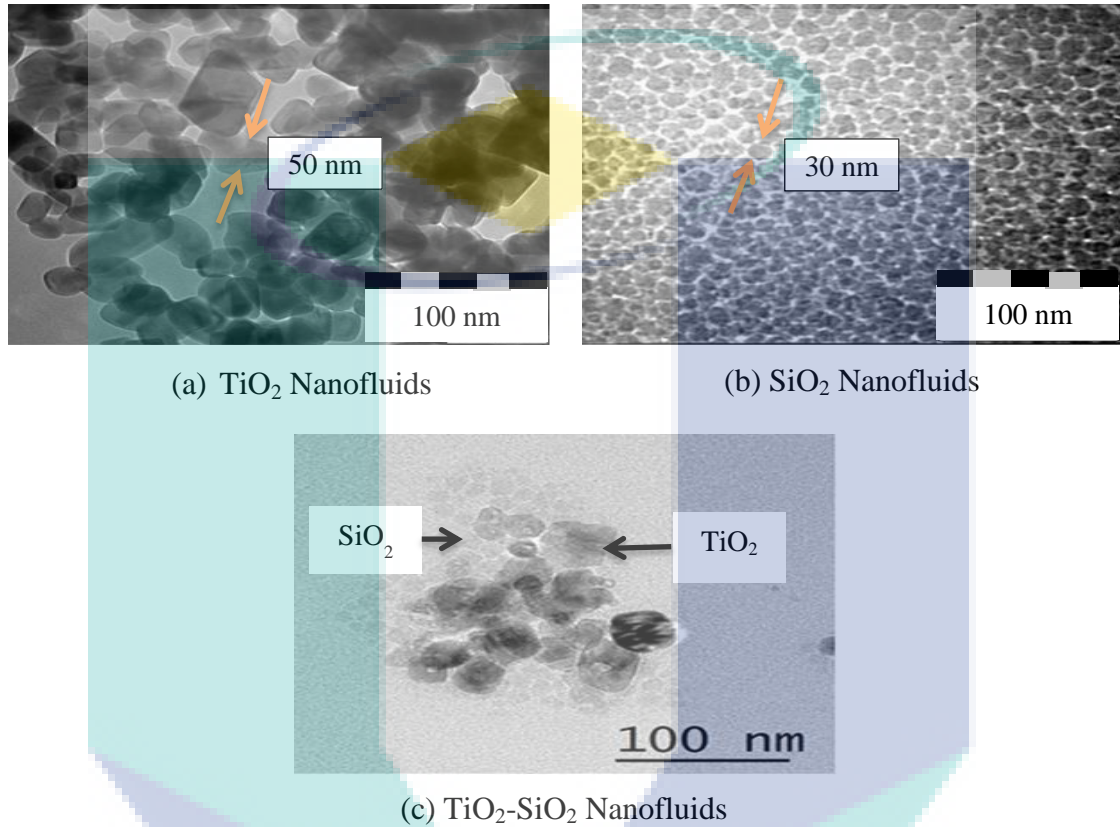


Figure 4.3 TEM images (100 nm scales) for single type nanofluid of TiO_2 and SiO_2 , and TiO_2 - SiO_2 hybrid nanofluids for 1.0% volume concentrations

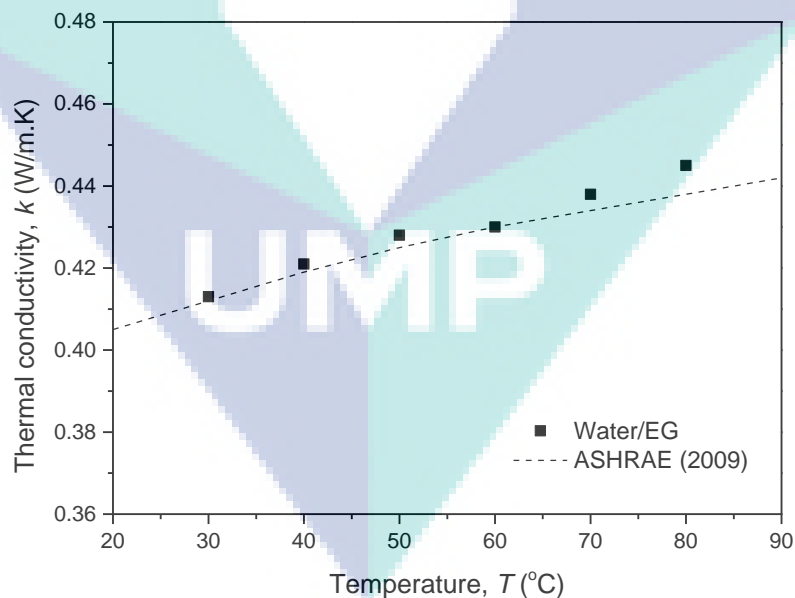
4.3 Thermo-physical Properties

The effectiveness of thermo-physical properties such as thermal conductivity, dynamic viscosity, specific heat and density enhanced the performance of heat transfer. The previous study shows that good performance of heat transfer coefficient is found at the highest value of thermal conductivity, specific heat and density but lowest value of dynamic viscosity. The thermal conductivity and dynamic viscosity of TiO_2 - SiO_2 nanofluids at different volume concentrations (0.5 to 3.0%) with various temperatures (30 to 80°C) are shown in Figure 4.4, Figure 4.5, and Figure 4.6. From the figure, the

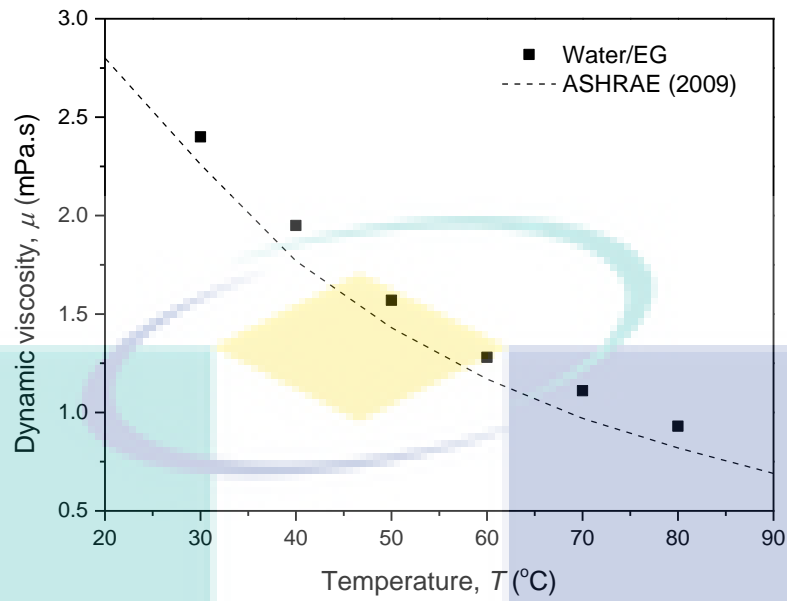
base fluid properties were validated by comparing the experimental data to ASHRAE (2009). It was found to be in good agreement for both properties.

4.3.1 Properties Measurement Validation

The thermal conductivity and viscosity measurements were validated by comparing the present data of water/EG (60:40) mixture with ASHRAE (2009). Figure 4.4 (a) shows the benchmark test for the thermal conductivity measurement. The maximum deviation for the mixture of water/EG data from ASHRAE results was found to be 1.6%. Reddy and Rao (Reddy & Rao, 2013) performed a similar validation and found maximum deviation of 2.5% for their base fluid. Hence, the thermal conductivity measurements of the present study are reliable due to the small deviation. The same validation was also performed for the viscosity measurements. The present viscosity data is in good agreement with the data from ASHRAE (2009) and shown in Figure 4.4 (b). The measured data for the base fluid of water/EG mixture followed a similar trend with ASHRAE (2009). It shows that the viscosity decreases with increase of temperature.



(a) Thermal Conductivity



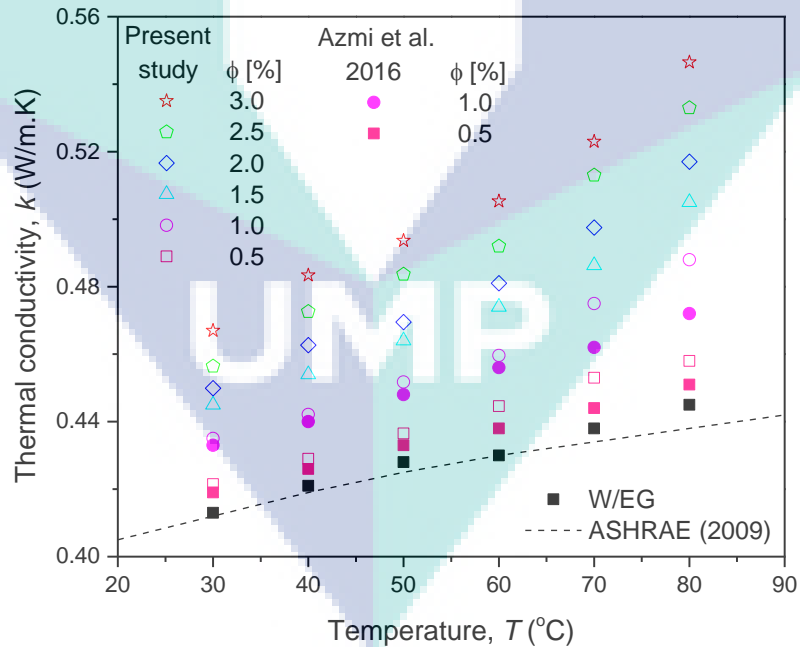
(b) Dynamic Viscosity

Figure 4.4 Comparison of water/EG (60:40) thermal conductivity and viscosity experimental results with ASHRAE (2009)

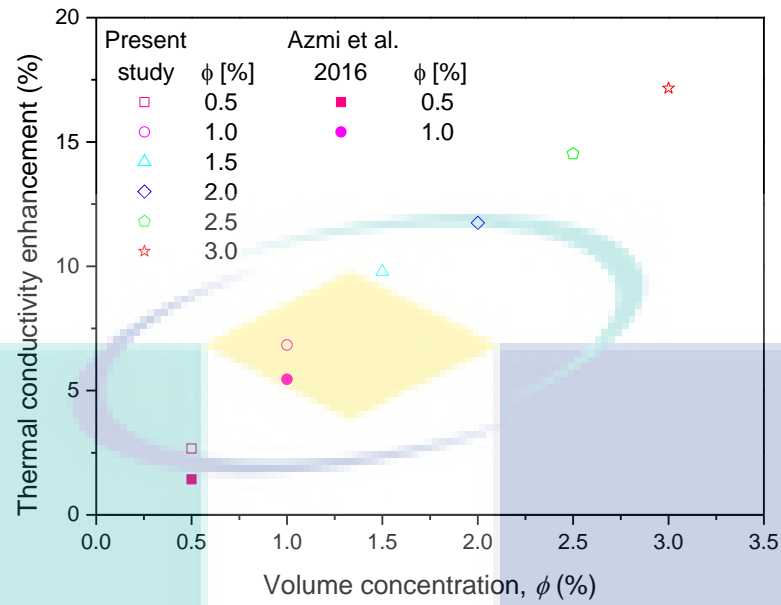
4.3.2 Thermal Conductivity of TiO₂-SiO₂ Nanofluids

Figure 4.5 (a) shows the thermal conductivity of TiO₂-SiO₂ nanofluids for the experimental data of various volume concentrations (0.5 – 3.0%) and different temperatures (30 – 80 °C) with comparing by previous study for single nanofluids. As observed in Figure 4.5 (a), the thermal conductivity of TiO₂-SiO₂ nanofluids is enhanced with increase of volume concentration and temperature. The highest enhancement was found at the temperature of 80 °C and volume concentration of 3.0% with 22.8% higher than the based fluids. This happens because the collision of particles is more at high temperatures and affects the kinetic energy for the enhancement of thermal conductivity (Azmi et al., 2016a; Keblinski et al., 2002; Teng et al., 2010a). The thermal conductivity of TiO₂-SiO₂ nanofluids is always higher than the base fluid for all volume concentrations. The same pattern was also observed by previous researchers such as Suresh et al. (2011), Baghbanzadeh et al. (2012) and Hemmat Esfe et al. (2015c).

The clear presentation of enhancement for the range of concentration and temperature is shown in Figure 4.5 (b). The figure presents the thermal conductivity ratio of TiO₂-SiO₂ nanofluids compared to the base fluid. The ratio of thermal conductivity of TiO₂-SiO₂ nanofluids is nearly proportional to the volume concentration. The higher volume concentration of the hybrid nanofluids and the greater number of particles suspended in the base solution may lead to enhancement of surface-to-volume ratio and collisions between particles (S.Harandi et al., 2016). This effect can also be due to the Brownian motion of the nanoparticles in the base fluid (Teng et al., 2010b). Other previous studies encountered similar results to the present study (Baghbanzadeh et al., 2012; Hemmat Esfe et al., 2015d; Kumar et al., 2016b). Beside that, from the Figure 4.5 also shows the comparison of single TiO₂ nanofluids by previous study with the present study of hybrid nanofluids for the same of base fluid mixture ratio. The hybrid nanofluids was improve the thermal conductivity of single nanofluids with 46.4% and 20.2% enhancement for volume concentration of 0.5 and 1.0%, respectively.



(a) Experimental Thermal Conductivity



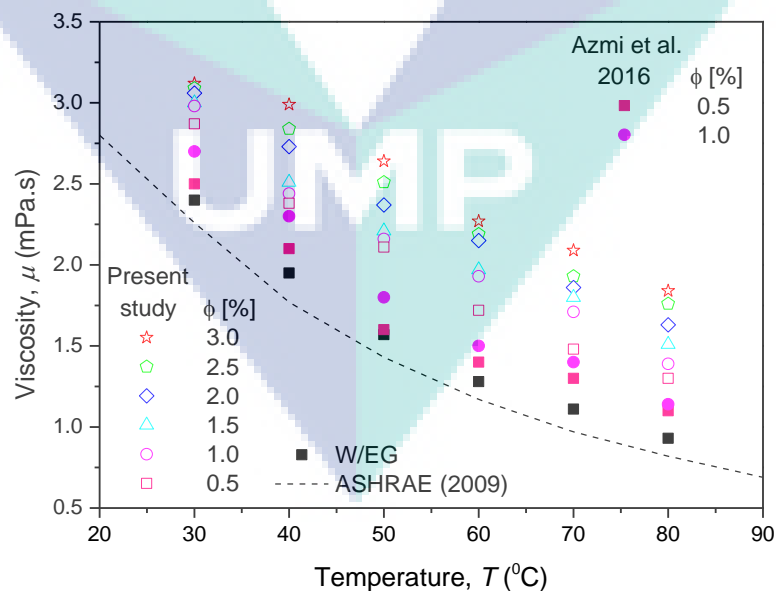
(b) Enhancement of Thermal Conductivity

Figure 4.5 Thermal conductivity of $\text{TiO}_2\text{-SiO}_2$ and single TiO_2 nanofluids

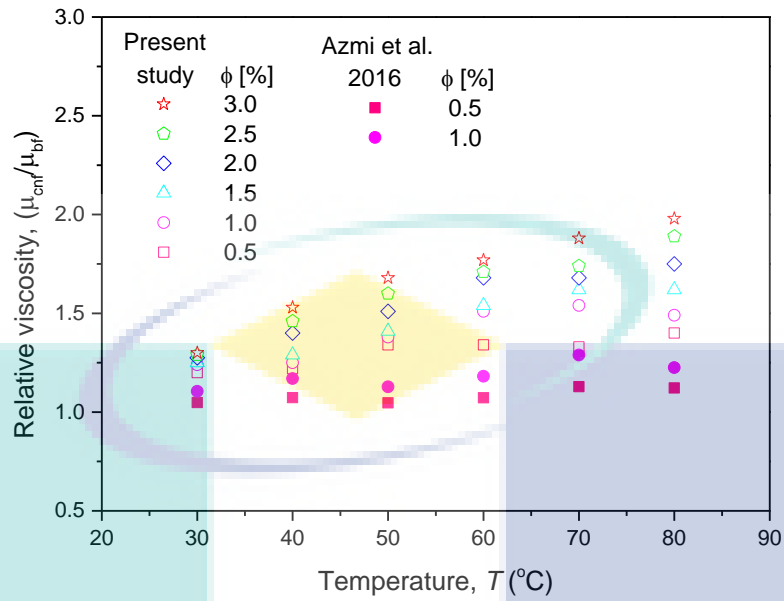
4.3.3 Dynamic Viscosity of $\text{TiO}_2\text{-SiO}_2$ Nanofluids

Figure 4.6 (a) shows the variation of viscosity for different concentrations and temperatures. The viscosity of $\text{TiO}_2\text{-SiO}_2$ nanofluids increases with increasing volume concentrations and decreases with increasing temperature, which follows the trend of the base fluid and single TiO_2 nanofluids. Nguyen et al. (2007a) and Hemmat Esfe et al. (2017) highlighted that the fluid internal shear stress is greater at high volume concentrations whereas the increment of the temperature weakened the inter-molecular interaction. The increase in viscosity with respect to particle concentration is clearly much greater than base fluid at high volume concentrations. The interaction between $\text{TiO}_2\text{-SiO}_2$ nanoparticles and base fluid (water/EG) also contribute to the greater enhancement as compared to a single type of nanofluids. This was also discovered by Bahrami et al. (2016) and Soltani and Akbari (2016a). The viscosity of nanofluids followed the base fluid trend which decreased with the increase of temperature. This is because the intermolecular interactions between the molecules become weak when the temperature rises, hence lowering the viscosity (Afrand et al., 2016b; Nguyen et al., 2007b).

The relative viscosity of $\text{TiO}_2\text{-SiO}_2$ nanofluid is shown in Figure 4.6 (b). The viscosity ratio shows increments with increasing volume concentrations. However, the relative viscosity is almost constant with temperature with a small fluctuation. The lowest average relative viscosity was observed for 0.5% volume concentration with 25.9%. Meanwhile, the highest average relative viscosity of 62.5% increment was obtained for 3.0% concentration. The maximum relative viscosity value was noticed for 3.0% concentration and 80 °C temperature. Generally, the relative viscosities within the present range of volume concentration and temperature increased from 21.3 to 80.0% when compared to the water/EG mixture. However, the variation of the relative viscosity in the range of the temperature studied was undetermined. Nevertheless, this behaviour may be related to the difference in the structure and thickness of the diffused fluid layers around the nanoparticles in the base fluids, which affects the effective volume concentration, and ultimately the viscosity of the suspension (Timofeeva et al., 2011). The dynamic viscosity for single type of TiO_2 nanofluids also were shown in Figure 4.6. The pattern of graph are same with hybrid nanofluids and the base fluid which affect by the volume concentration and temperature. The viscosity increment of $\text{TiO}_2\text{-SiO}_2$ nanofluids compared with single TiO_2 nanofluids are 16.93% and 15.24% for volume concentration of 0.5% and 1.0%, respectively.



(a) Experimental Dynamic Viscosity



(b) Relative Dynamic Viscosity

Figure 4.6 Variation of dynamic viscosity of TiO₂-SiO₂ and TiO₂ nanofluids

4.3.4 Properties Regression Equations

Equation 4.1 and 4.2 were developed from the experimental data for the estimation of thermal conductivity and dynamic viscosity of TiO₂-SiO₂ nanofluids, respectively. The equations were applicable for TiO₂-SiO₂ nanofluids ratio of 50:50 in water/EG mixture (60:40) with volume concentrations up to 3.0% and the temperatures range from 30 to 80 °C. The average deviation, standard deviation and maximum deviation for thermal conductivity were 1.4%, 1.4% and 4.6%, respectively, while for viscosity were 3.7%, 2.6% and 9.5%, respectively. The measurement data for both properties is in good agreement with the estimated values from Equation 4.1 and 4.2 based on the statistical analysis shown in Figure 4.7 and Figure 4.8.

$$k_r = \frac{k_{hnf}}{k_{bf}} = \left(1 + \frac{\phi}{100}\right)^{5.5} \left(\frac{T}{80}\right)^{0.01} \quad 4.1$$

$$\mu_r = \frac{\mu_{hnf}}{\mu_{bf}} = 37 \left(0.1 + \frac{\phi}{100}\right)^{1.59} \left(0.1 + \frac{T}{80}\right)^{0.31} \quad 4.2$$

where k_r is thermal conductivity ratio in W/m.K; k_{hnf} is thermal conductivity of hybrid nanofluids in W/m.K; k_{bf} is thermal conductivity of base fluid in W/m.K; μ_r is viscosity ratio in mPa.s; μ_{hnf} is viscosity of hybrid nanofluids in mPa.s; μ_{bf} is viscosity of base fluid in mPa.s; ϕ is volume concentration in %; T is temperature in °C.

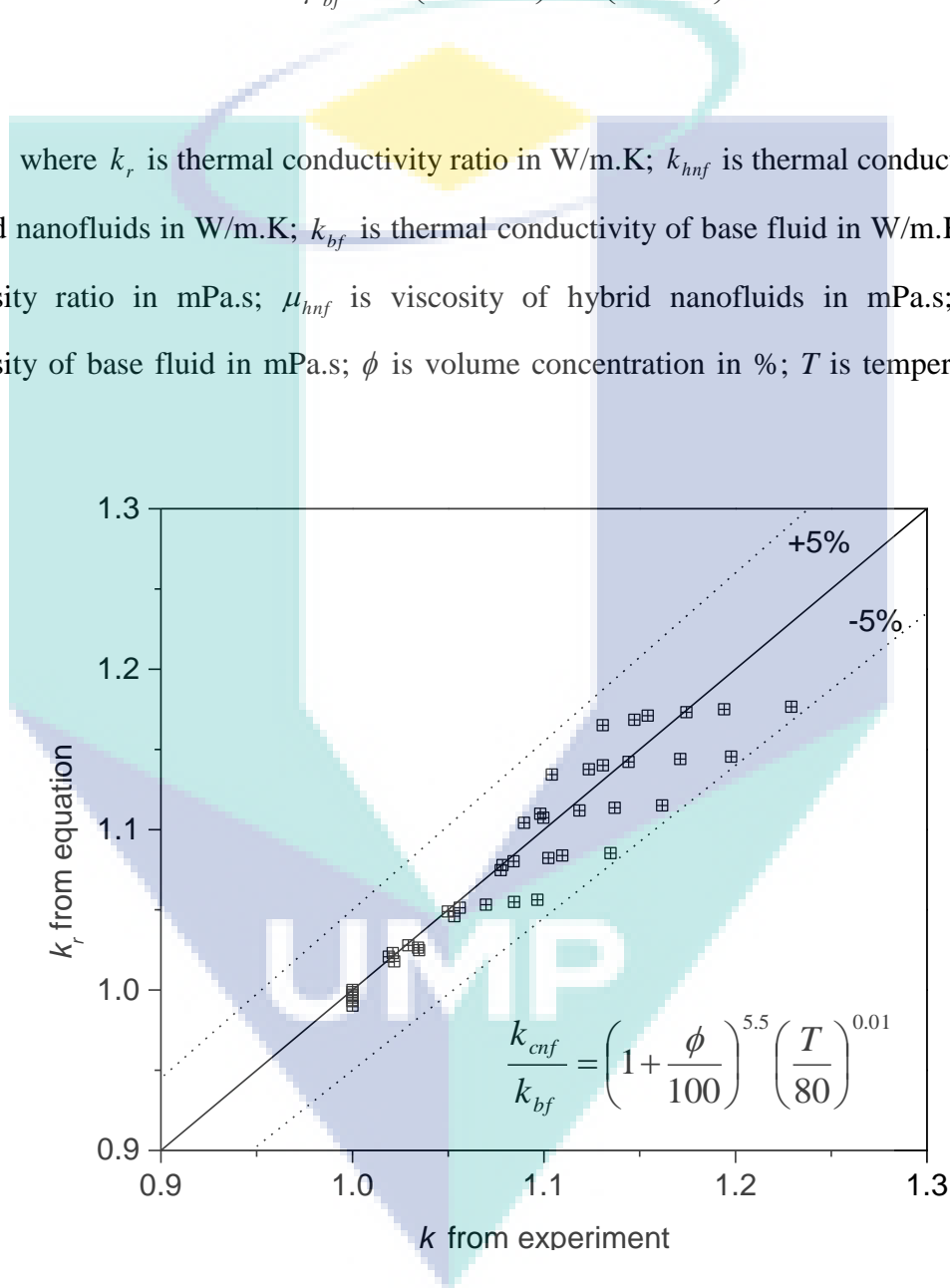


Figure 4.7 Comparison of thermal conductivity ratio with Eq. 4.1

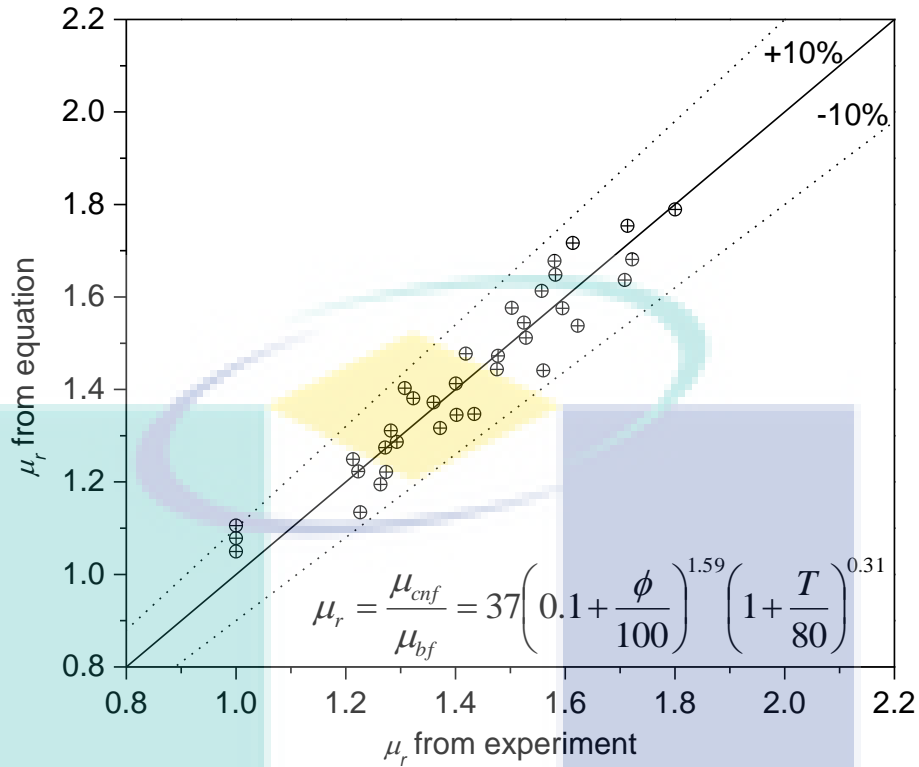


Figure 4.8 Comparison of relative viscosity with Eq. 4.2

4.3.5 Comparison with Literature

Figure 4.9 (a) demonstrates a comparison of thermal conductivity ratio in the present study with the data from S.Harandi et al. (2016) and Ahammed et al. (2016). Meanwhile, Figure 4.9 (b) displays the comparison of relative viscosity from the present study compared to Ahammed et al. (2016). The present study obtained the thermal conductivity ratio of the TiO₂-SiO₂ nanofluids between 1.02 to 1.23 times higher than the base fluid. Ahammed et al. (2016) conducted an investigation of thermal conductivity and viscosity of Al₂O₃-graphene (G) nanofluids in a water base. They observed that the thermal conductivity ratio was more than 1.1 times higher than the water base for 0.1% volume concentration. In another paper, S.Harandi et al. (2016) measured that the thermal conductivity ratio for *f*-MWCBT-Fe₃O₄ was lower than Al₂O₃-G even at higher volume concentrations of 0.8%. Meanwhile, the present study observed that the thermal conductivity enhancement was more than 1.15 times higher than the water/EG mixture for 3.0% concentration. Figure 4.9 (b) shows the relative viscosity for 0.17% volume concentration. The data from the present study shows lower increment viscosity ratios compared to the literatures for temperatures between 30 to

50 °C. This is because the viscosity strongly depends on the volume concentration. According to Sundar et al. (2017), the magnitude of enhancement in thermal conductivity and relative viscosity strongly depend on types of the nanoparticles and base fluid.

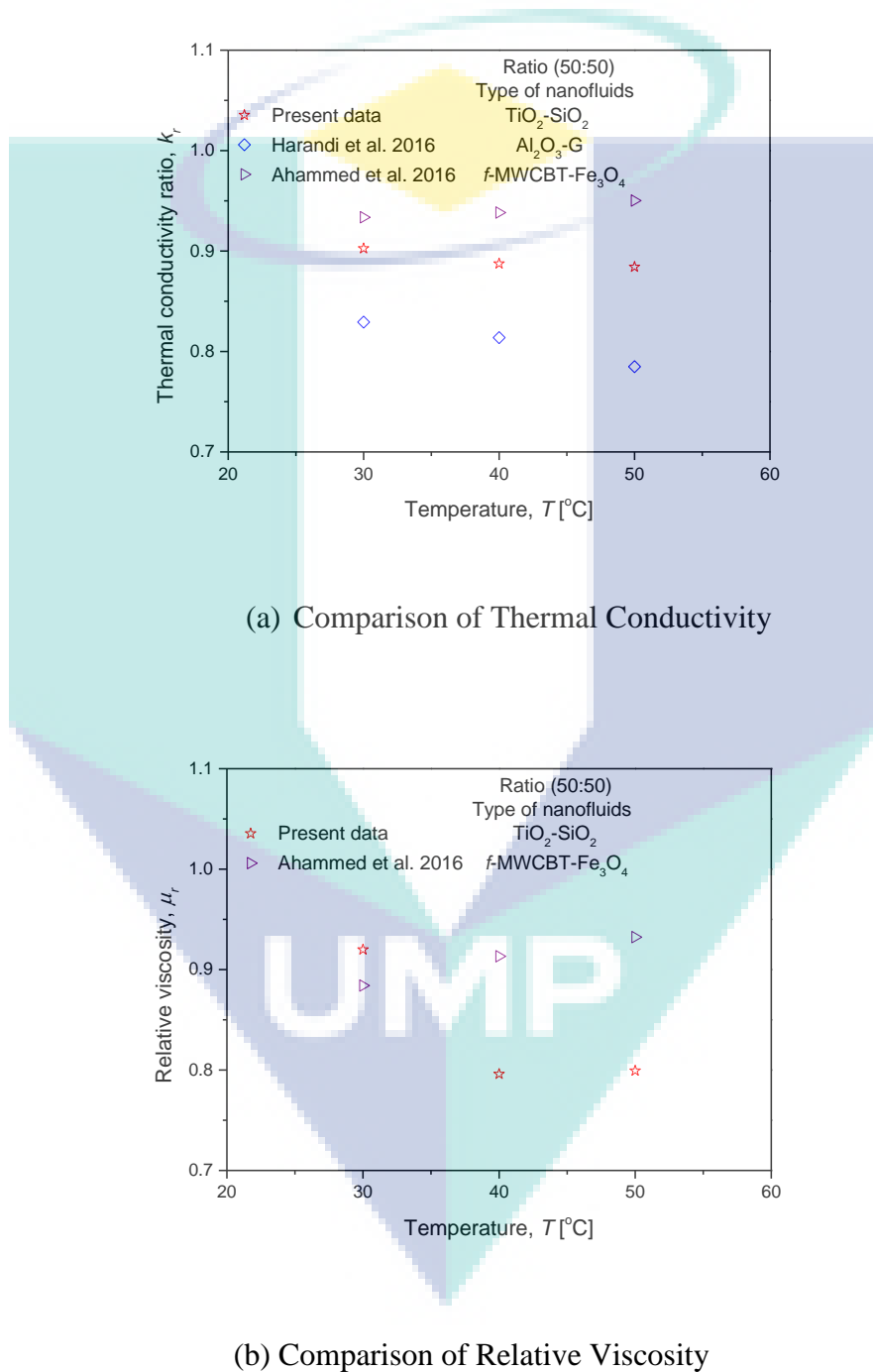


Figure 4.9 Comparison of TiO₂-SiO₂ nanofluids properties with the data from literatures

4.3.6 Properties Enhancement Ratio

The property enhancement ratio, PER is given by the dynamic viscosity increment ratio over the enhancement of thermal conductivity (Azmi et al., 2014b; Garg et al., 2008). Figure 4.10 represents the property enhancement ratio and it was plotted against temperature for different volume concentrations. According to Garg et al. (2008), a PER value of below 5 presents the nanofluids to behave as a good heat transfer fluid. The PER is higher than 5 for volume concentrations of 0.5 and 1.0% as shown in Figure 4.10. Meanwhile, it can be seen that $TiO_2 - SiO_2$ nanofluids at concentrations of $\phi \geq 1.5\%$ is expected to behave as a good heat transfer fluid with PER less than 5. However, at low concentrations of $\phi = 0.5\%$, the PER is greater than 5 and not suggested for heat transfer applications. Further experimental heat transfer investigation is necessary to confirm the present prediction.

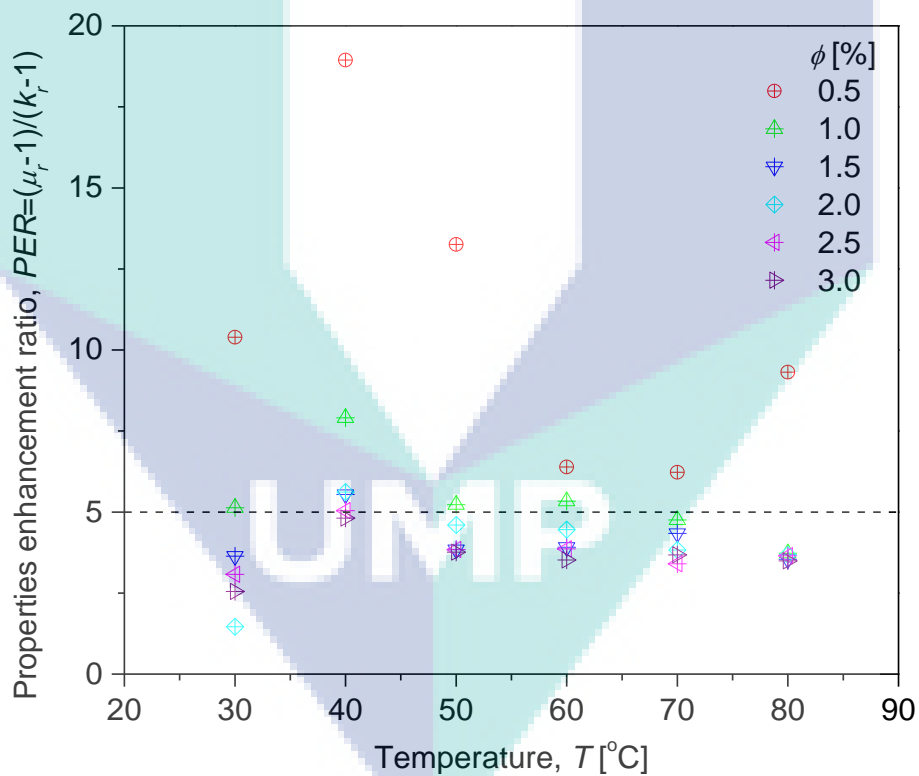


Figure 4.10 Variation of property enhancement ratio with concentration and temperature

4.4 Convective Heat Transfer Experimental Study

The result from the experimental of forced convection heat transfer study was obtained from the heat transfer analysis as in section 3.7. The Nusselt number of base fluid was validated with the Dittus-Boelter (1930) relation and then followed by the discussion of heat transfer performances. Finally, the friction factor and pressure drop of experiments were discussed in details.

4.4.1 Experimental Validation

Section 3.7 shows the analysis of heat transfer that was used in the estimation of Nusselt number, pressure drop and friction factor. The present validation of Nusselt number of based fluid (water/EG) is shown in Figure 4.11. From the experimental study, the Nusselt number values of based fluid for the temperature of 30, 50 and 70 °C shows a good agreement with the Dittus-Boelter (1930) relation by 0.91, 2.88 and 1.78% of maximum deviation, respectively. The previous researchers also used Dittus-Boelter (1930) relation as a benchmark for the validation of Nusselt number (Abdolbaqi et al., 2017; Azmi et al., 2014b).

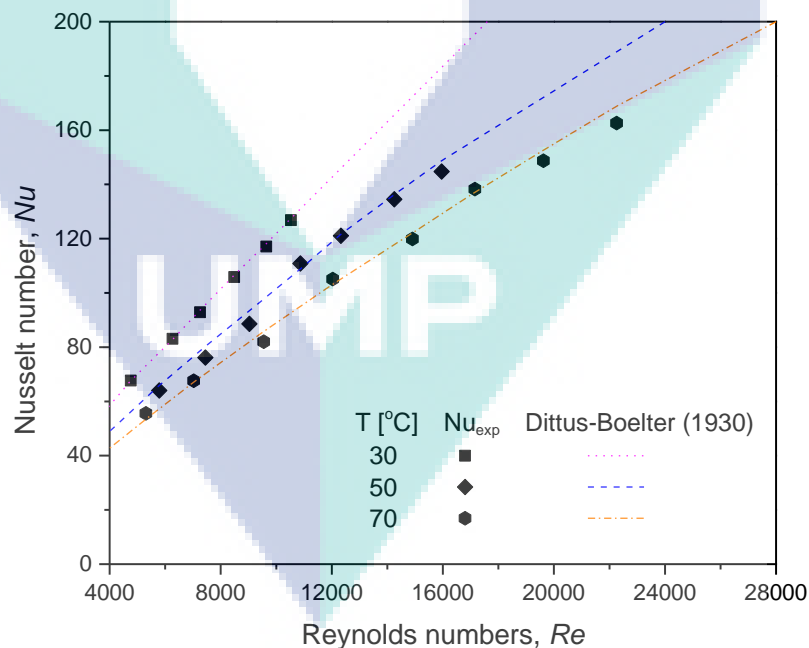
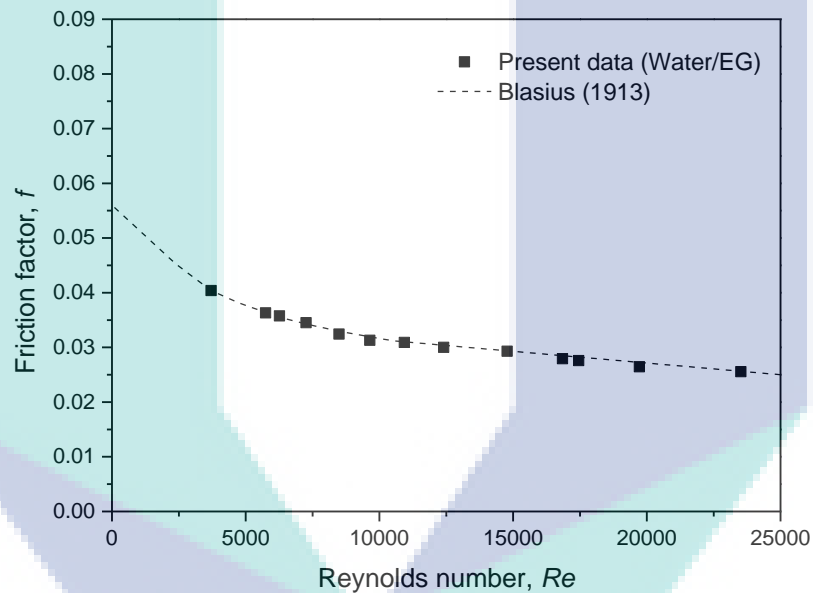


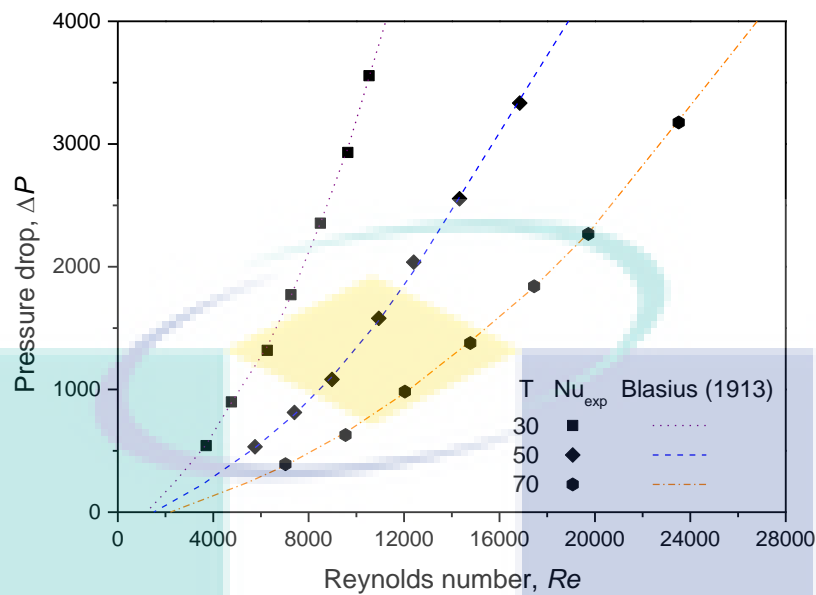
Figure 4.11 Validation of Nusselt number

Figure 4.12 shows the validation of based fluid friction factor and pressure drop by comparing with Blasius (1913) equations. Based on Figure 4.12 (a), the friction

factor of based fluid value is closed to Blasius (1913) equations lines. The maximum and minimum deviation value are 2.9 and 0%, respectively compared with Blasius (1913) relation. The same pattern was shown for the pressure drop of based fluid as in Figure 4.12 (b). The pressure drop of based fluid distribution are scattered near to the Blasius (1913) line. The average deviation of based fluid pressure drop compared with Blasius (1913) equation at 30, 50 and 70 °C are 0.66, 1.19, and 1.29%, respectively. Based on the deviation of based fluid friction factor and pressure drop, the validation data are in good agreement with Blasius (1913) relation. Then, the experimental of $\text{TiO}_2\text{-SiO}_2$ nanofluids is undertaken at the same operating condition and procedure.



(a) Friction factor



(b) Pressure drop

Figure 4.12 Validation of friction factor and pressure drop

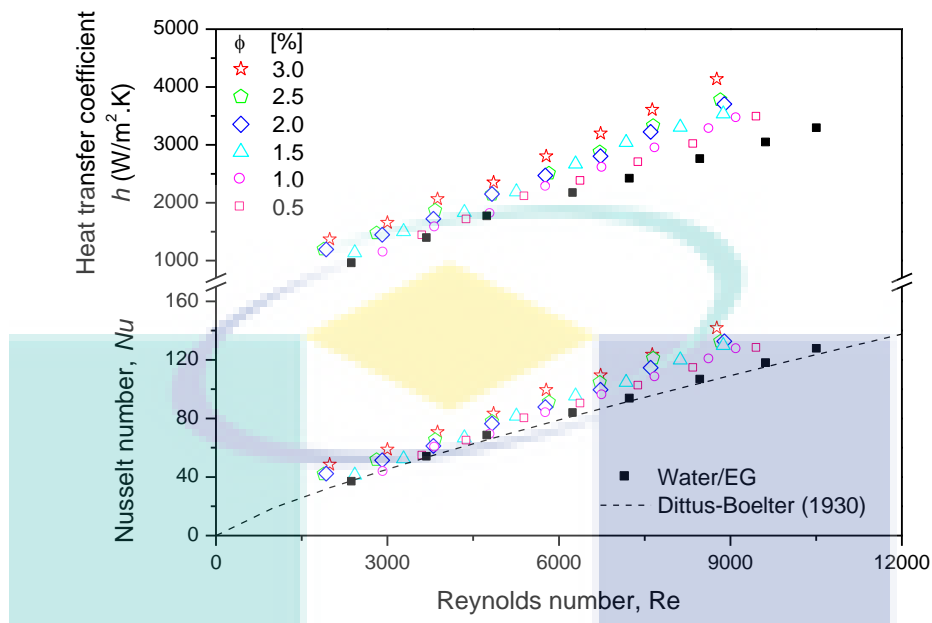
4.4.2 Heat Transfer Coefficient and Nusselt Number

The experimental Nusselt number for water/EG (60:40) mixture at different working temperatures of 30, 50 and 70 °C is presented in Figure 4.11. The experimental results were compared with the Dittus-Boelter (1930) relation given by Equation (3.13) for data validation (Azmi et al., 2016a; Azmi et al., 2017; Hamid et al., 2016). As observed in Figure 4.11, the experimental value is in agreement with the Dittus-Boelter (1930) relation. The maximum deviations were found up to be 0.9, 2.9 and 1.8% for working temperatures of 30, 50 and 70 °C, respectively. For this reason, the reliability and consistency of the present experimental setup is further confirmed and being used for the TiO_2-SiO_2 nanofluids heat transfer evaluation.

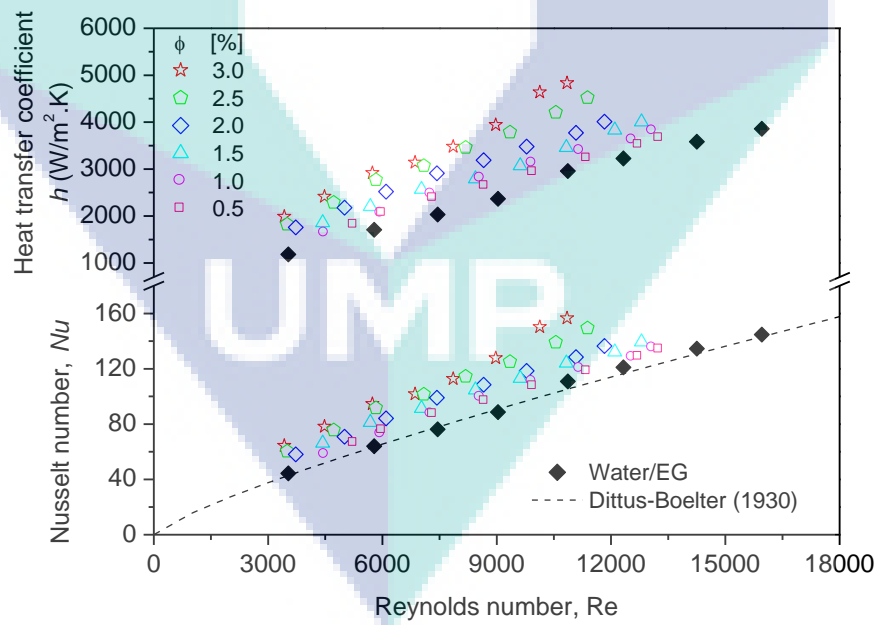
Figure 4.13 shows the heat transfer coefficient and Nusselt number of TiO_2-SiO_2 nanofluids at three different working temperatures of 30, 50 and 70 °C in turbulent flow. It can be observed that the experimental data for TiO_2-SiO_2 nanofluids is in good agreement with the data trend given by Dittus and Boelter (2 1930) and the base fluid

but is also applicable for different working temperatures as shown in Figure 4.13 (a) - (c). Figure 4.13 (a) shows the heat transfer coefficient and Nusselt number of $\text{TiO}_2\text{-SiO}_2$ nanofluids for bulk temperature of 30 °C. The Reynolds number was influenced the increasing of heat transfer coefficient and Nusselt number by 45.9% maximum enhancement were found at volume concentration of 3.0% whereas 9.7% enhancement occurs at 0.5% concentration. However, all of the concentration is higher than the base fluid and improved more than 9.0% compared with based. The same pattern was shown for the heat transfer coefficient and Nusselt number as in Figure 4.13 (b). The figure shows the heat transfer coefficient and Nusselt number increased with the increasing of volume concentration and Reynolds number. At bulk temperature of 50 °C, the heat transfer coefficient was enhanced more than 11% compared with the base fluid. Meanwhile, the maximum enhancement were occur at 3.0% volume concentration of $\text{TiO}_2\text{-SiO}_2$ nanofluids by 67.5% for bulk temperature of 50 °C. It can be seen that the increasing of temperature from 30 °C to 50 °C, clearly shows greater augmentation for value of heat transfer coefficient by the concentration (Hajjar et al., 2014).

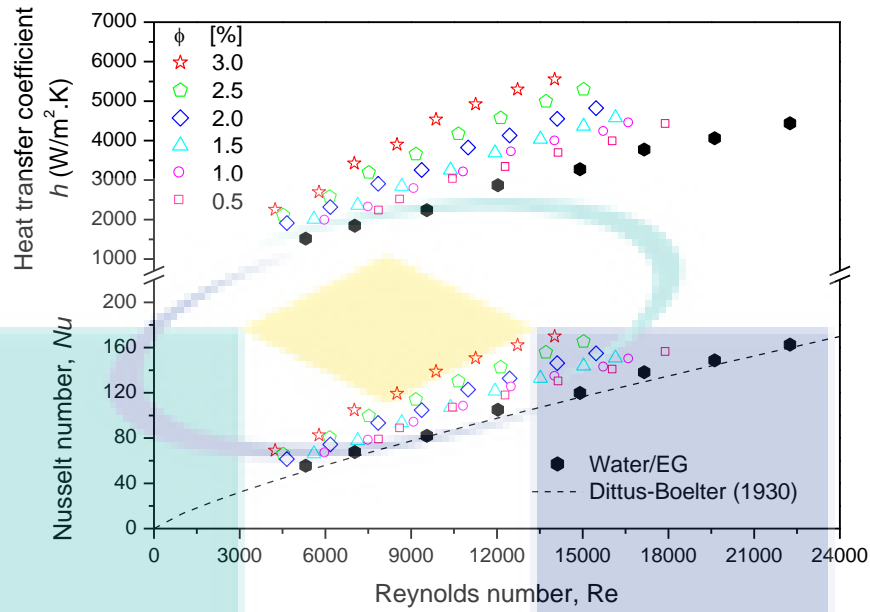
The heat transfer coefficient and Nusselt number for $\text{TiO}_2\text{-SiO}_2$ nanofluids at bulk temperature of 70 °C were shown as in Figure 4.13 (c). The increasing of temperature, volume concentration and Reynolds number were enhanced the heat transfer coefficient and Nusselt number. At 70 °C the range of Reynolds number is higher up to 24,000. This happened due to the decreasing of viscosity because of higher temperature. The maximum enhancement of heat transfer coefficient is observed to be up to 81% for the working temperature of 70 °C and 3.0% volume concentration while the lowest heat transfer enhancement is found at 15.1% with the volume concentration of 0.5%. The highers of thermal properties would improved the heat transfer coefficient (Hemmat Esfe et al., 2016).



(a) Temperature 30 °C



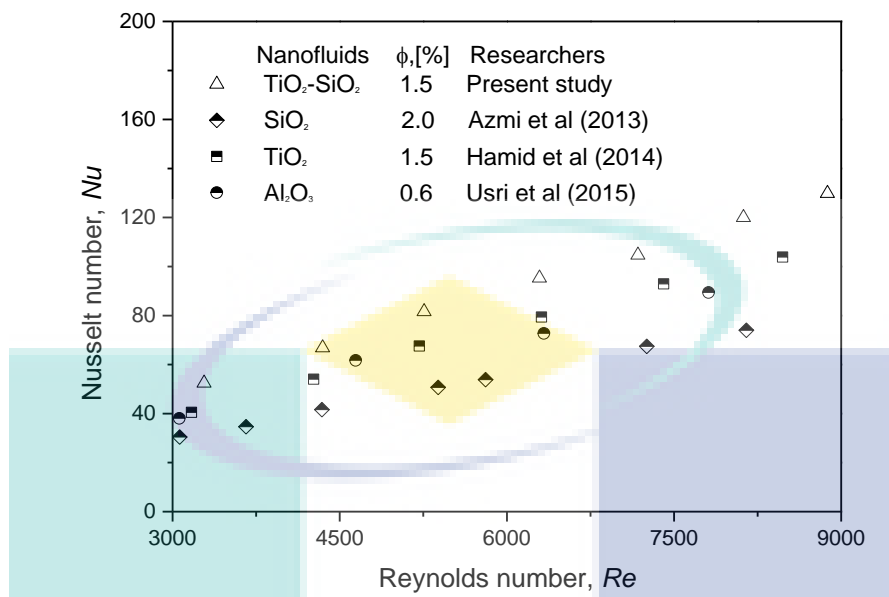
(b) Temperature 50 °C



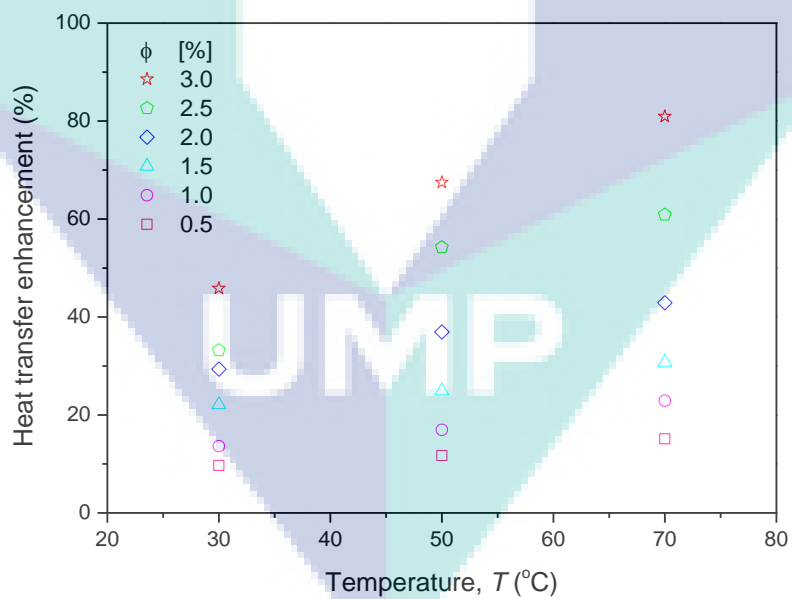
(c) Temperature 70 °C

Figure 4.13 Variation of the Nusselt number and heat transfer coefficient with Reynolds number of $\text{TiO}_2\text{-SiO}_2$ hybrid nanofluids at various temperature.

The experimental Nusselt number of $\text{TiO}_2\text{-SiO}_2$ nanofluids were compared with single nanofluids from the previous study (Abdul Hamid et al., 2014; Azmi et al., 2013b; Usri et al., 2015) in Figure 4.14 (a). Interestingly, the $\text{TiO}_2\text{-SiO}_2$ nanofluids at 1.5% volume concentration in the figure displays the highest Nusselt number in comparison with SiO_2 nanofluids (Azmi et al., 2013b), TiO_2 nanofluids (Abdul Hamid et al., 2014) and Al_2O_3 nanofluids (Usri et al., 2015). Figure 4.14 (b) shows the summary of heat transfer enhancement of $\text{TiO}_2\text{-SiO}_2$ nanofluids for different concentrations and temperatures. It can be concluded that the heat transfer coefficient of $\text{TiO}_2\text{-SiO}_2$ nanofluids is increased with increasing volume concentrations and working temperatures. The improvement of heat transfer coefficient using hybrid nanofluids is also discussed by Selvakumar and Suresh (2012b). From their research work, they stated that the percentage increment of pumping power is less than the enhancement of heat transfer coefficient for $\text{Al}_2\text{O}_3\text{-Cu}$ nanofluids. Therefore, the hybrid nanofluids are able to improve the performance of single nanofluids and it was recommended for the heat transfer applications.



(a) Comparison of Nusselt number experimental with previous study



(b) Heat transfer enhancement

Figure 4.14 Variations of experimental Nusselt number comparison and heat transfer enhancement

4.4.3 Friction Factor and Pressure Drop

Figure 4.15 presents the friction factor of $\text{TiO}_2\text{-SiO}_2$ nanofluids for different volume concentrations and working temperatures. The experimental results for the water/EG (60:40) mixture were compared with Blasius (1913) given by Equation (3.15) and found to be in good agreement. From the graph, it can also be seen that the friction factor of $\text{TiO}_2\text{-SiO}_2$ nanofluids is slightly higher than the base fluids, however insignificantly. The distribution of friction factor was very close to the Blasius (1913) line for all concentrations, hence the $\text{TiO}_2\text{-SiO}_2$ nanofluids does not significantly affect the friction factor. The same findings have been found by Azmi et al. (2017), Pak and Cho (1998) and Abdolbaqi et al. (2017). The internal friction forces between particles were influenced by temperature and viscosity of $\text{TiO}_2\text{-SiO}_2$ nanofluids. When the temperature is increased, the viscosity of $\text{TiO}_2\text{-SiO}_2$ nanofluids decreased and consequently causes low internal force between the molecules. However, the viscosity of $\text{TiO}_2\text{-SiO}_2$ nanofluids increases with increasing concentration due to the strong nanoparticle bonding, hence slightly affect the friction factor increment.

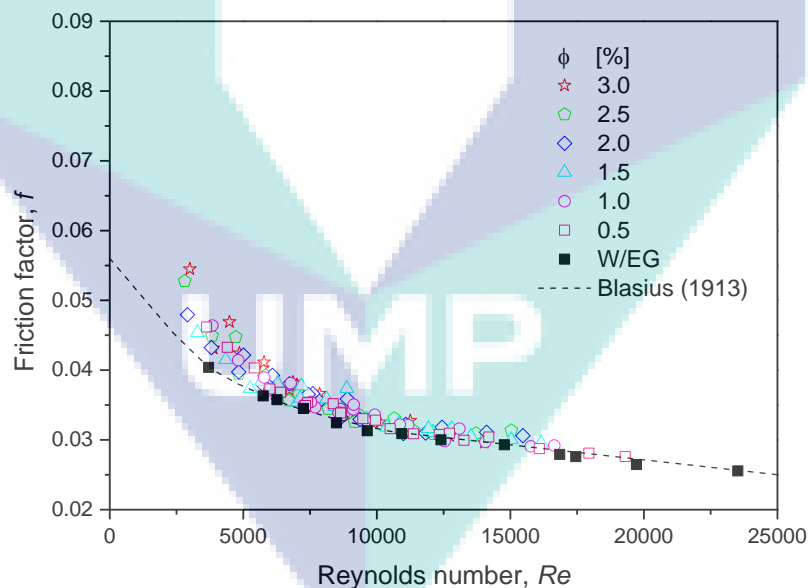
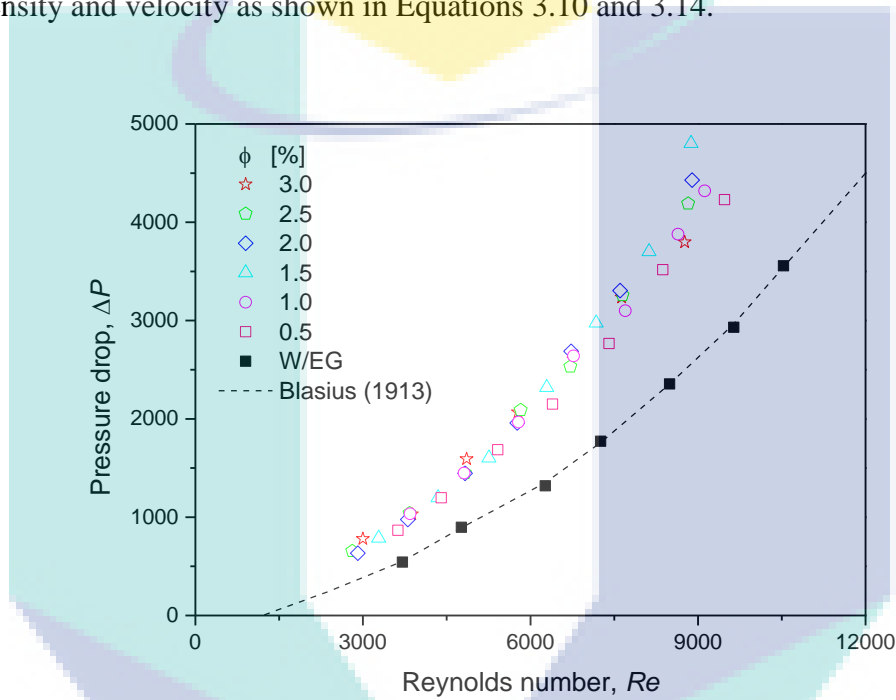


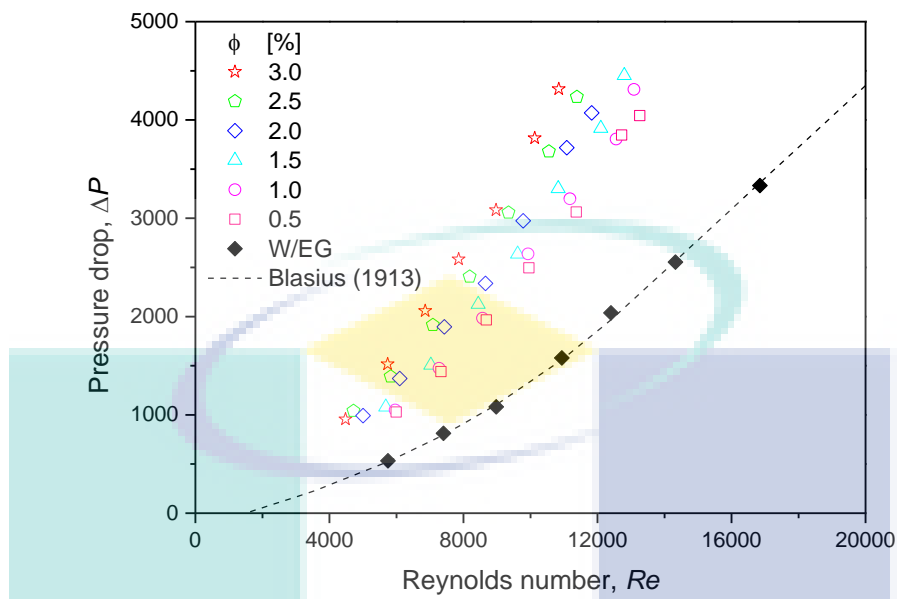
Figure 4.15 Friction factor in bulk temperature at 30, 50 and 70 °C

The variation of the pressure drop with Reynolds number of $\text{TiO}_2\text{-SiO}_2$ nanofluids at various temperature was shown in Figure 4.16 (a-c). The range of flow

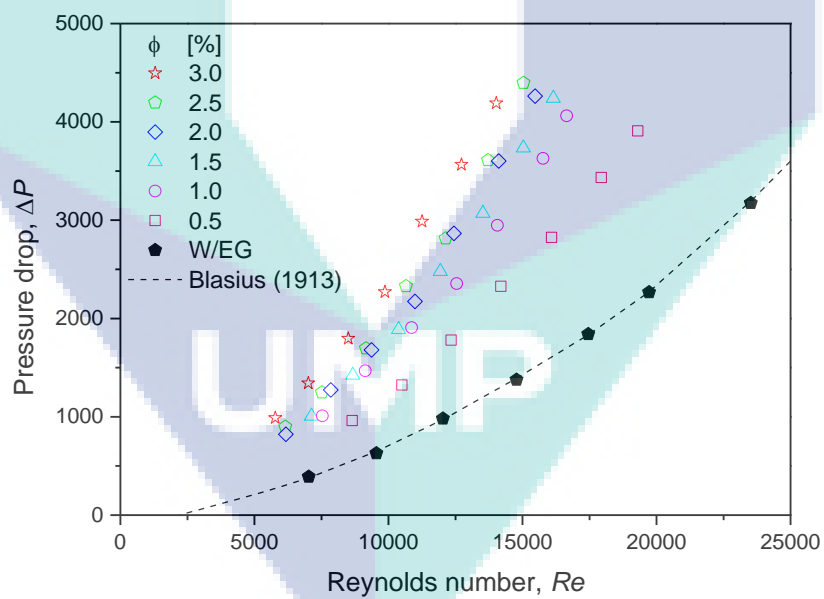
rate are constantly controlled in between 4 to 20 LPM with Reynolds number can be achieved more than 9000, 13000 and 19000 for temperature of 30, 50 and 70 °C, respectively. The effect of decreasing in viscosity influenced the increasing of Reynolds number. This can be proven from the experimental data that was shown in Figure 4.16 (a-c) that the increasing the temperature will reduce the viscosity of nanofluids and higher of Reynolds number. The pressure drop of TiO₂-SiO₂ nanofluids shows higher than based fluid. This happen due to the pressure drop is proportionally increased with the density and velocity as shown in Equations 3.10 and 3.14.



(a) Temperature 30 °C



(b) Temperature 50 °C



(c) Temperature 70 °C

Figure 4.16 Variation of the Pressure drop with Reynolds number of $\text{TiO}_2\text{-SiO}_2$ nanofluids at various temperatures

4.5 Experimental Regression Correlation

The regression model is developed for the estimation of Nusselt number and friction factor of TiO₂-SiO₂ nanofluids flow in a tube. The Reynolds number, Prandtl number, temperature and volume concentrations are among the main variables which affect the regression model of Nusselt number. The development of regression correlation for the TiO₂-SiO₂ nanofluids dispersed in 60:40 (water/EG) mixture base fluid was discussed in details in the next sections.

4.5.1 Nusselt Number

The Nusselt number regression model for TiO₂-SiO₂ nanofluids in water/EG (60:40) mixture base fluid was developed by using 170 experimental data at different volume concentrations and temperatures. The Nusselt number correlation is applicable for TiO₂-SiO₂ nanofluids in water/EG (60:40) mixture base fluid, volume concentration up to 3.0% and working temperature of 30 to 70 °C. The Nusselt number correlation was obtained with a maximum deviation of 9.9%, average deviation of 3.8% and standard deviation of 4.2%. The Nusselt number regression model is given as Equation 4.3. The comparison of Nusselt number between regression model and experimental data is shown in Figure 4.17.

$$Nu_{hnf} = 0.023Re^{0.8} Pr^{0.4} \left(0.01 + \frac{T}{70}\right)^{0.05} \left(1.0 + \frac{\phi}{100}\right)^{6.9} \quad 4.3$$

where Nu_{hnf} is Nusselt number of hybrid nanofluids; Re is Reynolds number; Pr is Prandtl number; T is temperature in °C; ϕ is volume concentration in %.

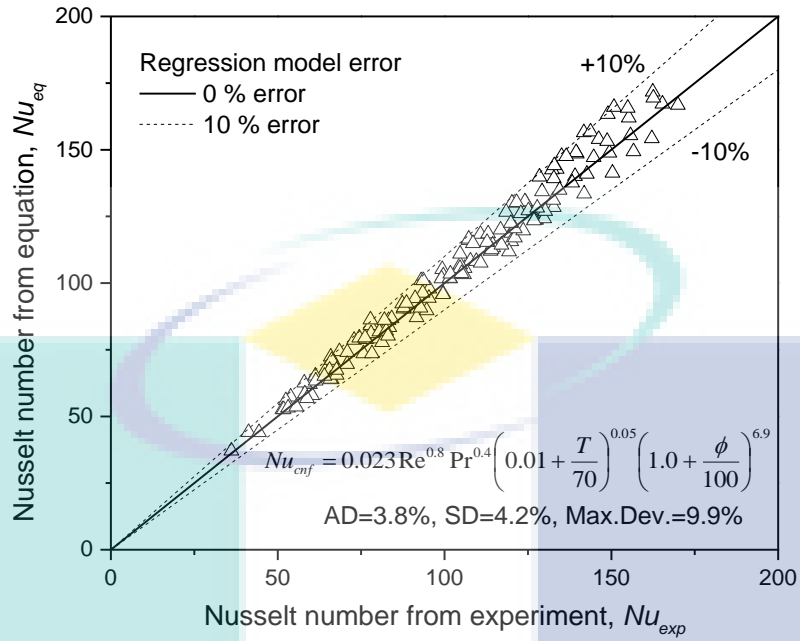


Figure 4.17 Comparison of Nusselt number regression model with experimental data

4.5.2 Friction Factor

The friction factor regression model for TiO₂-SiO₂ nanofluids in the water/EG (60:40) mixture was prepared using 170 experimental data at different volume concentrations and temperatures. The regression model is valid for TiO₂-SiO₂ nanofluids in water/EG (60:40) mixture and volume concentration up to 3.0%. The friction factor correlation is given by Equation 4.4 with maximum deviation, average deviation and standard deviation of 7.8%, 2.2% and 2.9%, respectively. Figure 4.18 represents the error validation of friction factor estimated by present regression model in comparison with the experimental data.

$$f_{hnf} = \frac{0.3164}{Re^{0.25}} \left(1.0 + \frac{\phi}{100}\right)^{2.8} \quad 4.4$$

where f_{hnf} is friction factor of hybrid nanofluids; Re is Reynolds number; ϕ is volume concentration in %.

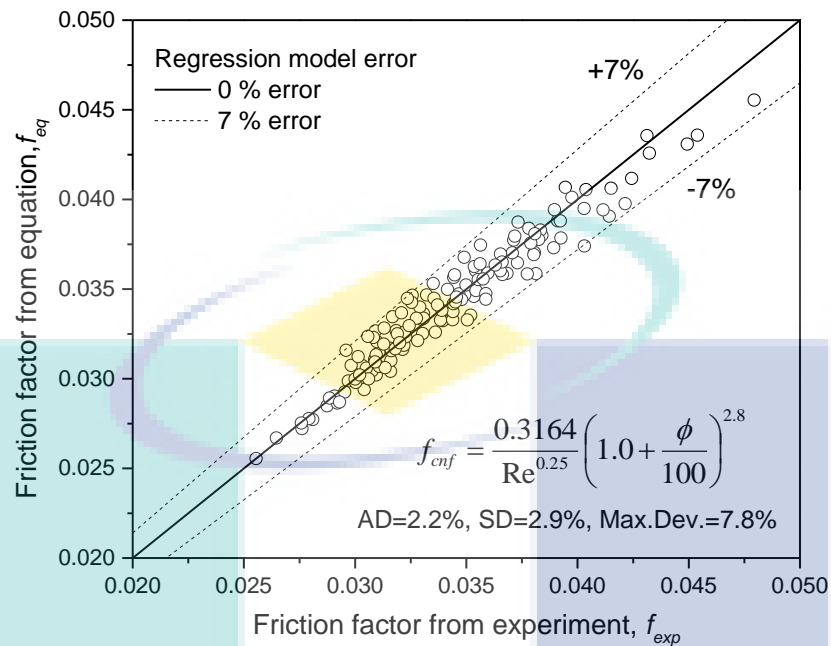


Figure 4.18 Comparison of friction factor regression model with experimental data

4.6 Thermal Hydraulic Performance

The thermal hydraulic performance or also known as thermal performance factor was evaluated for the present experimental data of TiO_2-SiO_2 nanofluids convective heat transfer. The experimental Nusselt number and friction factor were used to determine the thermal performance factor.

4.6.1 Nusselt Number Ratio

Figure 4.19 shows the experimental Nusselt number ratio for TiO_2-SiO_2 nanofluids against the Reynolds number for all volume concentrations and various temperatures. From the figure, it is clearly observed that the ratio of Nusselt number tend to increase with increasing of volume concentration. A small number of the Nusselt number ratio for volume concentrations of 0.5 and 1.0% was found with less than 1.0. Meanwhile, most of the present data with Nusselt number ratio more than 1.0. The maximum ratio was observed for volume concentration of 3.0%. The trend is agreement with the previous heat transfer data as presented in Figure 4.13.

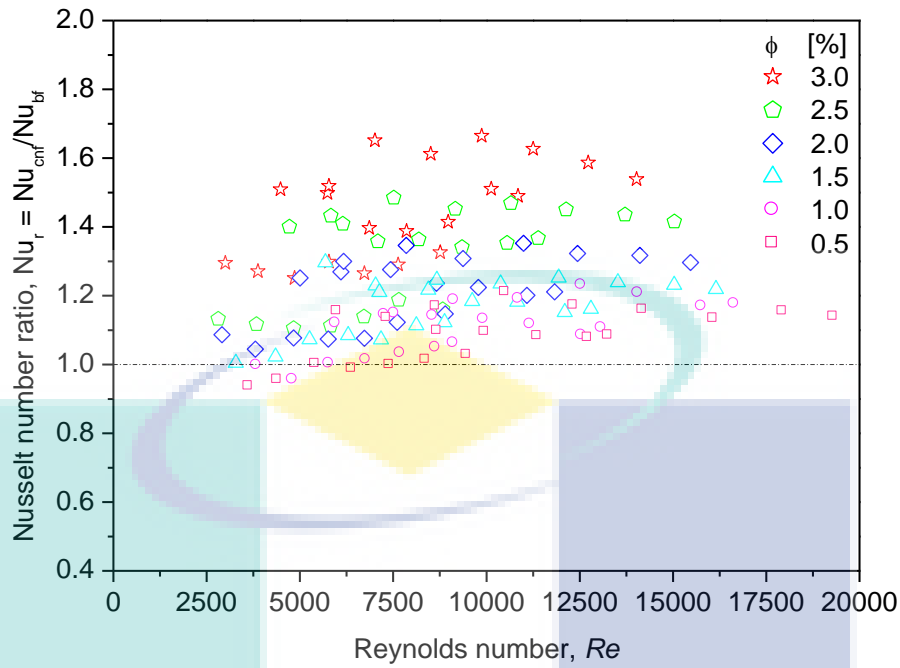


Figure 4.19 Variation of Nusselt number ratio with Reynolds number for different volume concentration of $\text{TiO}_2\text{-SiO}_2$ nanofluids at various temperature

4.6.2 Friction Factor Ratio

The variation data for the experimental friction factor ratio of $\text{TiO}_2\text{-SiO}_2$ nanofluids against Reynolds number is shown in Figure 4.20. The figure was plotted for the experimental data of different volume concentrations and for the temperature of 30, 50 and 70 °C. The graph shows that the friction factor ratio are within the range of 1.0 to 1.1. The friction factor ratios are slightly decrease with increasing of Reynolds number whereas increases with volume concentration. However, small increment has been seen for all volume concentration. Therefore, the friction factor is slightly increase however insignificantly. Again, the trend is agreement with the previous friction data as presented in Figure 4.15.

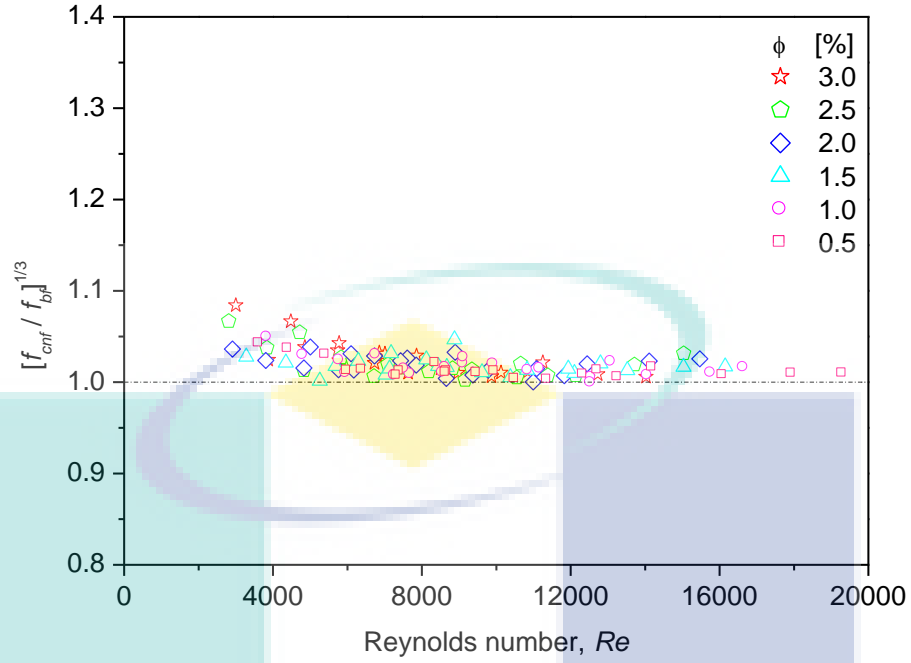


Figure 4.20 Variation of friction factor ratio with Reynolds number for different volume concentration of TiO₂-SiO₂ nanofluids at various temperature

4.6.3 Thermal Performance Factor

The thermal performance factor, η of TiO₂-SiO₂ nanofluids against Reynolds number were shown in Figure 4.21 for temperatures of 30, 50 and 70 °C. The thermal performance factor can be defined as the ratio of heat transfer for nanofluids with heat transfer of base fluid at similar pumping power (Abdolbaqi et al., 2016a). The mathematical expression is given as in Equation 4.5. The equation was used to determine the thermal performance factor of nanofluids (Abdolbaqi et al., 2016a; Eiamsa-ard et al., 2013a; Kumar et al., 2016a; Webb & Kim, 2005).

$$\eta = \left[\frac{\frac{Nu_{hnf}}{Nu_{bf}}}{\left(\frac{f_{hnf}}{f_{bf}} \right)^{\frac{1}{3}}} \right] \quad 4.5$$

where η is thermal performance factor; h_{hnf} is heat transfer coefficient of hybrid nanofluids; h_{bf} is heat transfer coefficient of base fluid; Nu_{hnf} is Nusselt number of hybrid nanofluids; Nu_{bf} is Nusselt number of base fluid; f_{hnf} is friction factor of hybrid nanofluids; f_{bf} is friction factor of base fluid.

Figure 4.21 shows the thermal performance factor against Reynolds number for the TiO₂-SiO₂ nanofluids at different temperatures. It can be observed that the thermal performance factor are more than 1.0 for almost all volume concentrations. However, some data show lesser than 1.0 for volume concentration of 0.5 and 1.0%. The maximum and minimum performance factor were occur at volume concentration of 3.0% and 0.5%, respectively. The thermal performance factor is agreement with the trend of Nusselt number ratio in Figure 4.19. This proved that the friction factor increment does not affect to the thermal performance factor of TiO₂-SiO₂ nanofluids. The highest of heat transfer coefficient with small increments of friction factor would enhance the thermal performance factor of heat transfer (Eiamsa-ard et al., 2013b; Kumar et al., 2016a). Therefore, TiO₂-SiO₂ nanofluids are recommended for applications in various heat transfer system without extra penalty with the pumping power and pressure drop.

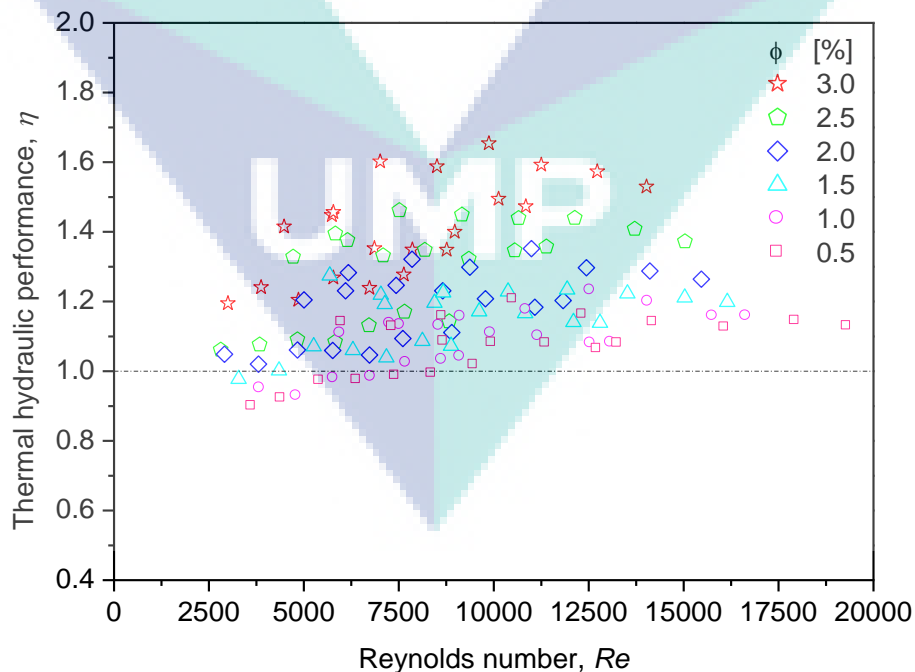


Figure 4.21 Variation of thermal performance factor with Reynolds number for TiO₂-SiO₂ nanofluids at various temperatures

CHAPTER 5

CONCLUSIONS

5.1 Introduction

This chapter summarized the present study on the investigation of thermo-physical properties and thermal-hydraulic performance of $\text{TiO}_2\text{-SiO}_2$ nanofluids. Based on the results and findings were described in chapter 4, the overall conclusions of the study was presented. Finally, this chapter was ended with recommendations for the future study.

5.2 Conclusions

The thermal conductivity and dynamic viscosity of $\text{TiO}_2\text{-SiO}_2$ nanofluids in a water:ethylene glycol mixture were investigated for volume concentrations from 0.5 to 3.0% and temperatures of 30 to 80 °C. The nanofluids with 90 minutes sonication time were observed to be the most stable sample with absorbance ratio of more than 70% for 275 hours sedimentation time. The maximum thermal conductivity of nanofluids was enhanced up to 22.8% for 3.0% volume concentration and temperature of 80 °C. Meanwhile, the highest average relative viscosity was obtained for 3.0% concentration with 62.5% increment. According to the properties enhancement ratio, the $\text{TiO}_2\text{-SiO}_2$ nanofluids were recommended to behave as a good heat transfer fluid for volume concentrations higher than 1.5%. The regression equations for the estimation of thermal conductivity ratio and relative viscosity were presented with good accuracy. The equations are applicable for volume concentrations up to 3.0% and working temperatures of 30 to 70 °C.

The heat transfer performance and friction factor of TiO₂-SiO₂ nanofluids in a water/EG (60:40) mixture has been investigated for volume concentrations of up to 3.0% and working temperatures of 30 to 70°C. The heat transfer coefficient of TiO₂-SiO₂ nanofluids increased with increasing volume concentrations and temperatures. The maximum enhancement of heat transfer coefficient is observed up to 81% for the working temperature of 70°C and 3.0% volume concentration. The heat transfer performance of TiO₂-SiO₂ nanofluids is higher than TiO₂ nanofluids for the same volume concentration. The friction factor of TiO₂-SiO₂ nanofluids is slightly higher than the base fluids however insignificantly. The regression models for the estimation of Nusselt number and friction factor were presented with good accuracy. The correlations are applicable for water/EG (60:40) mixture and TiO₂-SiO₂ nanofluids with volume concentrations of 0.5 to 3.0% and working temperatures of 30 to 70 °C.

As addition for the research work, the thermal hydraulic performance were determined using the experimental Nusselt number and friction factor. It can be observed that the thermal performance factor in the present study are more than 1.0 for almost all volume concentrations with exception for a few data at volume concentration of 0.5 and 1.0%. This was proved that the friction factor increment does not affect to the overall performance of TiO₂-SiO₂ nanofluids. Therefore, it was expected that the TiO₂-SiO₂ nanofluids are recommended for various heat transfer system applications and insignificantly effect on the pressure drop of the system.

5.3 Recommendations for the Future Work

Several investigations that can be cover for the future research of hybrid nanofluids are recommended as below:

- i. Experiments with other based fluid such as Bio-Glycol, water/Bio-Glycol mixture and oils may be undertaken to determine the performance of heat transfer.
- ii. Experiments with different combinations of nanoparticles either in combination of metallic and non-metallic or with various ratio of based fluid such as 20:80, 40:60, 70:30 and etc. (water/EG) for the comparison of the highest enhancement of heat transfer.

REFERENCES

- Abbasi, S. M., Rashidi, A., Nemati, A., & Arzani, K. (2013). The effect of functionalisation method on the stability and the thermal conductivity of nanofluid hybrids of carbon nanotubes/gamma alumina. *Ceramics International*, 39(4), 3885-3891.
- Abdolbaqi, M. K., Azmi, W. H., Mamat, R., Mohamed, N. M. Z. N., & Najafi, G. (2016a). Experimental investigation of turbulent heat transfer by counter and co-swirling flow in a flat tube fitted with twin twisted tapes. *International Communications in Heat and Mass Transfer*, 75, 295-302.
- Abdolbaqi, M. K., Mamat, R., Sidik, N. A. C., Azmi, W. H., & Selvakumar, P. (2017). Experimental investigation and development of new correlations for heat transfer enhancement and friction factor of BioGlycol/water based TiO₂ nanofluids in flat tubes. *International Journal of Heat and Mass Transfer*, 108, 1026-1035.
- Abdolbaqi, M. K., Sidik, N. A. C., Aziz, A., Mamat, R., Azmi, W. H., Yazid, M. N. A. W. M., & Najafi, G. (2016b). An experimental determination of thermal conductivity and viscosity of BioGlycol/water based TiO₂ nanofluids. *International Communications in Heat and Mass Transfer*, 77, 22-32.
- Abdolbaqi, M. K., Sidik, N. A. C., Rahim, M. F. A., Mamat, R., Azmi, W. H., Yazid, M. N. A. W. M., & Najafi, G. (2016c). Experimental investigation and development of new correlation for thermal conductivity and viscosity of BioGlycol/water based SiO₂ nanofluids. *International Communications in Heat and Mass Transfer*, 77, 54-63.
- Abdul Hamid, K., Azmi, W. H., Mamat, R., & Usri, N. A. (2014). Heat transfer performance of titanium oxide in ethylene glycol based nanofluids under transition flow. *Applied Mechanics and Materials*, 660, 684-688.
- Afrand, M. (2017). Experimental study on thermal conductivity of ethylene glycol containing hybrid nano-additives and development of a new correlation. *Applied Thermal Engineering*, 110, 1111-1119.
- Afrand, M., Nazari Najafabadi, K., & Akbari, M. (2016a). Effects of temperature and solid volume fraction on viscosity of SiO₂-MWCNTs/SAE40 hybrid nanofluid as a coolant and lubricant in heat engines. *Applied Thermal Engineering*, 102, 45-54.

- Afrand, M., Toghraie, D., & Ruhani, B. (2016b). Effects of temperature and nanoparticles concentration on rheological behavior of Fe_3O_4 -Ag/EG hybrid nanofluid: An experimental study. *Experimental Thermal and Fluid Science*, 77, 38-44.
- Agarwal, D. K., Vaidyanathan, A., & Sunil Kumar, S. (2015). Investigation on convective heat transfer behaviour of kerosene- Al_2O_3 nanofluid. *Applied Thermal Engineering*, 84, 64-73.
- Ahammed, N., Asirvatham, L. G., & Wongwises, S. (2016). Entropy generation analysis of graphene-alumina hybrid nanofluid in multiport minichannel heat exchanger coupled with thermoelectric cooler. *International Journal of Heat and Mass Transfer*, 103, 1084-1097.
- Ahuja, A. S. (1975). Augmentation of heat transport in laminar flow of polystyrene suspensions. I. Experiments and results. *Journal of Applied Physics*, 46(8), 3408-3416.
- Allahyar, H. R., Hormozi, F., & ZareNezhad, B. (2016). Experimental investigation on the thermal performance of a coiled heat exchanger using a new hybrid nanofluid. *Experimental Thermal and Fluid Science*, 76, 324-329.
- Asadi, M., & Asadi, A. (2016). Dynamic viscosity of MWCNT/ZnO-engine oil hybrid nanofluid: An experimental investigation and new correlation in different temperatures and solid concentrations. *International Communications in Heat and Mass Transfer*, 76, 41-45.
- ASHRAE. (2009). *ASHRAE Handbook - Fundamentals (SI Edition)*. Atlanta: American Society of Heating, Refrigerating and Air-Conditioning Engineers, Inc.
- Azmi, W. H., Abdul Hamid, K., Mamat, R., Sharma, K. V., & Mohamad, M. S. (2016a). Effects of working temperature on thermo-physical properties and forced convection heat transfer of TiO_2 nanofluids in water – ethylene glycol mixture. *Applied Thermal Engineering*, 106, 1190-1199.
- Azmi, W. H., Abdul Hamid, K., Usri, N. A., Mamat, R., & Mohamad, M. S. (2016b). Heat transfer and friction factor of water and ethylene glycol mixture based TiO_2 and Al_2O_3 nanofluids under turbulent flow. *International Communications in Heat and Mass Transfer*, 76, 24-32.
- Azmi, W. H., Sharma, K. V., Mamat, R., Alias, A. B. S., & Misnon, I. I. (2012). Correlations for thermal conductivity and viscosity of water based nanofluids. *IOP Conference Series: Materials Science and Engineering*, 36, 012029.

- Azmi, W. H., Sharma, K. V., Mamat, R., & Anuar, S. (2013a). Nanofluid properties for forced convection heat transfer: An overview. *Journal of Mechanical Engineering and Sciences*, 4, 397-408.
- Azmi, W. H., Sharma, K. V., Mamat, R., Najaf, G., & Mohamad, M. S. (2016c). The enhancement of effective thermal conductivity and effective dynamic viscosity of nanofluids – A review. *Renewable and Sustainable Energy Reviews*, 53, 1046-1058.
- Azmi, W. H., Sharma, K. V., Mamat, R., Najafi, G., & Mohamad, M. S. (2016d). The enhancement of effective thermal conductivity and effective dynamic viscosity of nanofluids – A review. *Renewable and Sustainable Energy Reviews*, 53, 1046-1058.
- Azmi, W. H., Sharma, K. V., Sarma, P. K., & Mamat, R. (2010). *Influence of certain thermo-physical properties on prandtl number of water based nanofluids*. Paper presented at the National Conference in Mechanical Engineering Research and Postgraduate Students (1st NCMER), Universiti Malaysia Pahang, Malaysia.
- Azmi, W. H., Sharma, K. V., Sarma, P. K., Mamat, R., Anuar, S., & Dharma Rao, V. (2013b). Experimental determination of turbulent forced convection heat transfer and friction factor with SiO₂ nanofluid. *Experimental Thermal and Fluid Science*, 51, 103-111.
- Azmi, W. H., Sharma, K. V., Sarma, P. K., Mamat, R., Anuar, S., & Syam Sundar, L. (2014a). Numerical validation of experimental heat transfer coefficient with SiO₂ nanofluid flowing in a tube with twisted tape inserts. *Applied Thermal Engineering*, 73(1), 296-306.
- Azmi, W. H., Sharma, K. V., Sarma, P. K., Mamat, R., & Najafi, G. (2014b). Heat transfer and friction factor of water based TiO₂ and SiO₂ nanofluids under turbulent flow in a tube. *International Communications in Heat and Mass Transfer*, 59, 30-38.
- Azmi, W. H., Usri, N. A., Mamat, R., Sharma, K. V., & Noor, M. M. (2017). Force convection heat transfer of Al₂O₃ nanofluids for different based ratio of water:ethylene glycol mixture. *Applied Thermal Engineering*, 112, 707-719.
- Baby, T. T., & Ramaprabhu, S. (2011). Experimental investigation of the thermal transport properties of a carbon nanohybrid dispersed nanofluid. *Nanoscale*, 3(5), 2208-2214.

- Baby, T. T., & Ramaprabhu, S. (2013). Synthesis of silver nanoparticle decorated multiwalled carbon nanotubes-graphene mixture and its heat transfer studies in nanofluid. *AIP Advances*, 3(1), 012111.
- Baghbanzadeh, M., Rashidi, A., Rashtchian, D., Lotfi, R., & Amrollahi, A. (2012). Synthesis of spherical silica/multiwall carbon nanotubes hybrid nanostructures and investigation of thermal conductivity of related nanofluids. *Thermochimica Acta*, 549, 87-94.
- Baghbanzadeh, M., Rashidi, A., Soleimanisalim, A. H., & Rashtchian, D. (2014). Investigating the rheological properties of nanofluids of water/hybrid nanostructure of spherical silica/MWCNT. *Thermochimica Acta*, 578, 53-58.
- Bahrami, M., Akbari, M., Karimipour, A., & Afrand, M. (2016). An experimental study on rheological behavior of hybrid nanofluids made of iron and copper oxide in a binary mixture of water and ethylene glycol: Non-Newtonian behavior. *Experimental Thermal and Fluid Science*, 79, 231-237.
- Bhosale, G. H., & Borse, S. L. (2013). Pool boiling CHF enhancement with Al₂O₃-CuO/H₂O hybrid nanofluid. *International Journal of Engineering Research & Technology (IJERT)*, 2(10), 946-950.
- Blasius, H. (1913). Das ähnlichkeitsgesetz bei reibungsvorgängen in flüssigkeiten *Mitteilungen über Forschungsarbeiten auf dem Gebiete des Ingenieurwesens* (Vol. 131, pp. 1-41): Springer.
- Botha, S. S., Ndungu, P., & Bladergroen, B. J. (2011). Physicochemical properties of oil-based nanofluids containing hybrid structures of silver nanoparticles supported on silica. *Industrial and Engineering Chemistry Research*, 50(6), 3071-3077.
- Chen, L., & Xie, H. (2010). Surfactant-free nanofluids containing double- and single-walled carbon nanotubes functionalized by a wet-mechanochemical reaction. *Thermochimica Acta*, 497(1-2), 67-71.
- Chiam, H. W., Azmi, W. H., Usri, N. A., Mamat, R., & Adam, N. M. (2017). Thermal conductivity and viscosity of Al₂O₃ nanofluids for different based ratio of water and ethylene glycol mixture. *Experimental Thermal and Fluid Science*, 81, 420-429.

- Choi, & Stephen, U. S. (1995). Enhancing thermal conductivity of fluids with nanoparticles in developments and applications of non-newtonian flows. *D. A. Singer and H.P. Wang, Eds., American Society of Mechanical Engineers, New York, FED-231/MD-66*, 99–105.
- Das, S. K., Choi, S. U. S., & Patel, H. E. (2006). Heat transfer in nanofluids - A review. *Heat Transfer Engineering*, 27(10), 3-19.
- Deepak Selvakumar, R., & Dhinakaran, S. (2016). Nanofluid flow and heat transfer around a circular cylinder: A study on effects of uncertainties in effective properties. *Journal of Molecular Liquids*, 223, 572-588.
- Dewan, A., Mahanta, P., Sumithra Raju, K., & Suresh Kumar, P. (2004). Review of passive heat transfer augmentation techniques. *Proceedings of the Institution of Mechanical Engineers, Part A: Journal of Power and Energy*, 218(7), 509-527.
- Dittus, F. W., & Boelter, L. M. K. (2 1930). Heat transfer in automobile radiators of the tubular type.
- Dittus, F. W., & Boelter, L. M. K. (1930). Heat transfer in automobile radiators of the tubular type (Vol. 2, pp. 443–461). Berkeley: University of California Publications on Engineering 2.
- Duangthongsuk, W., & Wongwises, S. (2008). Effect of thermophysical properties models on the predicting of the convective heat transfer coefficient for low concentration nanofluid. *International Communications in Heat and Mass Transfer*, 35(10), 1320-1326.
- Eastman, J. A., Choi, S., Li, S., Yu, W., & Thompson, L. (2001). Anomalously increased effective thermal conductivities of ethylene glycol-based nanofluids containing copper nanoparticles. *Applied physics letters*, 78(6), 718-720.
- Eiamsa-ard, S., Kongkaitpaiboon, V., & Nanan, K. (2013a). Thermohydraulics of Turbulent Flow Through Heat Exchanger Tubes Fitted with Circular-rings and Twisted Tapes. *Chinese Journal of Chemical Engineering*, 21(6), 585-593.
- Eiamsa-ard, S., Nanan, K., Thianpong, C., & Eiamsa-ard, P. (2013b). Thermal Performance Evaluation of Heat Exchanger Tubes Equipped with Coupling Twisted Tapes. *Experimental Heat Transfer*, 26(5), 413-430.
- G.H.Bhosale, & S.L.Borse. (2013). Pool boiling CHF enhancement with Al₂O₃-CuO/H₂O hybrid nanofluid. *International Journal of Engineering Research and Technology (IJERT)*, 2(10), 946-950.

- Garg, J., Poudel, B., Chiesa, M., Gordon, J., Ma, J., Wang, J., . . . Nanda, J. (2008). Enhanced thermal conductivity and viscosity of copper nanoparticles in ethylene glycol nanofluid. *Journal of Applied Physics*, *103*(7), 074301.
- Ghadimi, A., Saidur, R., & Metselaar, H. S. C. (2011). A review of nanofluid stability properties and characterization in stationary conditions. *International Journal of Heat and Mass Transfer*, *54*(17-18), 4051-4068.
- Gou, S., Dong, S., & Wang, E. (2008). Gold/platinum hybrid nanoparticles supported on multiwalled carbon nanotube/silica coaxial nanocables: Preparation and application as electrocatalysts for oxygen reduction. *American Chemical Society*, *112*, 2389-2393.
- Hajjar, Z., Rashidi, A. m., & Ghozatloo, A. (2014). Enhanced thermal conductivities of graphene oxide nanofluids. *International Communications in Heat and Mass Transfer*, *57*, 128-131.
- Hamid, K. A., Azmi, W. H., Mamat, R., & Sharma, K. V. (2016). Experimental investigation on heat transfer performance of TiO₂ nanofluids in water–ethylene glycol mixture. *International Communications in Heat and Mass Transfer*, *73*, 16-24.
- Hamid, K. A., Azmi, W. H., Mamat, R., Usri, N. A., & Najafi, G. (2015). Effect of temperature on heat transfer coefficient of titanium dioxide in ethylene glycol-based nanofluid. *Journal of Mechanical Engineering and Sciences*, *8*, 1367-1375.
- Han, W. S., & Rhi, S. H. (2011). Thermal characteristics of grooved heat pipe with hybrid nanofluids. *Thermal Science*, *15*(1), 195-206.
- Harandi, S. S., Karimipour, A., Afrand, M., Akbari, M., & D'Orazio, A. (2016). An experimental study on thermal conductivity of F-MWCNTs–Fe₃O₄/EG hybrid nanofluid: Effects of temperature and concentration. *International Communications in Heat and Mass Transfer*, *76*, 171-177.
- Hatwar, S., & Kriplani, V. M. (2014). A review on heat transfer enhancement with nanofluid. *International Journal of Advance Research in Science and Engineering*, *3*(3), 175-183.
- Hemmat Esfe, M., Abbasian Arani, A. A., Rezaie, M., Yan, W.-M., & Karimipour, A. (2015a). Experimental determination of thermal conductivity and dynamic viscosity of Ag–MgO/water hybrid nanofluid. *International Communications in Heat and Mass Transfer*, *66*, 189-195.

- Hemmat Esfe, M., Abbasian Arani, A. A., Rezaie, M., Yan, W. M., & Karimipour, A. (2015b). Experimental determination of thermal conductivity and dynamic viscosity of Ag–MgO/water hybrid nanofluid. *International Communications in Heat and Mass Transfer*, 66, 189-195.
- Hemmat Esfe, M., Afrand, M., Rostamian, S. H., & Toghraie, D. (2017). Examination of rheological behavior of MWCNTs/ZnO-SAE40 hybrid nano-lubricants under various temperatures and solid volume fractions. *Experimental Thermal and Fluid Science*, 80, 384-390.
- Hemmat Esfe, M., Afrand, M., Yan, W.-M., Yarmand, H., Toghraie, D., & Dahari, M. (2016). Effects of temperature and concentration on rheological behavior of MWCNTs/SiO₂(20–80)-SAE40 hybrid nano-lubricant. *International Communications in Heat and Mass Transfer*, 76, 133-138.
- Hemmat Esfe, M., Saedodin, S., Yan, W.-M., Afrand, M., & Sina, N. (2015c). Study on thermal conductivity of water-based nanofluids with hybrid suspensions of CNTs/Al₂O₃ nanoparticles. *Journal of Thermal Analysis and Calorimetry*, 124(1), 455-460.
- Hemmat Esfe, M., Wongwises, S., Naderi, A., Asadi, A., Safaei, M. R., Rostamian, H., . . . Karimipour, A. (2015d). Thermal conductivity of Cu/TiO₂–water/EG hybrid nanofluid: Experimental data and modeling using artificial neural network and correlation. *International Communications in Heat and Mass Transfer*, 66, 100-104.
- Hjerrild, N. E., Mesgari, S., Crisostomo, F., Scott, J. A., Amal, R., & Taylor, R. A. (2016). Hybrid PV/T enhancement using selectively absorbing Ag–SiO₂/carbon nanofluids. *Solar Energy Materials and Solar Cells*, 147, 281-287.
- Ho, C. J., Huang, J. B., Tsai, P. S., & Yang, Y. M. (2010). Preparation and properties of hybrid water-based suspension of Al₂O₃ nanoparticles and MEPCM particles as functional forced convection fluid. *International Communications in Heat and Mass Transfer*, 37(5), 490-494.
- Ho, C. J., Huang, J. B., Tsai, P. S., & Yang, Y. M. (2011). On laminar convective cooling performance of hybrid water-based suspensions of Al₂O₃ nanoparticles and MEPCM particles in a circular tube. *International Journal of Heat and Mass Transfer*, 54(11-12), 2397-2407.
- Hormozi, F., ZareNezhad, B., & Allahyar, H. R. (2016). An experimental investigation on the effects of surfactants on the thermal performance of hybrid nanofluids in helical coil heat exchangers. *International Communications in Heat and Mass Transfer*, 78, 271-276.

- Huang, D., Wu, Z., & Sunden, B. (2016). Effects of hybrid nanofluid mixture in plate heat exchangers. *Experimental Thermal and Fluid Science*, 72, 190-196.
- Hwang, Y., Park, H. S., Lee, J. K., & Jung, W. H. (2006). Thermal conductivity and lubrication characteristics of nanofluids. *Current Applied Physics*, 6, e67-e71.
- Jana, S., Salehi-Khojin, A., & Zhong, W. H. (2007). Enhancement of fluid thermal conductivity by the addition of single and hybrid nano-additives. *Thermochimica Acta*, 462(1-2), 45-55.
- Javadi, F., Sadeghipour, S., Saidur, R., BoroumandJazi, G., Rahmati, B., Elias, M., & Sohel, M. (2013a). The effects of nanofluid on thermophysical properties and heat transfer characteristics of a plate heat exchanger. *International Communications in Heat and Mass Transfer*, 44, 58-63.
- Javadi, F. S., Sadeghipour, S., Saidur, R., BoroumandJazi, G., Rahmati, B., Elias, M. M., & Sohel, M. R. (2013b). The effects of nanofluid on thermophysical properties and heat transfer characteristics of a plate heat exchanger. *International Communications in Heat and Mass Transfer*, 44, 58-63.
- Karami, M., Akhavan Bahabadi, M. A., Delfani, S., & Ghozatloo, A. (2014). A new application of carbon nanotubes nanofluid as working fluid of low-temperature direct absorption solar collector. *Solar Energy Materials and Solar Cells*, 121, 114-118.
- Karami, N., & Rahimi, M. (2014). Heat transfer enhancement in a hybrid microchannel-photovoltaic cell using Boehmite nanofluid. *International Communications in Heat and Mass Transfer*, 55, 45-52.
- Keblinski, P., Eastman, J. A., & Cahill, D. G. (2005). Nanofluids for thermal transport. *Materials Today*, 8(6), 36-44.
- Keblinski, P., Phillpot, S., Choi, S., & Eastman, J. (2002). Mechanisms of heat flow in suspensions of nano-sized particles (nanofluids). *International Journal of Heat and Mass Transfer*, 45(4), 855-863.
- Kumar, A., Kumar, M., & Chamoli, S. (2016a). Comparative study for thermal-hydraulic performance of circular tube with inserts. *Alexandria Engineering Journal*, 55(1), 343-349.
- Kumar, M. S., Vasu, V., & Gopal, A. V. (2016b). Thermal conductivity and rheological studies for Cu–Zn hybrid nanofluids with various basefluids. *Journal of the Taiwan Institute of Chemical Engineers*, 66, 321-327.

- Kumar, N., & Sonawane, S. S. (2016). Experimental study of Fe₂O₃/water and Fe₂O₃/ethylene glycol nanofluid heat transfer enhancement in a shell and tube heat exchanger. *International Communications in Heat and Mass Transfer*, 78, 277-284.
- Kumaresan, V., Mohaideen Abdul Khader, S., Karthikeyan, S., & Velraj, R. (2013). Convective heat transfer characteristics of CNT nanofluids in a tubular heat exchanger of various lengths for energy efficient cooling/heating system. *International Journal of Heat and Mass Transfer*, 60, 413-421.
- Kumaresan, V., & Velraj, R. (2012). Experimental investigation of the thermo-physical properties of water-ethylene glycol mixture based CNT nanofluids. *Thermochimica Acta*, 545, 180-186.
- Lee, J., & Mudawar, I. (2007). Assessment of the effectiveness of nanofluids for single-phase and two-phase heat transfer in micro-channels. *International Journal of Heat and Mass Transfer*, 50(3), 452-463.
- Li, H., Ha, C. S., & Kim, I. (2009a). Fabrication of carbon nanotube/SiO₂ and carbon nanotube/SiO₂/Ag nanoparticles hybrids by using plasma treatment. *Nanoscale Res Lett*, 4(11), 1384-1388.
- Li, H., Ha, C. S., & Kim, I. (2009b). Fabrication of carbon nanotube/SiO₂ and carbon nanotube/SiO₂/Ag nanoparticles hybrids by using plasma treatment. *Nanoscale Research Letters*, 4(11), 1384-1388.
- Li, Y., Zhou, J. e., Tung, S., Schneider, E., & Xi, S. (2009c). A review on development of nanofluid preparation and characterization. *Powder Technology*, 196(2), 89-101.
- Madhesh, D., & Kalaiselvam, S. (2014). Experimental analysis of hybrid nanofluid as a coolant. *Procedia Engineering*, 97, 1667-1675.
- Madhesh, D., Parameshwaran, R., & Kalaiselvam, S. (2014). Experimental investigation on convective heat transfer and rheological characteristics of Cu-TiO₂ hybrid nanofluids. *Experimental Thermal and Fluid Science*, 52, 104-115.
- Mahesh, J., Rahul, A., Diksha, B., Amol, B., & Mayura, M. (2016). Review on enhancement of heat transfer by active method. *International Journal of Current Engineering and Technology (IJCET)*(06), 221-225.

- Mariano, A., Pastoriza-Gallego, M. J., Lugo, L., Camacho, A., Canzonieri, S., & Piñeiro, M. M. (2013). Thermal conductivity, rheological behaviour and density of non-Newtonian ethylene glycol-based SnO₂ nanofluids. *Fluid Phase Equilibria*, 337, 119-124.
- Mechiri, S. K., V, V., A, V. G., & R, S. B. (2015). Thermal conductivity of Cu-Zn hybrid newtonian nanofluids: experimental data and modeling using neural network. *Procedia Engineering*, 127, 561-567.
- Mehmood, A., & Iqbal, M. S. (2016). Heat transfer analysis in natural convection flow of nanofluid past a wavy cone. *Journal of Molecular Liquids*, 223, 1178-1184.
- Minea, A. A. (2017). Hybrid nanofluids based on Al₂O₃, TiO₂ and SiO₂: Numerical evaluation of different approaches. *International Journal of Heat and Mass Transfer*, 104, 852-860.
- Moffat, R. J. (1988). Describing the uncertainties in experimental results. *Experimental Thermal and Fluid Science*, 1(1), 3-17.
- Moghadassi, A., Ghomi, E., & Parvizian, F. (2015). A numerical study of water based Al₂O₃ and Al₂O₃-Cu hybrid nanofluid effect on forced convective heat transfer. *International Journal of Thermal Sciences*, 92, 50-57.
- Naghash, A., Sattari, S., & Rashidi, A. (2016). Experimental assessment of convective heat transfer coefficient enhancement of nanofluids prepared from high surface area nanoporous graphene. *International Communications in Heat and Mass Transfer*, 78, 127-134.
- Nguyen, C., Desgranges, F., Roy, G., Galanis, N., Maré, T., Boucher, S., & Mintsa, H. A. (2007a). Temperature and particle-size dependent viscosity data for water-based nanofluids – Hysteresis phenomenon. *International Journal of Heat and Fluid Flow*, 28(6), 1492-1506.
- Nguyen, C. T., Desgranges, F., Roy, G., Galanis, N., Maré, T., Boucher, S., & Angue Mintsa, H. (2007b). Temperature and particle-size dependent viscosity data for water-based nanofluids - Hysteresis phenomenon. *International Journal of Heat and Fluid Flow*, 28(6), 1492-1506.
- Nuim Labib, M., Nine, M. J., Afrianto, H., Chung, H., & Jeong, H. (2013). Numerical investigation on effect of base fluids and hybrid nanofluid in forced convective heat transfer. *International Journal of Thermal Sciences*, 71, 163-171.

- Pak, B. C., & Cho, Y. I. (1998). Hydrodynamic and heat transfer study of dispersed fluids with submicron metallic oxide particles. *Experimental Heat Transfer an International Journal*, 11(2), 151-170.
- Paul, G., Philip, J., Raj, B., Das, P. K., & Manna, I. (2011). Synthesis, characterization, and thermal property measurement of nano-Al₉₅Zn₀₅ dispersed nanofluid prepared by a two-step process. *International Journal of Heat and Mass Transfer*, 54(15-16), 3783-3788.
- Ramachandran, R., Ganesan, K., Rajkumar, M. R., Asirvatham, L. G., & Wongwises, S. (2016). Comparative study of the effect of hybrid nanoparticle on the thermal performance of cylindrical screen mesh heat pipe. *International Communications in Heat and Mass Transfer*, 76, 294-300.
- Reddy, M. C. S., & Rao, V. V. (2013). Experimental studies on thermal conductivity of blends of ethylene glycol-water-based TiO₂ nanofluids. *International Communications in Heat and Mass Transfer*, 46, 31-36.
- S. Harandi, S., Karimipour, A., Afrand, M., Akbari, M., & D'Orazio, A. (2016). An experimental study on thermal conductivity of F-MWCNTs-Fe₃O₄/EG hybrid nanofluid: Effects of temperature and concentration. *International Communications in Heat and Mass Transfer*, 76, 171-177.
- Said, Z., Sajid, M. H., Alim, M. A., Saidur, R., & Rahim, N. A. (2013). Experimental investigation of the thermophysical properties of AL₂O₃-nanofluid and its effect on a flat plate solar collector. *International Communications in Heat and Mass Transfer*, 48, 99-107.
- Saleh, R., Putra, N., Wibowo, R. E., Septiadi, W. N., & Prakoso, S. P. (2014). Titanium dioxide nanofluids for heat transfer applications. *Experimental Thermal and Fluid Science*, 52, 19-29.
- Sarkar, J., Ghosh, P., & Adil, A. (2015). A review on hybrid nanofluids: Recent research, development and applications. *Renewable and Sustainable Energy Reviews*, 43, 164-177.
- Selvakumar, P., & Suresh, S. (2012a). Use of Al₂O₃-Cu/water hybrid nanofluids in an electronic heat sink. *IEEE Transactions On Components, Packaging And Manufacturing Technology*, 2, 1600-1607.

- Selvakumar, P., & Suresh, S. (2012b). Use of Al₂O₃-Cu/water hybrid nanofluids in an electronic heat sink. Institute of Electrical and Electronics Engineers (IEEE) Transactions On Components, Packaging And Manufacturing Technology, 2, 1600-1607.
- Sidik, N. A. C., Adamu, I. M., Jamil, M. M., Kefayati, G. H. R., Mamat, R., & Najafi, G. (2016). Recent progress on hybrid nanofluids in heat transfer applications: A comprehensive review. *International Communications in Heat and Mass Transfer*, 78, 68-79.
- Sidik, N. A. C., Mohammed, H. A., Alawi, O. A., & Samion, S. (2014). A review on preparation methods and challenges of nanofluids. *International Communications in Heat and Mass Transfer*, 54, 115-125.
- Sivashanmugam, P. (2012). Application of Nanofluids in Heat Transfer. In S. N. Kazi (Ed.), *An Overview of Heat Transfer Phenomena: InTech* (Online).
- Soltani, O., & Akbari, M. (2016a). Effects of temperature and particles concentration on the dynamic viscosity of MgO-MWCNT/ethylene glycol hybrid nanofluid: Experimental study. *Physica E: Low-Dimensional Systems and Nanostructures*, 84, 564-570.
- Soltani, O., & Akbari, M. (2016b). Effects of temperature and particles concentration on the dynamic viscosity of MgO-MWCNT/ethylene glycol hybrid nanofluid: Experimental study. *Physica E: Low-dimensional Systems and Nanostructures*, 1-20.
- Sonawane, T., Patil, P., Abhay, C., & Dusane, B. M. (2016). A review on heat transfer enhancement by passive methods. *International Research Journal of Engineering and Technology (IRJET)*, 03(09), 1567-1574.
- Sundar, L. S., Farooky, M. H., Sarada, S. N., & Singh, M. K. (2013a). Experimental thermal conductivity of ethylene glycol and water mixture based low volume concentration of Al₂O₃ and CuO nanofluids. *International Communications in Heat and Mass Transfer*, 41, 41-46.
- Sundar, L. S., Sharma, K. V., Singh, M. K., & Sousa, A. C. M. (2017). Hybrid nanofluids preparation, thermal properties, heat transfer and friction factor – A review. *Renewable and Sustainable Energy Reviews*, 68, 185-198.
- Sundar, L. S., Singh, M. K., & Sousa, A. C. M. (2013b). Thermal conductivity of ethylene glycol and water mixture based Fe₃O₄ nanofluid. *International Communications in Heat and Mass Transfer*, 49, 17-24.

- Sundar, L. S., Singh, M. K., & Sousa, A. C. M. (2013c). Thermal conductivity of ethylene glycol and water mixture based Fe_3O_4 nanofluid. *International Communications in Heat and Mass Transfer*, 49(0), 17-24.
- Sundar, L. S., Singh, M. K., & Sousa, A. C. M. (2014). Enhanced heat transfer and friction factor of MWCNT- Fe_3O_4 /water hybrid nanofluids. *International Communications in Heat and Mass Transfer*, 52, 73-83.
- Sundar, L. S., Venkata Ramana, E., Graça, M. P. F., Singh, M. K., & Sousa, A. C. M. (2016). Nanodiamond- Fe_3O_4 nanofluids: Preparation and measurement of viscosity, electrical and thermal conductivities. *International Communications in Heat and Mass Transfer*, 73, 62-74.
- Sundar, L. S., Venkata Ramana, E., Singh, M. K., & De Sousa, A. C. M. (2012). Viscosity of low volume concentrations of magnetic Fe_3O_4 nanoparticles dispersed in ethylene glycol and water mixture. *Chemical Physics Letters*, 554, 236-242.
- Suresh, S., Venkataraj, K. P., Selvakumar, P., & Chandrasekar, M. (2011). Synthesis of Al_2O_3 -Cu/water hybrid nanofluids using two step method and its thermo physical properties. *Colloids and Surfaces A: Physicochemical and Engineering Aspects*, 388(1-3), 41-48.
- Suresh, S., Venkataraj, K. P., Selvakumar, P., & Chandrasekar, M. (2012). Effect of Al_2O_3 -Cu/water hybrid nanofluid in heat transfer. *Experimental Thermal and Fluid Science*, 38, 54-60.
- Takabi, B., & Salehi, S. (2015). Augmentation of the heat transfer performance of a sinusoidal corrugated enclosure by employing hybrid nanofluid. *Advances in Mechanical Engineering*, 6, 147059.
- Takabi, B., & Shokouhmand, H. (2015). Effects of Al_2O_3 -Cu/water hybrid nanofluid on heat transfer and flow characteristics in turbulent regime. *International Journal of Modern Physics C*, 26(04), 1550047.
- Teng, T.-P., Hung, Y.-H., Teng, T.-C., Mo, H.-E., & Hsu, H.-G. (2010a). The effect of alumina/water nanofluid particle size on thermal conductivity. *Applied Thermal Engineering*, 30(14), 2213-2218.
- Teng, T. P., Hung, Y. H., Teng, T. C., Mo, H. E., & Hsu, H. G. (2010b). The effect of alumina/water nanofluid particle size on thermal conductivity. *Applied Thermal Engineering*, 30(14-15), 2213-2218.

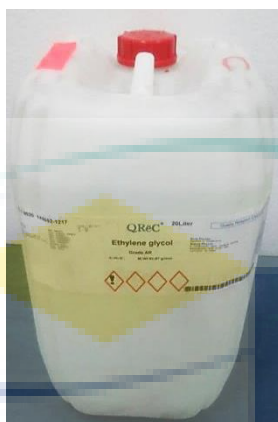
- Timofeeva, E. V., Yu, W., France, D. M., Singh, D., & Routbort, J. L. (2011). Base fluid and temperature effects on the heat transfer characteristics of SiC in ethylene glycol/H₂O and H₂O nanofluids. *Journal of Applied Physics*, 109(1), 014914.
- Turgut, A., Tavman, I., Chirtoc, M., Schuchmann, H., Sauter, C., & Tavman, S. (2009). Thermal conductivity and viscosity measurements of water-based TiO₂ nanofluids. *International Journal of Thermophysics*, 30(4), 1213-1226.
- Usri, N. A., Azmi, W. H., Mamat, R., Hamid, K. A., & Najafi, G. (2015). Heat transfer augmentation of Al₂O₃ nanofluid in 60:40 water to ethylene glycol mixture. *Energy Procedia*, 79, 403-408.
- Webb, R. L., & Kim, N. (2005). *Enhanced Heat Transfer*. Taylor and Francis, NY.
- Wong, K. V., & De Leon, O. (2015). Applications of nanofluids: Current and future. *Advances in Mechanical Engineering*, 2, 519659.
- Wu, J. M., & Zhao, J. (2013). A review of nanofluid heat transfer and critical heat flux enhancement—Research gap to engineering application. *Progress in Nuclear Energy*, 66, 13-24.
- Xie, H., Lee, H., Youn, W., & Choi, M. (2003). Nanofluids containing multiwalled carbon nanotubes and their enhanced thermal conductivities. *Journal of Applied Physics*, 94(8), 4967-4971.
- Yarmand, H., Gharekhani, S., Ahmadi, G., Shirazi, S. F. S., Baradaran, S., Montazer, E., . . . Dahari, M. (2015). Graphene nanoplatelets–silver hybrid nanofluids for enhanced heat transfer. *Energy Conversion and Management*, 100, 419-428.
- Yarmand, H., Gharekhani, S., Shirazi, S. F. S., Amiri, A., Montazer, E., Arzani, H. K., . . . Kazi, S. N. (2016a). Nanofluid based on activated hybrid of biomass carbon/graphene oxide: Synthesis, thermo-physical and electrical properties. *International Communications in Heat and Mass Transfer*, 72, 10-15.
- Yarmand, H., Gharekhani, S., Shirazi, S. F. S., Goodarzi, M., Amiri, A., Sarsam, W. S., . . . Kazi, S. N. (2016b). Study of synthesis, stability and thermo-physical properties of graphene nanoplatelet/platinum hybrid nanofluid. *International Communications in Heat and Mass Transfer*, 77, 15-21.
- Yoo, D. H., Hong, K. S., & Yang, H. S. (2007). Study of thermal conductivity of nanofluids for the application of heat transfer fluids. *Thermochimica Acta*, 455(1–2), 66-69.

- Yu, W., & Xie, H. (2012). A review on nanofluids: preparation, stability mechanisms, and applications. *Journal of Nanomaterials*, 2012, 1-17.
- Yu, W., Xie, H., Li, Y., Chen, L., & Wang, Q. (2012). Experimental investigation on the heat transfer properties of Al₂O₃ nanofluids using the mixture of ethylene glycol and water as base fluid. *Powder Technology*, 230, 14-19.
- Zakaria, I., Azmi, W. H., Mohamed, W. A. N. W., Mamat, R., & Najafi, G. (2015). Experimental Investigation of Thermal Conductivity and Electrical Conductivity of Al₂O₃ Nanofluid in Water - Ethylene Glycol Mixture for Proton Exchange Membrane Fuel Cell Application. *International Communications in Heat and Mass Transfer*, 61, 61-68.
- Zamzamian, A., Oskouie, S. N., Doosthoseini, A., Joneidi, A., & Pazouki, M. (2011). Experimental investigation of forced convective heat transfer coefficient in nanofluids of Al₂O₃/EG and CuO/EG in a double pipe and plate heat exchangers under turbulent flow. *Experimental Thermal and Fluid Science*, 35(3), 495-502.



UMP

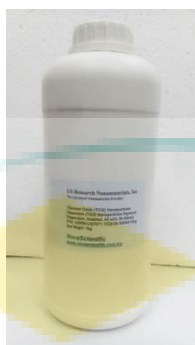
APPENDIX A
ETHYLENE GLYCOL



Product name	: Ethylene glycol, reagent grade
Product code	: E7152-1-2500
Formula	: C ₂ H ₆ O ₂
M. wt	: 62.07 g/mol
CAS No.	: 107-21-1
Packing	: 2.5 L

Parameter	Specification	
Assay	min. 99.5	%
Acidity	max. 0.0002	meg/g
Formaldehyde	max. 0.005	%
Chlorides (Cl)	max. 0.00002	%
Iron (Fe)	max. 0.00002	%
KMnO ₄ red. Matter (as O)	max. 0.0003	%
Substances darkened by H ₂ SO ₄	passes test	
Sulfated ash	max. 0.005	%
Water	max. 0.1	%

APPENDIX B
TITANIUM OXIDE (TiO₂) NANOFLUIDS



Trade name	: Titanium (IV) oxide, Anatase, 40% in water, Dispersion
Stock number	: USRN-US7071-TiO ₂ / 30-50 NM
Manufacturer/Supplier	: US Research Nanomaterials, Inc./NovaScientific Resources (M) Sdn. Bhd.

Handling and storage

1. Handling

- Information for safe handling:
Keep container tightly sealed.
Store in cool, dry place in tightly closed containers.
Ensure good ventilation at the workplace.
Prevent formation of dust.
- Information about protection against explosions and fires:
No special measures required.

2. Storage

- Requirements to be met by storerooms and receptacles:
No special requirements.
- Informations about storage in one common storage facility:
Not required.
- Further information about storage conditions:
Keep container tightly sealed.
Store in cool, dry conditions in well-sealed containers.

Personal protective equipment

- General protective and hygienic measures:
The usual precautionary measures for handling chemicals should be followed.
Keep away from foodstuffs, beverages, and feed.
Remove all soiled and contaminated clothing immediately.
Wash hands before breaks and at the end of work.
- Breathing equipment:
Use suitable respirator when high concentrations are present.
- Protection of hands:
Impervious gloves.
- Eye protection:
Safety glasses.
- Body protection:
Protective work clothing.

Physical and chemical properties

Form	: Powder
Color	: White
Odor	: Odorless
Melting point/Melting range	: 1830-1850 °C
Boiling point/Boiling range	: 2500-3000 °C
Sublimation temperature/start	: Not determined
Flash point	: Not applicable
Ignition temperature	: Not determined
Decomposition temperature	: Product does not present an explosion hazard
Danger of explosion	: Not determined
Vapor pressure	: 4.23 g/cm ³
Density at 20 °C	: Insoluble
Water solubility	

APPENDIX C

SILICON OXIDE (SiO₂) NANOFUIDS



Trade name	: Silicon oxide, 25% in water, Dispersion
Stock number	: USRN-US7040-SiO ₂ / 30 NM
Manufacturer/Supplier	: US Research Nanomaterials, Inc./NovaScientific Resources (M) Sdn. Bhd.

Handling and storage

1. Handling

- Information for safe handling:
Keep container tightly sealed.
Store in cool, dry place in tightly closed containers.
Ensure good ventilation at the workplace.
Prevent formation of dust.
- Information about protection against explosions and fires:
The product is not flammable.

2. Storage

- Requirements to be met by storerooms and receptacles:
No special requirements.
- Informations about storage in one common storage facility:
Do not store together with acids.
Store away from Halogens.
Store away from oxidizing agents.
- Further information about storage conditions:
Protect from humidity and water.
Keep container tightly sealed.
Store in cool, dry conditions in well sealed containers.

Personal protective equipment

- General protective and hygienic measures:
The usual precautionary measures for handling chemicals should be followed.
Keep away from foodstuffs, beverages, and feed.
Remove all soiled and contaminated clothing immediately.
Wash hands before breaks and at the end of work.
- Breathing equipment:
Use suitable respirator when high concentrations are present.
- Protection of hands:
Impervious gloves.
- Eye protection:
Safety glasses.
- Body protection:
Protective work clothing.

Physical and chemical properties

Form	: Powder
Color	: White
Odor	: Odorless
Melting point/Melting range	: 1610-1728 °C
Boiling point/Boiling range	: 2230 °C
Sublimation temperature/start	: Not determined
Flash point	: Not determined
Ignition temperature	: Not determined
Decomposition temperature	: Product does not present an explosion hazard
Danger of explosion	: Not determined
Vapor pressure	: 2.17-2.66 g/cm ³
Density at 20 °C	: Insoluble
Water solubility	

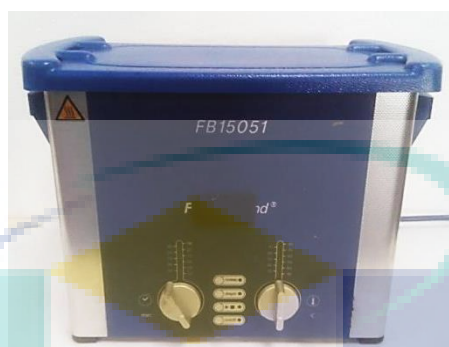
APPENDIX D STIRRING HOTPLATE



Model	: HS070V2
Serial number	: 6844
Design	: Flat shaped stirrer and hot plate

<u>Performance specifications</u>	
Speed range	: 100-1500 rpm
Voltage	: 230 V
Frequency	: 50 Hz
Power input	: 1020 W
Shaking movement	: Orbital
Temperature range	: 50-500 °C
Overall dimensions (w x l x h)	: 220 x 295 x 115 mm
Plate dimensions	: 80%
Permissible relative humidity	

APPENDIX E
ULTRASONIC BATH



Model	: Fisherbrand FB15051
--------------	-----------------------

<u>Unit Features</u>	
Normal	: For sample preparation, e.g. mixing, dissolving and dispersing
Pulse	: Activatable additional power through increased peak performance
Sweep	: For a uniform distribution of the ultrasonic power throughout the tank
Degas	: For a quick degassing of samples and HPLC solvents
Power control	: Optimised power regulation for special cleaning and laboratory applications
Pause	: Interrupts the operation
Auto start	: Automatic start when set temperature is reached
<u>Technical Data</u>	
Tank max. capacity	: 2.75 L
Tank internal dimension (W/H/D)	: 240 x 137 x 100 mm
Unit external dimension (W/H/D)	: 300 x 179 x 214 mm
Basket internal dimension (W/H/D)	: 198 x 106 x 50 mm
Voltage	: 220-240 V
Power consumption total	: 300 W
Ultrasonic frequency	: 37 Hz
Ultrasonic power effective	: 120 W
Ultrasonic peak power	: 400 W
Sweep	: integrated
Pulse	: activatable
Heating power	: 200 W

APPENDIX F
UV-VIS SPECTROPHOTOMETER



Model	: DU-8200
-------	-----------

<u>Specifications</u>	
Wavelength range	: 190-1100 nm
Optical system	: Single beam, blazed holographic grating (1200 lines/mm)
Wavelength accuracy	: ± 0.8 nm
Wavelength repeatability	: ≤ 0.2 nm
Wavelength setting	: Auto, Resolution 0.1 nm
Photometric range	: 0~200% T, -0.3~3 A, 0~9999 C
Photometric accuracy	: ± 0.002 A (0~0.5 A), ± 0.004 A (0.5~1 A), $\pm 0.3\%$ T (0~100% T)
Photometric repeatability	: ≤ 0.001 A (0~0.5 A), ≤ 0.002 A (0.5~1 A), $\leq 0.2\%$ T (0~100% T)
Stray light	: $\leq 0.1\%$ T (220/360 nm)
Scan speed	: High, Medium, Low. Max. 1000 nm/min
Baseline flatness	: ± 0.003 A
Stability	: 0.002 A/h (500 nm, 0 A)
Noise	: $\leq 0.2\%$ T / 3 min (250/500 nm, 0% T); $\leq 0.5\%$ T / 3 min (250/500 nm, 100% T)
Sample compartment	: Accommodate 5-100 nm pathlength cuvette
Detector	: Silicon Photodiode
Lamps	: Tungsten lamp & Deuterium lamp (Pre-aligned)
Display	: Graphic LCD (128x64 Dots)
Keypad	: 11-key Membrane Keypad
Output port	: USB port & RS232 port
Printer	: Mini serial printer; PC printer
PC software	: Optional PC scanning software
Power requirements	: AC 90-250V, 50/60 Hz
Dimension	: 431x318x195 mm
Net weight / Gross weight	: 9kgs / 13kgs

Features

1. Small fine design, space saving
2. The excellent optical and electric system
3. Low noise and low stray light
4. Large LCD display (128*64 Dots), can display curve
5. High quality grating, detector and lamps
6. Data and curve can be stored in real-time
7. Auto setting WL, auto blank
8. Easy to change Pri-aligned lamps
9. Reinforced baseboard and bracket assures durability

Function

Photometric
Quantitative

: T%, Abs

:Standard curve system utility

*WL scan (spectrum scan – PC)

*Time scan (Kinetics – PC)

*DNA/Protein test (PC)

*Multi-WL test (PC)



UMP

APPENDIX G

TRANSMISSION ELECTRON MICROSCOPE (TEM)



Standard Operating Procedures

1. Sign in the Log Book and log in to CM120 computer
 - Take a look at previous comments made by the last few users.
 - Write your name, username, date, and time in the Log Book.
 - Samples have to be examined.
 - Write down the IGP and P3 numbers (on vacuum page).

2. Check the following
 - On VACUUM page: make sure the vacuum is ready (HIVAC and UHV should be lit).
 - For normal operation $IGP < 30$ and $P3 < 30$.
 - Check V3, V4, V5 and V7 are opened.
 - On Configuration page make sure Cathode is set to LaB6 and Filament Limit is highlighted.

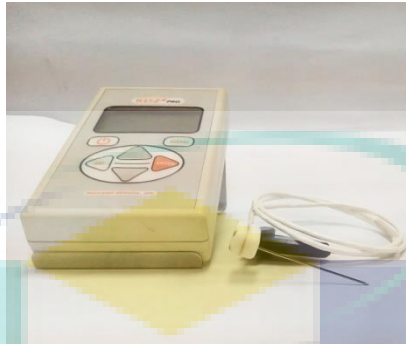
3. Loading and inserting specimen
 - Load the specimen in the standard single tilt holder. Make sure the specimen is properly fastened in the specimen holder
 - Check that the O-ring of the holder is clean.
 - Make sure the filament is completely desaturated.
 - Carefully insert the holder into the goniometer compustage with the pin on the holder in the 5 o'clock position. The prepumping cycle will initiate and the red indicator light will come on.
 - When the red light goes off (about 1 minute), rotate the specimen holder fully counterclockwise until unable to rotate further and insert into the microscope carefully as it will be sucked into the vacuum of the microscope.
 - Wait for $IGP < 30$ before proceed furthermore. Do not use the microscope if the IGP reading is higher than 30 to prevent damage to the LaB6 filament.
 - Reverse these directions to remove the specimen holder from the microscope. The filament should be fully desaturated!

4. Bringing the microscope to operating conditions

- Check High Tension (i.e. 120kV) in Parameters, Cathode (LaB6 highlighted) and Fil Limit (highlighted, reading 20 to 30) in Configuration.
 - To saturate the filament turn the Filament knob clockwise until Filament Limit is reached. The process is automated; every step will take 5s. The whole procedure should be completed in 2-3 min.
 - From Page Menu set the desired Mode: TEM Bright Field or Low Dose TEM Bright Field.
 - Go to 5600x MAG and Reset Holder in COMPUSTAGE/COMPUCTRL. Set Spotsize to 3-4, find a small recognizable object on viewing screen using Joystick X/Y control, adjust illumination (Intensity knob) and press the Auto Focus knob.
 - Press A-WOBBLER in COMPUSTAGE (this will initiate forth and back tilting of the goniometer to +/- 15 deg.) Using Z Control on the joystick, align Z High by minimizing the apparent movement of the centered feature.
 - Stop A-WOBBLER and focus desired object using the Focus knob.
5. Taking pictures on the CCD Camera
- Open and Start EMMENU4. Create new View Port (up to 16)
 - Set Camera Format (2K x 2K, 2K x 1K, 1K x 1K), Bin (no, 2, 4, 8)
 - Choose or create Image Folder and Image Name.
 - Find the object of the interest, set appropriate MAG, align illumination
 - Press the Camera Button to acquire image on CCD camera.
 - Rename images (if necessary) and save in your folder.
6. Ending your session
- Set MAG to 5600X.
 - Spread the beam over the viewing screen
 - Reset Holder
 - Completely desaturate the filament
 - Take out the holder and remove your grid

APPENDIX H

KD2 PRO THERMAL PROPERTY ANALYZER



KD2 Pro Overview

The KD2 Pro is a battery-operated, menu-driven device that measures thermal conductivity and resistivity, volumetric specific heat capacity and thermal diffusivity. We designed the KD2 Pro for ease of use and maximum functionality.

Specifications

Operating Environment

Controller : 0 to 50 °C
 Sensors : -50 to +150 °C

Controller

Power : 4 AA batteries
 Battery life : At least 500 readings in constant use or three years with no use (battery drain in sleep mode < 50 uA)
 Case size : 15.5 cm x 9.5 cm x 3.5 cm
 Display : 3 cm x 6 cm, 128 x 64 pixel graphics LCD
 Keypad : 6 key, sealed membrane
 Data storage : 4095 measurements in flash memory (both raw and processed data are stored for download)
 Interface : 9-pin serial
 Read modes : Manual and Auto Read

KS- 1 Sensor

Size : 1.3 mm diameter x 6 cm long
 Range : 0.02 to 2.00 W/m.K (thermal conductivity)
 50 to 5000 °C.cm/W (thermal resistivity)
 Accuracy : (Conductivity): ±5% from 0.2 to 2 W/m.K ±0.01 W/m.K from
 0.02 to 0.2 W/m.K
 Cable length : 0.8 m

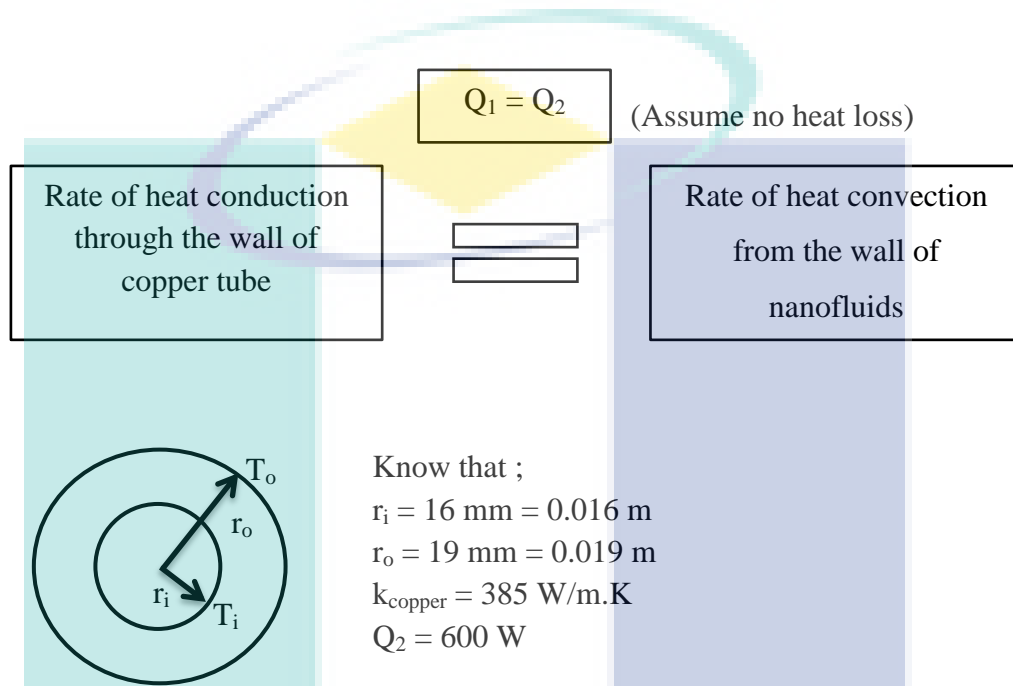
APPENDIX I
BROOKFIELD LVDV III ULTRA RHEOMETER



<u>Specifications</u>	
Speed ranges for viscosity test	: 0.01-250 rpm (0.01 increments from 0.01 to 0.99, 0.1 rpm increments from 1.0 to 250 rpm)
Speed ranges for yield test	: Pre shear = 0.01 to 200 rpm Zero = 0.01 to 0.5 rpm Yield test = 0.01 to 5 rpm
Time intervals for yield tests	: 100 msec – 1000 msec
Viscosity accuracy	: ± 1.0% of full scale range for a specific spindle running at a specific speed
Temperature sensing range	: -100 to 300 °C
Temperature accuracy	: ±1.0 °C from -100 °C to 150 °C ±2.0 °C from +150 °C to 300 °C
Analog torque output	: 0 – 1 Volt DC (0 – 100% torque)
Analog temperature output	: 0 – 4 Volt DC (10 mV / °C)
Printer output	: Centronics, parallel or serial
Computer interface	: RS-232 USB
Torque accuracy	: ±1.0% of full scale range
Torque repeatability	: ±2.0%

APPENDIX J
Sample Calculation of the Effect of Tube Thickness

For 0.5% volume concentration of TiO₂-SiO₂ nanofluids at bulk temperature of 30 °C with flow rate of 19.31 LPM.



From the experiment data ;
 $T_b = 30 \text{ }^\circ\text{C}$
 $T_{s,\text{avg}} = 31.42 \text{ }^\circ\text{C}$

$Q_1 = Q_2$ (assume no heat loss)

$$\frac{T_i - T_o}{\left[\frac{\ln(r_o / r_i)}{2\pi k L} \right]} = 600$$

$$T_i = 600 \left[\frac{\ln(0.019/0.016)}{2\pi(385)(1.5)} \right] + 31.33$$

$$T_i = 0.0284 + 31.33 = 31.36$$

Therefore, the reading of thermocouple are ;

$$T_o = 31.33 \text{ }^\circ\text{C} ; T_i = 31.36 \text{ }^\circ\text{C}$$

$$\% \text{ error / difference} = 0.0957\%$$

APPENDIX K
UNCERTAINTY OF PARAMETER ANALYSIS

No.	Heat transfer and friction parameter	Maximum uncertainty (%)	Minimum uncertainty (%)
1	Reynolds number, Re $\text{Re} = \frac{\rho \bar{V} D}{\mu}$	$\frac{U_{\text{Re}}}{\text{Re}} = \sqrt{\left(\frac{U_{\rho}}{\rho}\right)^2 + \left(\frac{U_{\bar{V}}}{\bar{V}}\right)^2 + \left(\frac{U_{\mu}}{\mu}\right)^2}$ $= \sqrt{(0.1)^2 + (0.25063)^2 + (0.1)^2}$ $= 0.28777$	$\frac{U_{\text{Re}}}{\text{Re}} = \sqrt{\left(\frac{U_{\rho}}{\rho}\right)^2 + \left(\frac{U_{\bar{V}}}{\bar{V}}\right)^2 + \left(\frac{U_{\mu}}{\mu}\right)^2}$ $= \sqrt{(0.1)^2 + (0.04902)^2 + (0.1)^2}$ $= 0.14968$
2	Heat flux, q $q = \frac{Q}{A} = \frac{VI}{\pi DL}$	$\frac{U_q}{q} = \sqrt{\left(\frac{U_V}{V}\right)^2 + \left(\frac{U_I}{I}\right)^2}$ $= \sqrt{(0.00908)^2 + (0.18349)^2}$ $= 0.18371$	$\frac{U_q}{q} = \sqrt{\left(\frac{U_V}{V}\right)^2 + \left(\frac{U_I}{I}\right)^2}$ $= \sqrt{(0.00908)^2 + (0.18349)^2}$ $= 0.18371$
3	Heat transfer coefficient, h $h = \frac{q}{(T_w - T_b)}$	$\frac{U_h}{h} = \sqrt{\left(\frac{U_q}{q}\right)^2 + \left(\frac{U_{(T_w - T_b)}}{(T_w - T_b)}\right)^2}$ $\frac{U_{(T_w - T_b)}}{(T_w - T_b)} = \sqrt{(0.72314)^2 + (0.48682)^2}$ $= 0.87173$	$\frac{U_h}{h} = \sqrt{\left(\frac{U_q}{q}\right)^2 + \left(\frac{U_{(T_w - T_b)}}{(T_w - T_b)}\right)^2}$ $\frac{U_{(T_w - T_b)}}{(T_w - T_b)} = \sqrt{(0.29429)^2 + (0.19989)^2}$ $= 0.35575$

		$\frac{U_h}{h} = \sqrt{(0.18371)^2 + (0.87173)^2}$ $= 0.89088$	$\frac{U_h}{h} = \sqrt{(0.18371)^2 + (0.35575)^2}$ $= 0.40039$
4	Nusselt number, Nu $Nu = \frac{hD}{k}$	$\frac{U_{Nu}}{Nu} = \sqrt{\left(\frac{U_h}{h}\right)^2 + \left(\frac{U_k}{k}\right)^2}$ $= \sqrt{(0.89088)^2 + (0.1)^2}$ $= 0.89647$	$\frac{U_{Nu}}{Nu} = \sqrt{\left(\frac{U_h}{h}\right)^2 + \left(\frac{U_k}{k}\right)^2}$ $= \sqrt{(0.40039)^2 + (0.48682)^2}$ $= 0.41269$
5	Friction factor, f $f = \frac{\Delta P}{\left(\frac{L}{D}\right)\left(\frac{\rho \bar{V} D}{2}\right)}$	$\frac{U_f}{f} = \sqrt{\left(\frac{U_{\Delta P}}{\Delta P}\right)^2 + \left(\frac{U_{\rho}}{\rho}\right)^2 + \left(\frac{U_{\bar{V}}}{\bar{V}}\right)^2}$ $= \sqrt{(0.13333)^2 + (0.1)^2 + 2 \times (0.25063)^2}$ $= 0.39167$	$\frac{U_f}{f} = \sqrt{\left(\frac{U_{\Delta P}}{\Delta P}\right)^2 + \left(\frac{U_{\rho}}{\rho}\right)^2 + \left(\frac{U_{\bar{V}}}{\bar{V}}\right)^2}$ $= \sqrt{(0.00696)^2 + (0.1)^2 + 2 \times (0.04902)^2}$ $= 0.12188$
6	Thermo-physical properties	0.1	0.1

APPENDIX L LIST OF PUBLICATIONS

The list of publications during my master study is stated as below:

LIST OF ISI JOURNALS:

1. **M.F. Nabil**, W.H. Azmi, K.A. Hamid, N.N.M. Zawawi, G. Priyandoko, R. Mamat. 2016. Thermo-physical properties of hybrid nanofluids and hybrid nanolubricants: A comprehensive review on performance. *International Communications in Heat and Mass Transfer* 83:30-39. **Published Q1 (IF = 3.718)**
2. **M.F. Nabil**, W.H. Azmi, K.A. Hamid, R. Mamat. 2017. An experimental study on the thermal conductivity and dynamic viscosity of TiO₂ - SiO₂ nanofluids in water : ethylene glycol mixture. *International Communications in Heat and Mass Transfer* 86:181-189. **Published Q1 (IF = 3.718)**
3. **M.F. Nabil**, W.H. Azmi, K.A. Hamid, R. Mamat. Experimental investigation of heat transfer and friction factor of TiO₂-SiO₂ nanofluids in water:ethylene glycol mixture. *International Journal of Heat and Mass Transfer*. **Published Q1 (IF = 3.458) In Press**
4. K.A Hamid, W.H. Azmi, **M.F. Nabil**, K.V. Sharma, R. Mamat. Experimental investigation of thermal conductivity and dynamic viscosity on nanoparticle mixture ratios of TiO₂-SiO₂ nanofluids. *International Journal of Heat and Mass Transfer* 116:1143–1152. **Published Q1 (IF = 3.458)**
5. K.A. Hamid, W.H. Azmi, **M.F. Nabil**, R. Mamat. Experimental investigation of heat transfer performance on nanoparticle mixture ratio of TiO₂-SiO₂ nanofluids under turbulent flow. *International Journal of Heat and Mass Transfer* 118: 617–627. **Published Q1 (IF = 3.458)**

LIST OF CONFERENCE PROCEEDING JOURNALS:

6. **M.F. Nabil**, W.H. Azmi, K.A. Hamid, R. Mamat. Heat transfer and friction factor of composite TiO₂-SiO₂ nanofluids in water-ethylene glycol (60:40) mixture. *4th International Conference on Mechanical Engineering Research (ICMER2017)* 257 012066. **Published (Scopus)**
7. K.A. Hamid, W.H. Azmi, **M.F. Nabil**, R. Mamat. Improved thermal conductivity of TiO₂-SiO₂ hybrid nanofluid in ethylene glycol and water mixture. *4th International Conference on Mechanical Engineering Research (ICMER2017)* 257 012067. **Published (Scopus)**
8. **M.F. Nabil**, W.H. Azmi, K.A. Hamid, R. Mamat. Heat transfer performance of TiO₂-SiO₂ nanofluids in water-ethylene glycol mixture. *International Conference on Advances in Mechanical Engineering (ICAME) 2017*. **Published (Scopus)**
9. K.A. Hamid, W.H. Azmi, **M.F. Nabil**, R. Mamat. Heat transfer augmentation of difference binary ratio of TiO₂-SiO₂ nanofluids. *International Conference on Advances in Mechanical Engineering (ICAME) 2017*. **Published (Scopus)**

LIST OF AWARDS:

11. **Silver Medal** in Advanced Innovation and Engineering Exhibition (AiNEX 2017), 3 Mei 2017, Dewan Astaka, UMP Gambang, Kuantan, Pahang Darul Makmur, Malaysia.
12. **Best Paper Award** in International Conference on Mechanical Engineering Research (ICMER 2017), 1-2 August 2017, Swiss-Garden Resort, Kuantan, Pahang Darul Makmur, Malaysia. M.F. Nabil, W.H. Azmi, K.A. Hamid and Rizalman Mamat. 2017. Heat transfer and friction factor of composite TiO₂-SiO₂ nanofluids in water-ethylene glycol (60:40) mixture.

13. **Best Paper Award** in International Conference on Advances in Mechanical Engineering (ICAME 2017), 16-18 August 2017, Ao Nang Villa Resort, Krabi, Thailand. K.A. Hamid, W.H. Azmi, M.F. Nabil, and Rizalman Mamat. 2017. Heat transfer augmentation of mixture ratio TiO_2 to SiO_2 in hybrid nanofluids.

